The Proteins LIN-39 HOX, LIN-12 NOTCH and LIN-31 Forkhead Coordinately Control the Cell Cycle of the *C. elegans* Vulva

---

Dissertation

zur

Erlangung der naturwissenschaflichen Doktorwürde
(Dr. sc. nat.)

vorgelegt der

Mathematish-naturwissenschaftlichen Fakultät

der

Universität Zürich

von

Daniel Maria Roiz Lafuente

aus

Spanien

Promotionskomitee

Prof. Dr. Alex Hajnal (Vorsitz)
Prof. Dr. Konrad Basler
Prof. Dr. Fritz Müller

Zürich, 2015

To all who contributed on the way

Zusammenfassung

Entwicklung nennt man den Prozess vom Einzell-embryo bis hin zur Bildung eines funktionellen erwachsenen Organismus. Ein sehr wichtiger Teil der Entwicklung ist die Organogenese oder die de-novo Bildung von Organen. Die Organogenese ist ein komplexer Ablauf, der Protein-Protein Interaktionen involviert, wobei sowohl Interaktionen mit löslichen, als auch membrangebundenen Proteinen stattfinden und über die Regulierung von Transkriptionsfaktoren das zelluläre Programm bestimmt wird. So führen zum Beispiel Ligand-Rezeptorinteraktionen, die zu konservierten RAS, WNT und NOTCH Signalwegen gehören, zur Modifikation von HOX-, ETS- oder Forkhead- Transkriptionsfaktoren, welche jeder Zelle eines Organs eine bestimmte Identität zuweisen.

Man kann die Organogenese in vier Stufen unterteilen: Die Spezifikation oder der Erwerb einer bestimmten Organidentität; die Differenzierung, bei der ähnliche Zellen innerhalb eines Organs sich zu bestimmten Zelltypen spezialisieren; die Zellvermehrung, bei der die verschiedenen Zelltypen proliferieren und zu Organwachstum führen; die Morphogenese, bei der verschiedene Zellen eine bestimmte 3D-struktur ausbilden. Vom Wurm zum Mensch spielen viele Mitglieder der HOX-Familie eine grundlegende Rolle bei der Organentwicklung und dem Körperbauplan. Jedoch fehlt uns bis heute ein vollständiges Verständnis der Rolle dieser Traskriptionsfaktoren in den vier oben beschriebenen Phasen der Entwicklung.

Die Vulvaentwicklung des Fadenwurms *C. elegans* ist ein geeignetes Modell, um besser zu verstehen, wie Hoxgene die Organogenese regulieren, da konservierte Signalwege in einem eizelnen HOX-Gen, *lin-39*, zusammenlaufen.

Darüberhinaus, eignet sich dieses System, um die Funktion von *lin-39* in der Kontrolle und Koordination der Zellteilung zu untersuchen, ein Phänomen, welches bislang fast nicht untersucht wurde und wenig verstanden ist.

An Hand von genetischen Analysen verschiedener Gene, die die Vulvaentwicklung steuern, konnte ich zeigen, dass die Vulva-Organanlage von Tieren, die keine *lin-39* Aktivität aufweisen, auf das induktive LIN3 (EGF) Signal reagiert, aber den lateralen Signalweg auf Grund des Verlusts der *lag-2 delta* und *lin-12 Notch* Expression nicht anschalten kann. Zudem habe ich herausgefunden, dass Lin-12 NOTCH mit LIN-39 kooperiert, um die Zellteilung zu fördern, während der LIN-31 Forkhead-Transkriptionsfaktor, unabhängig von LIN-1, die Proliferation verhindert und LIN-39 antagonisiert. Ausserdem habe ich mit Reporteranalysen und Chromatin-Immunpräzipitationsexperimenten gezeigt, dass *cye-1* und möglicherweise *cki-1* und *cdk-4* direkte Zielgene von LIN-39 sind. Dabei basiert die Bindung

auf einem funktionell konservierten, neuartigen Bindugsmotiv, welches sich im Promotor dieser Gene befindet und eine wichtige Rolle bei der Aktivierung des Zellzyklus der Vulvavorläuferzellen (VPC) spielt.
Zusammenfassend stelle ich in dieser Arbeit ein Modell vor, bei dem LIN-39 den Zellzyklus sowohl direkt durch die Interaktion mit Zellzykluskomponenten in der Vulva Organanlage als auch indirekt über die Aktivierung des LIN-12 Notch Signalwegs, steuert. Auf diese Weise, ermöglicht LIN-39 den Zellen der Vulva-Organanlage die Hinderung des Zellzyklus durch LIN-31 zu überwinden.

Summary

The processes occurring between the one-cell stage embryo and the formation of a functional adult organism is known as "development". Among the different processes that take place during development, organogenesis or the *novo* formation of organs, plays a central role.
Organogenesis is a complex process that involves protein-protein interactions where both soluble and cell associated ligand-receptor interactions take place and transcriptional regulation, where a broad range of transcription factors are necessary to reshape the cellular program. Thus, ligand-receptor interactions belonging to RAS, WNT and NOTCH conserved signaling pathways, lead to the modification of transcription factors of HOX, ETS-domain or the Forkhead families, that will give a particular identity to the each cell of a given organ.
In addition, the organogenesis can be divided in four steps: "specification", or the acquisition of a defined organ identity; "differentiation", where cells alike within an organ specialize in subsequent cell types; "proliferation", where the multiple cell lineages multiply leading to organ growth; and "morphogenesis", where the different cell lineages assemble into a specific 3D conformation.
From worms to humans many members of the *hox* family have been reported to play a fundamental role in the organogenesis and development of the animal body plan. However, we lack a complete picture of their role during the different phases of organogenesis and don't have a clear picture of how those *hox* genes coordinate the different processes taking place during animal development.
Thus, the development of the vulva of *C. elegans,* where the highly conserved signaling pathways converge in a single *hox* gene, *lin-39,* to produce a functional organ, is a great model to better understand how *hox* genes coordinate organogenesis. Yet, *lin-39* coordination of cell proliferation is a less studied mechanism and therefore poorly understood.
By performing genetic analysis of different genes implicated in vulval development, I discovered that the vulval primordium of animals lacking *lin-39* activity responds to the inductive LIN-3 EGF signal, but cannot activate lateral signaling due to the loss of *lag-2 delta* and *lin-12 Notch* expression. Moreover, the LIN-12 NOTCH pathway cooperates with LIN-39 to promote proliferation, while LIN-31 independently of LIN-1, prevents proliferation and antagonizes LIN-39. Furthermore, using reporter analysis and Chromatin Immuno-Precipitation (ChIP) experiments I found that *cye-1* and possibly *cki-1* and *cdk-4* are direct targets of LIN-39 and contain a functional conserved novel LIN-39 binding motif in the enhancer regions that play an important role in the activation of the cell cycle in the vulval precursor cells (VPC). Taken together, I propose a model where LIN-39 promotes cell cycle

progression by directly inducing the expression of cell cycle components in the vulval primordium and indirectly by activating the LIN-12 NOTCH pathway. This way, LIN-39 allows the vulval primordium to overcome the proliferation block imposed by LIN-31.

Table of Contents

1

Introduction

1.1 Organs development in multicellular organisms

Animal organogenesis involves the remodelling of epithelia into organs (Trinkaus, 1969). This process is guided by both soluble and cell associated ligand-receptor interactions and can be divided in four steps: specification, differentiation and proliferation of multiple cell lineages that will assemble into a specific form (morphogenesis) (Ackermann and Paw, 2003).

Specification is the acquisition of a defined identity by a cell or a group of cells. In many organisms, the specification process is the integrative product of different extracellular and intercellular signals (Clark et al., 1993; Rogers et al., 2011; Kim and Nirenberg, 1989) that include: the RAS, NOTCH and WNT signaling pathways (Eisenmann et al., 1998; Christensen et al., 1996; Gleason et al., 2006). The balance between the different inputs leads, in general, to the expression of homeobox genes that will remodel the transcriptional programs toward a specific fate (Clark et al., 1993; Kim and Nirenberg, 1989; Koh et al., 2002; Maloof et al., 1999; Costa et al., 1988) **(Fig. 1.1A)**.

Once the cell has acquired a specific cell fate, it enters in the differentiation process. During this process, cells alike within an organ specialize in subsequent cell types. In this phase, the cross-talk between the different cells of the organ primordium, as well as with the neighbouring tissues plays, a crucial role (Sundaram, 2004; Sundaram, 2005) **(Fig. 1.1A)**.

After differentiation, the organ primordium contains all the cell lineages necessary for adult organ formation. Still, the number of cells and their 3D location are not fully acquired. Therefore, the proliferation of those cells, coupled to the morphogenesis of the organ, must take place. Both processes, differentiation and morphogenesis, are mainly controlled by signal transduction pathways such the RAS, NOTCH and WNT signaling pathways (Aktas et al., 1997; Go et al., 1998) and a diverse range of transcription factors that act in parallel

(Pellegrino and Hajnal, 2014; Farooqui et al., 2012; Schindler and Sherwood, 2012) **(Fig. 1.1A)**.

An important aspect of organogenesis is the conservation throughout the evolution. For example, gastrulation, the process by which cells in the surface of the embryo internalize to originate the three germ layers, is highly conserved in a wide variety of organisms. The high conservation of the gastrulation movements throughout the animal kingdom may indicate that the acquisition in two dimensions of certain patterns and cell fates is fundamental to form complex structures (Wolpert, 1992). In addition, the molecular pathways controlling certain developmental processes are also highly conserved. For example, underneath the different morphological and functional structures among the animal kingdom lies an ancient structural fingerprint based on the expression of *hox* genes. Both, the establishment and maintenance of the spatial and temporal distribution of *hox* expression plays an important role in determining axial patterns from worms to humans (Gellon and McGinnis, 1998). However, these processes are very difficult to analyze in higher eukaryotes, due to their large and complex genome, the complexity and diversity of their cellular types and in many cases the redundancy of their biological processes. Moreover, the study of these processes in superior animals leads to ethical issues that can be circumvented using model organisms. Each of these models is suitable for different approaches and techniques. For example, while *C. elegans* comes very handy to analyse problems from a genetic point of view, the mouse (*mus musculus)* can be an excellent tool to understand the molecular basics of complex organs formation.

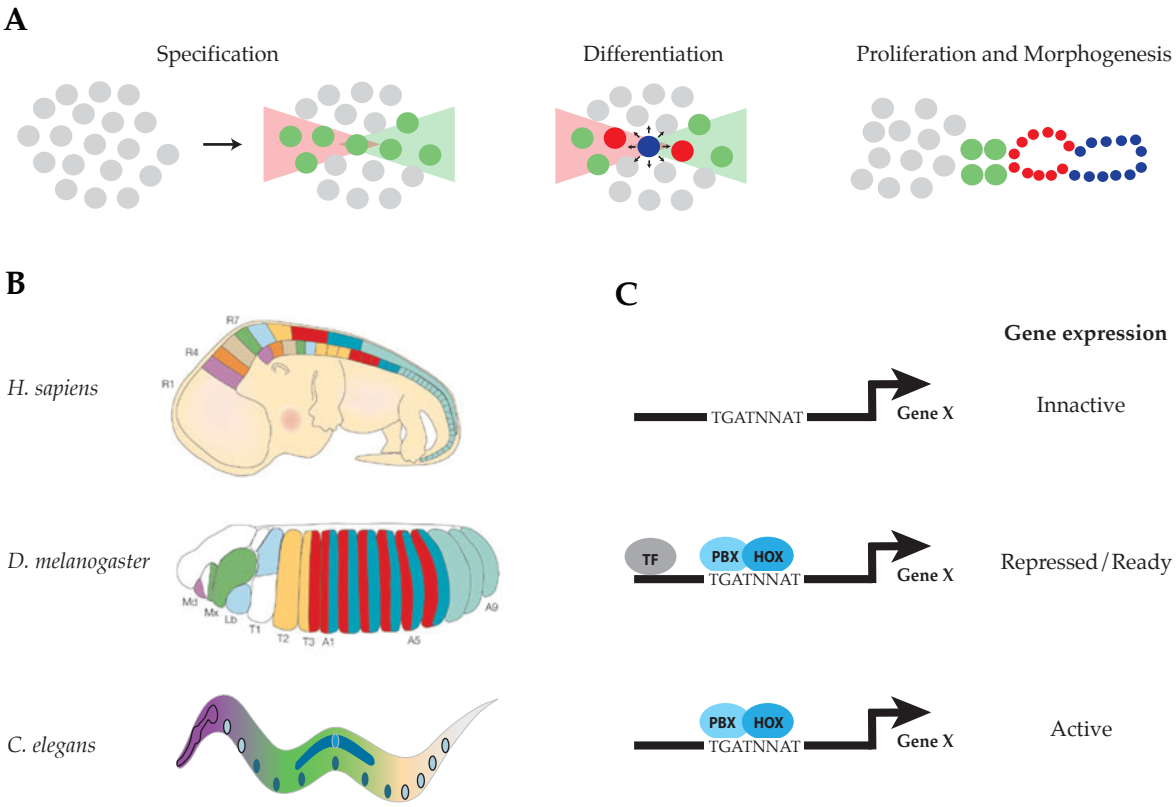

Figure 1.1: Steps of the organogenesis and role of *hox* genes in bilateria.
(A) Representation of the different steps of the organogenesis. **(B)** The *hox* genes and their spatial distribution along the Anterior-Posterior axis are conserved through evolution. Modified from (Pearson et al., 2005) **(C)** The combination of *hox* genes, their co-factors (PBX) and other transcription factors results in the modulation of the expression of different genes within the genome.

1.1.1 The role of HOX proteins in organogenesis

Up to date, more than 20 homeobox gene families have been described (e.g. HOX, *Dlx*, *PBC)* and most have been shown to affect animal development and organogenesis (Mann and Affolter, 1998). One of the most intensively studied families within the homeobox superfamily is the *hox* gene family.

The *hox* genes play fundamental roles in controlling the development and final morphology of bilaterian animals (Krumlauf, 1994; Pearson et al., 2005). Alterations in their activities often result in segmental transformation characterised by the appearance of organs in certain parts of the animal that normally should develop somewhere else (Rezsohazy et al., 2015). HOX proteins contain two distinctive and highly conserved domains: the hexapeptide motif and the homeodomain. The hexapeptide domain mediates contact with members of the PBX

class of proteins, a homology and functional group belonging to the homeobox gene superfamily and highly associated with *hox* function (for review: Moens and Selleri, 2006). The homeodomain is a widely use DNA segment of 180 base pairs encoding a helix-turn-helix type of DNA-binding protein motif of 60 amino acids. It was first described in *Drosophila* (Lufkin, 2005).

The *hox* genes are expressed in distinct domains along the anterior – posterior (A-P) axis of bilaterian animals, assigning different regional fates to these axial domains (Lemons and McGinnis, 2006) **(Fig. 1.1B)**. In addition, they are clustered in genomic regions so-called "*hox* clusters" and present collinear spatial expression **(Fig. 1.1B).** Thus, the order in the cluster mimics the expression order and their function along the A-P axis (de Rosa et al., 1999; Garcia-Fernàndez, 2005). In addition to the spatial collinearity, some *hox* clusters, mainly in vertebrates, show temporal collinearity (Duboule, 1994).

Although the origin of *hox* genes cannot be reconstructed, is widely accepted that the last common ancestor of protostomes and deuterostomes had a single *hox* cluster. During the Cambrian explosion, the cluster then expanded to include new members in several lineages (de Rosa et al., 1999; Powers and Amemiya, 2004), up to the 13 *hox* genes found in each vertebrate cluster, as well as duplicated resulting in the actual number of clusters in vertebrates. For example, 4 clusters with 39 *hox* genes in mammals and up to 14 clusters in fishes (Garcia-Fernàndez, 2005). Importantly, this expansion couple to variation in the expression pattern and protein activity has played a major role in the evolution and diversity of the animal body plan (Gellon and McGinnis, 1998).

Based on the scientific work of the last 30 years, recent reviews have compiled the functional diversity of the *hox* genes, which goes from controlling changes in cell shape and migration to differentiation (Cerdá-Esteban and Spagnoli, 2014; Taniguchi, 2014).

During this time a number of *hox* members have been described to regulate cell specification, differentiation, proliferation, migration or death, and many molecular functions have been attributed to them. This variety of molecular functions include non-transcriptional roles such replication and translation (Rezsohazy, 2014), and transcriptional regulation as transcription factors. It is thought that the *hox* genes function mainly relies on the selective activation or repression of downstream genes networks. However the molecular mechanisms underlying transcriptional regulation by HOX proteins are still poorly understood and only few HOX regulatory networks are well characterised.

hox genes relevance in animal development and morphogenesis starts as early as in the gastrulation, where *hox* genes are expressed in cells of the epiblast before their ingression. It has been suggested that this expression controls the migratory properties of cells and the timing of the process (Iimura and Pourquié, 2006). Subsequently, *hox* genes contribute in migration and in the establishment of cellular networks and circuits (Gavalas et. al., 1997).

For example, in *C. elegans*, the *hox* genes *lin-39* and *mab-5* control neuroblast cell migration (Whangbo and Kenyon, 1999). Furthermore, HOX genes control the collective cell migration of the mechanoreceptive lateral line in zebrafish (Breau et al., 2013). In all these cases, HOX proteins control receptor/ligand expression to modulate the interactions between the migrating cells and the environment. However, the previously mentioned is not the only way to control migration and tissue remodelling. For example, the HOXB1B protein of zebrafish has been shown to regulate microtubule dynamics during neural tube formation (Zigman et al., 2014), and the HOX LIN-39, through the transcription of *vab-23* (Pellegrino et al., 2011), controls vulval toroid formation during vulval development.

Other HOX proteins couple differentiation with morphogenesis, controlling cell fate decisions. For example, the HOXA5 determines epithelia from stromal cells in the lungs, gut and mammary glands of mice (Aubin et al., 2002; Boucherat et al., 2012; Garin et al., 2006). Again in this case, LIN-39, in *C. elegans,* plays a key role in the cell fate acquisition and morphogenesis of the vulval cells (Maloof and Kenyon, 1998).

The modulation of cell proliferation and cell cycle progression is another example of *hox* gene function. Thus, Antennapedia controls cell cycle exit in *Drosophila* neuroblasts (Baumgardt et al., 2014); HOXB8A controls cell proliferation of the lateral line primordium (Breau et al., 2013); HOXA9 directly regulates cell cycle in mouse (Collins et al., 2014); HOXB4 promotes cell cycle progression (Schiedlmeier et al., 2007) leading to the proliferation of the tissue; and HOXA10 promotes the expression of p21, a cell cycle inhibitor, to repress the cell cycle leading to differentiation (Bromleigh and Freedman, 2000).

Something that can be extracted from the functional diversity of the *hox* genes, taking in account the high degree of homology among them, is the importance of the cell context in conditioning the outcome. For example: HOXA9 is a severe oncogene, promoting leukaemia, in the hematopoietic lineage while a tumour suppressor in mammary glands (Gilbert et al., 2010; Sun et al., 2013); and HOXB13 inhibits growth in androgen-responsive prostate cancer (Hamid et al., 2014) while promotes cell cycle progression in androgen-refractory prostate tumours (Kim et al., 2010). In addition to the cell context, post-translational modifications can modulate HOX activity. Thus, the HOXA10 can act both as an activator and a repressor depending on its phosphorylation status (Bei et al., 2007).

HOX co-factors play an important role in the specificity of the functional diversity shown by the *hox* genes. The PBX family, previously described to interact with the HOX proteins through the Hexapeptide domain, are the most common HOX co-factors. The PBX proteins comprise also a conserved homeodomain and it is thought that in many cases the combination of both, the homeodomain from the HOX and the PBX, leads to the functional specificity (Phelan et al., 1995).

The consensus HOX-PBX DNA binding sequence is 5'-TGATNNATNN-3' (Mann and Affolter, 1998). The first four nucleotides bind the PBX protein and the reminding six are used for the HOX binding. This sequence is longer and different to the one recognised by the HOX monomers indicating that the interaction with the PBX modifies the HOX DNA binding properties (Rezsohazy et al., 2015).
Nowadays binding events are seen as probabilistic rather than as qualitative on/off events, this view indicates that there are not clear limits between relevant and non-relevant bindings (Biggin, 2011). In addition, evaluation of *Drosophila* Ubx and Dfd binding patterns revealed very little overlap despite sharing identical DNA binding sequences (Sorge et al., 2012). Moreover, other protein classes, such the *Meis* family or Chromatin remodelling factors, influence the activity of the HOX-PBX complex (Kroeger et al., 2008). All these facts indicate that the *in vivo* binding of HOX proteins is regulated beyond the intrinsic DNA binding potential.

1.1.2 Other transcription factors implicated in organogenesis: the ETS and Forkhead families

At the transcriptional level, organogenesis is a complex process that not only includes the homeobox superfamily genes. A great range of transcription factor families such the ETS-domain family and the Forkhead family play important roles, often in combination with members of the homeobox superfamily **(Fig. 1.1C)**.
The ETS-family is present in a broad range of species that goes from worms, where they have been described to play a role in the development of the vulva of the animal (Beitel et al., 1995), to humans, where they control diverse processes such angiogenesis (vessel formation) (Lelièvre et al., 2001) or corneal development (Yoshida et al., 2000). It includes more than 50 members characterised by a conserved DNA binding domain.
The ETS domain is an 85 amino acids variant of the winged helix – turn – helix motif located, in general, at the C-terminus of the proteins. It presents a high degree of structural conservation among the family members (Liang et al., 1994) and typically binds to the core DNA sequence GGAA/T in a very specific manner (Macleod et al., 1992; Sharrocks, 2001). The sequences flanking this core are variable and tend to regulate specificity (Lelièvre et al., 2001). In general, in most of the ETS family members, the N-terminus region regulates the DNA binding ability of the protein. Thus, in the absence of DNA, the ETS proteins fold to protect the DNA binding domain (Petersen et al., 1995). This auto-inhibitory function is reinforced, in many cases, through the phosphorylation of serine residues (Goetz et al., 2000). Another highly conserved domain is the *pointed* domain. This domain contains a threonine

residue that is targeted by RAS/MAPK signaling in *Drosophila* (Baker et al., 2001) and *C. elegans* (Beitel et al., 1995).

The activities of the ETS family members are controlled by their interaction with other transcription factors. It has been shown that in vertebrates, the ETS family members associate with AP1 to activate transcriptional programs. For example, in human T cells, the physical association between Ets-1 and AP-1 proteins is required for the normal transcriptional activity of the cells (Bassuk et al., 1995). Other factors shown to cooperate with the ETS family are CREB Binding Proteins and p300. Both are needed for the transcriptional activation of the human stromelysin1 and recruited to the promoter by Ets1 (Jayaraman et al., 1999). Finally another family of factors that is commonly linked to the ETS function is the Forkhead family. For example, the joint venture of the Forkhead FoxC2 and the ETS Etv2 is needed for vascular formation in Xenopus (De Val et al., 2008).

The Forkhead family of transcription factors is not among the largest transcription factor families, but display a great functional diversity. They are involved in a wide variety of morphogenetic processes, which suggests that the increasing complexity in body plan may have been the driving force behind the expansion of the Forkhead family (Carlsson and Mahlapuu, 2002). The name derives from the two spiked-head structures in the *Drosophila fork head* mutant embryos. The Forkhead family, in contrast to the ETS-domain family, shows high conservation in the 110 amino acids sequence as well as in the characteristic *winged-helix* tri-dimensional structure within the Forkhead domain (Weigel et al., 1989). On the other hand, and as opposed to other transcription factors described above, their consensus binding sequence is less stringent, being the core sequence: A/G-C/T-A/C-AA-C/T-A (Kaufmann et al., 1995; Overdier et al., 1994). For this reason, the structural basis for the differences in sequence specificity among the Forkhead family members remains elusive (Carlsson and Mahlapuu, 2002). Moreover, beside the high degree of homology within the DNA binding domain, there is an almost complete lack of similarity between the other domains of the proteins. These domains, which are thought to play a role in the activation or repression, are in many cases not well characterized. For this reason, very little is known about the mechanisms through which this protein family interacts with the transcriptional machinery.

Forkhead proteins have been shown to act mostly as transcriptional activators but not exclusively. For example, the *C. elegans* Forkhead *lin-31* is thought to act as either repressor or activator depending on its phosphorylation status (Tan et al., 1998). The Mammalian FoxG1 represses transcription by associating to other transcriptional co-repressors (Yao et al., 2001). In addition, in many cases, they are downstream transcriptional regulators of signal transduction pathways such the TGFß-Smad pathway, the Insulin pathway, the Hedgehog signaling pathway and the EGF/RAS/MAPK signaling cascade (Miller et al., 1993) among others (for a review: (Carlsson and Mahlapuu, 2002)).

Furthermore, Some Forkhead family members seem to play a role in cell cycle regulation. Thus, in mammals, the expression of *FoxM1* is confined to cycling cells and it is regulated in a cell cycle dependent manner (Korver et al., 1997), while FoxO4 blocks the cell cycle progression in G1 by activating the expression of p27 (Medema et al., 2000). Interestingly, the Forkhead protein LIN-31, in *C. elegans,* also promotes the expression of *cki-1,* the homologue of p27 (Clayton et al., 2008).
In summary, it should be notice that there is not an easy answer to the question what these transcription factors do. Yet, *C. elegans* is a great model organism to further understand their function.

1.2 The cell cycle and its regulation in organogenesis

Animal development requires cell division and proliferation. This is achieved through a process called *cell cycle*. The cell cycle can be divided in four main phases: the G1 –Gap 1 phase– characterized by the normal physiological functioning of the cell; the S phase –Synthesis phase– during which the DNA duplicates; the G2 phase –Gap 2 phase– where the cells sense diverse internal and external factors after duplicating the DNA, and finally the M phase –Mitosis– where two daughter cells are generated. In certain conditions or highly differentiated cell lineages, cells can go into the so-called G0 phase where the cell cycle is inactive (Vermeulen and Van Bockstaele, 2003).
Whether the cell enters into cell division or not, is in general decided based on internal and external factors. The external signals are only relevant until the cell is committed to go through the cell cycle at a time in G1 known as *Restriction point*. Interestingly, the cell cycle functions as a regulatory circuit that is established by positive or negative linear interactions among its components **(Fig. 1.1A)**. Some of those steps are known as *checkpoints* and function as quality control systems (Elledge, 1996). At those points the cell verifies the previous steps and decides whether to continue the process or stop it.
The core lineal regulatory circuit of the cell cycle is made of Cyclin-dependent kinases (CDK) and their corresponding Cyclin. These CDK-Cyclin complexes lead to the transition through the different phases of the cell cycle (Graña and Reddy, 1995; Koreth and van den Heuvel, 2005) **(Fig. 1.2A)**. The CDKs are small serine/threonine protein kinases that require a Cyclin for their activation and substrate specificity (Hochegger et al., 2008; Miller and Cross, 2001).

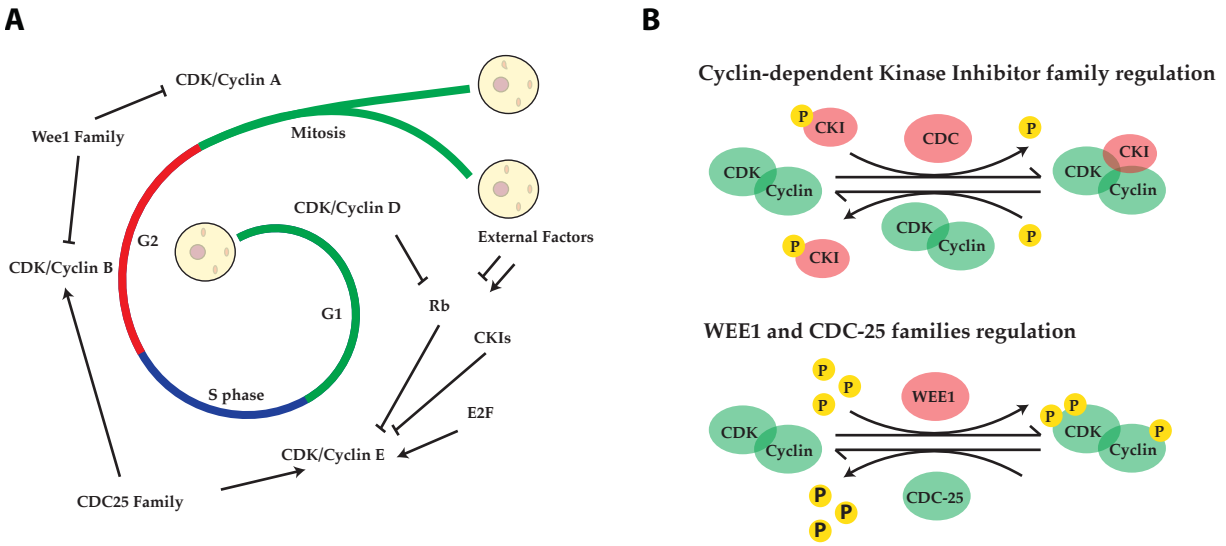

Figure 1.2: Cell cycle core machinery and its regulation

(A) Cell cycle regulation. The CDK/Cyclin *D* promotes the progression through the cell cycle by repression of Rb, this allows the transcription of *Cyclin E* and promotes the transition to the S phase. In addition to Rb, other proteins and transcriptional regulators as well as external factors influence the transition to the next step of the cell cycle. Upon this point, lineal interactions among the different CDK/Cyclin complexes control the progression through the cell cycle. **(B)** Among the most common regulators of the cell cycle are: the CKI family members, which bind and inhibit the CDK/Cyclin complexes when CKI is not phosphorylated, and the WEE1 kinase and CDC-25 phosphatase families that control the activity of the CDK/Cyclin complexes through phosphorylation.

A tight regulation ensures that the CDKs are constantly functioning with the correct Cyclin. This regulation focuses in both, the transcriptional and the protein level (Vermeulen and Van Bockstaele, 2003). Thus, the expression of the Cyclin E and A are tightly regulated by The Retinoblastoma (RB) family members (Du and Pogoriler, 2006) and their associated transcription factors from the E2F family (Attwooll et al., 2004). In addition, all of them contain either destruction boxes, in the case of the Cyclin A and D, or PEST domains, for Cyclin D and E. Both domains, the destruction box and the PEST domain, contribute to their degradation through ubiquitin-mediated proteolysis (Hershko, 1997) once the cell cycle moves on to the next phase (Glotzer et al., 1991; Rechsteiner and Rogers, 1996).

The Cyclin-dependent Kinase Inhibitor family plays an important role in the cell cycle regulation. They are a highly divergent group of small proteins that physically interact with the CDK-Cyclin complex inhibiting their function (Sherr and Roberts, 1999). While their main function is to inhibit the cell cycle progression at the G1/S phase transition, through direct binding to the CDK-Cyclin complexes, it has been shown that they can act as CDK/Cyclin assembly factors (LaBaer et al., 1997). Perhaps the easiest explanation to this *functional* contradiction is that beyond the inhibition of the cell cycle progression in the G1/S

phase, the CKIs secure sufficient levels of the CDK-Cyclin complex before progression through the cell cycle.
Other important regulators of the cell cycle are the WEEI Kinase and the cdc25 phosphatase families. The first one inhibits CDK/Cyclin function through Cyclin phosphorylation (McGowan and Russell, 1993; McGowan and Russell, 1995); and the second one promotes cell cycle progression activating the CDK-Cyclin complexes (Nilsson and Hoffmann, 2000)**(Fig. 1.2B)**.
External factors that trigger the progression through the cell cycle in the G1 phase play a key role in organogenesis. For example: RAS signaling controls cell cycle directly through phosphorylation and hence inhibition of the Rb protein (Peeper et al., 1997); WNT signaling promotes the expression of Cyclin D, which is responsible for the activation of the cell cycle and G1 entry, and other cell cycle components (Tetsu and McCormick, 1999); And Notch signaling promotes the cell cycle in human T cells (Joshi et al., 2009) and represses it in hepatocitic and small lung cells (Qi et al., 2003; Sriuranpong et al., 2001). In addition, transcription factors like the HOX genes and the Forkhead families (see above) have been linked to the regulation of the cell cycle through the animal kingdom.
In summary, one could describe the cell cycle of a cell in the context of organogenesis, as a linear process triggered by certain external factors. Those factors can activate/inhibit certain pathways that will have a direct effect in the cell cycle machinery, leading to the activation or repression of the process. A proper reading of those external factors by the cell in question is necessary for the normal development of organs in the context of the organism.
Once again, *C. elegans* is a great model to understand how the cell cycle and the cell fate, or its transcriptional network, interact. Its simplicity, compared to other models organisms, and its conservation allow us to answer complex question in a very simple manner.

1.3 *Caenorhabditis elegans* as a model for organogenesis

Caenorhabditis elegans is a 1mm free-living nematode that lives in nutrient rich and temperate soils (Wood, 1988). Its name derives from the Latin *caeno* - recent – for newly discover, *rhabditis* - rod-like – for its shape and *elegans* – elegant – for its elegant sinusoidal movement.
Sydney Brenner first established the nematode *C. elegans* as model organism in the early 70s. In 1974, he published an article where he described various aspects of the *C. elegans* biology, development and behaviour (Brenner, 1974). Since then, *C. elegans* has experimented a tremendous growth as model organism holding several Nobel prizes. Several features such the short generation time, the small size, the capability to keep the animals frozen

indefinitely, its transparency, its invariant cell lineage and most importantly their capacity to fertilize their own eggs while keeping inter-individual sexual reproduction, leading to clonal populations, has done of *C. elegans* a powerful genetic tool to study relevant developmental processes.

C. elegans generation time, from the fertilized egg to adulthood, is of 3.5 days at 20 degree Celsius. During this period the animals pass through an embryonic stage and four larval stages - L1 to L4 – before reaching adulthood. In addition to those four larval stages, the animals can go into the so-called *dauer* larval stage (Cassada and Russell, 1975). This stage is a "stress resistance" phase where the worm can live up to three months in extreme environmental conditions. (Golden and Riddle, 1984) **(Fig. 1.3)**.

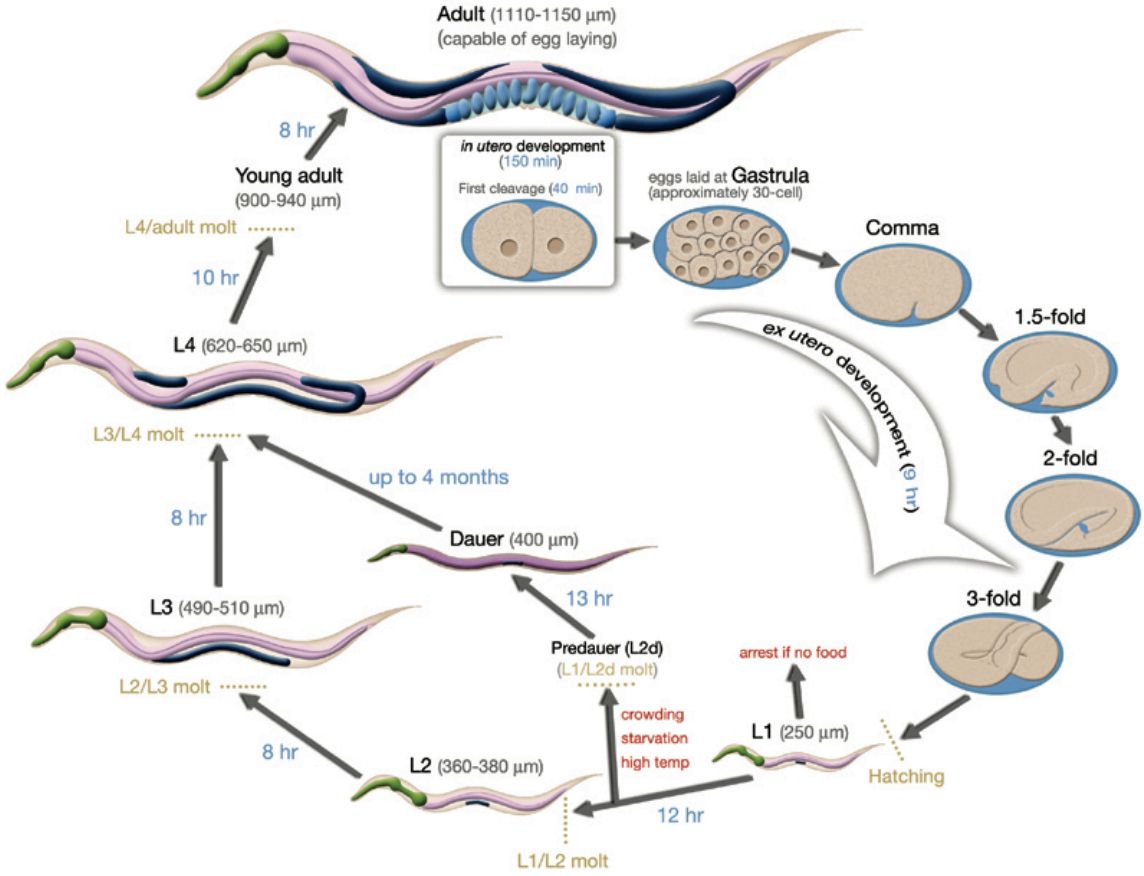

Fig. 1.3: Life cycle of *C. elegans*

Fertilized embryos start to develop inside the uterus and continue to grow outside the animal till they hatch outside the eggshell. The L1 larvae continue to develop through four molting larval stages and reach adulthood. In addition, in case of extreme conditions the larvae can adopt a fifth resistance larval stage, called the Dauer.

As previously mentioned, an extremely powerful characteristic of the worm is its hermaphroditism. Thus, the predominant sexual form is the hermaphrodite, which produces both eggs and sperm having the ability of self-fertilization. This, leads to genetically

homogeneous populations from a single individual. In addition, *C. elegans* has males in a proportion of 1 to 100. The present of males in the population allows the exchange of genetic material and variability within the population. This feature allows the study of genetic interactions among different genes in the laboratory (Brenner, 1974).
The genome of *C. elegans* encodes around 20000 genes packed in five pairs of autosomes and a pair of sexual chromosomes. Males lack one of the sexual chromosomes and therefore are generated spontaneously. It was the first animal genome to be completely sequenced (*C. elegans* Sequencing Consortium, 1998). From the nearly 20000 genes of the *C. elegans* genome, around 35% present direct human homologues and many others have functional analogy.

1.3.1 The Vulva of *C. elegans*

The egg-laying organ of the *C. elegans* hermaphrodite, known as "vulva" is located in the ventral side of the mid section of the body. A total of 22 cells form the adult vulva, which functions as the connection between the uterus of the animal and the environment.
In addition to laying eggs, the vulva is used during the mating process between hermaphrodite and male animals. Thus, a specialized structure of the male tail is able to penetrate the vulva and to release the sperm into the hermaphrodite.
The vulval development occurs through the four larval stages of the animal. The specification of the Vulval Precursor Cells (VPCs) takes place at the end of the first larval stage **(Fig. 1.4A)**. After specification, the VPCs keep their commitment until the end of the L2 stage, when they will adopt a specific differentiated fate **(Fig. 1.4B)**. Once they have adopted a differentiated cell fate, the vulval cells will proliferate in an invariant pattern and form a three-dimensional organ during the larval stages L3 and L4 **(Fig. 1.4C)**. Highly conserved signaling pathways such WNT, RAS or NOTCH signaling control this developmental process.
The vulval development allows us to study all the phases of the organogenesis using the 22 cells invariant pattern and the three-dimensional structure as tools to dissect the genetic interactions and functions of different genes, as well as to translate the knowledge to human organ development and diseases at the molecular level due to the high conservation of the pathways involved.

The Vulval Precursor Cells specification

During the L1 larval stage the Pn ventral neuro-ectoblasts (P1-P12) undergo an Anterior – Posterior round of division, leading to the anterior descendants (Pn.a) that will develop into ventral cord neurons, and their posterior sisters (Pn.p) that will adopt epithelial fate (Sulston

and Horvitz, 1977). Those Pn.p cells -P1.p to P12.p- will form an epithelial cell layer from head to tail.

In parallel, from the Posterior part of the animal, gradients of the WNT ligands *lin-44, egl-20* and *cwn-1* are formed (Gleason et al., 2006; Pan et al., 2006; Whangbo and Kenyon, 2010). These gradients lead to the activation of the *hox* genes cluster along the Anterior – Posterior axis of the animal (Austin et al., 1993; Maloof et al., 1999) **(Fig. 1.4A)**.

The activation of these *hox* genes in the Pn.p cells subdivides them in different competence groups that will adopt different cell fates (Maloof et al., 1999). Thus, the P1.p - P3.p group will express the HOX gene *ceh-13* that promotes the fusion with the hypodermis (Penigault and Felix, 2011), the P3.p – P8.p will express *lin-39* defining the VPCs competence group in the ventral middle part of the body and keeping their epithelial fate (Clandinin et al., 1997; Clark et al., 1993), the P7.p – P11.p group will express *mab-5* promoting as well the fusion to the hypodermis in hermaphrodite animals (Kenyon, 1986), and finally *elg-5* that will lead P12.p to differentiate into tail structures (Chrisholm, 1991).

Interestingly, in *C. elegans* these competence groups overlap with each other, leading to different sensitivity towards the WNT signaling within the same competence group. This fact explains why P3.p fuses in 50% of the cases; most probably due to the adoption of either *ceh-13* (fused) or *lin-39* (epithelial) fate (Penigault and Felix, 2011). In addition, *lin-39* seems to be epistatic to *mab-5* in hermaphrodite animals, explaining why P7.p and P8.p retain their epithelial fate in 100% of the cases (Chng and Kenyon, 1999).

At the end of the L1 stage only the middle body Pn.p cells (P3.p – P8.p) retain their epithelial fate. To keep the epithelial fate throughout the L2 larval stage, the LIN-39 protein, most probably through the expression of the transcription factors *egl-18* and *elt-6* (Koh et al., 2002), inhibits the expression of the fusion gene *eff-1* (Shemer and Podbilewicz, 2002). In addition, LIN-39 promotes the expression of epithelial receptors such the Notch receptor *lin-12* and possibly at least one of its ligands, *lag-2* (Takacs-Vellaia et al., 2007) **(Fig. 1.4A&B)**.

Other factors such *lin-1,* an ETS–like transcription factor, and *lin-31*, the *C. elegans* homologue of *forkhead*, play an important role in the maintenance of the VPCs quiescent stage throughout the L2 larval stage. Thus, the LIN-1/LIN-31 complex keeps the expression of *lin-39* in basal levels allowing the VPCs to escape fusion but not to differentiate into a vulval fate (Wagmaister et al., 2006b). In addition, the LIN-1/LIN-31 complex inhibits the expression of other *lin-39* putative targets like the Notch signaling ligand *lag-2* (Takacs-Vellaia et al., 2007; Zhang and Greenwald, 2011) **(Fig. 1.4A&B)**.

Induction of the vulval precursor cells

During the transition from the L2 to the L3 larval stage, a somatic gonadal cell, called the anchor cell (AC), located above P6.p, plays an important role in the re-activation of the VPCs

and their differentiation after induction. This allows the system to couple the development of the gonad/uterus with the vulva and it is a great example of inter-organ cross talk during development.

The AC releases LIN-3, the *C. elegans* homologous of the mammals epidermal growth factor (Sternberg, 1992). The stimulation of the VPCs with the LIN-3 gradient leads to the activation of the RAS signaling pathway. The activation of the pathway correlates with the positioning of the VPCs. Thus P6.p, the closest VPC to the AC, presents the strongest RAS signaling activation **(Fig. 1.4B)**.

The activation of the RAS signaling cascade leads to the phosphorylation and therefore disruption of the LIN-1/LIN-31 complex (Tan et al., 1998) releasing their repression over the promoter of *lin-39* (Wagmaister et al., 2006b; Wagmaister et al., 2006a) among other factors. Up-regulation of *lin-39* expression in P6.p leads to the adoption of the primary cell fate (1°) and the up-regulation of downstream genes like *lag-2* (Chen and Greenwald, 2004). As a direct consequence, P5.p and P7.p, the neighbouring cells, activate the NOTCH pathway. NOTCH activation inhibits RAS signaling in those two cells (Berset et al., 2001; Sternberg, 1988) and promotes the so-called secondary cell fate (2°). The other VPCs (P3.p, P4.p and P8.p) receive less LIN-3 stimulation and no lateral signaling, and therefore acquire the tertiary (3°) cell fate that results in the fusion to the hypodermis after the first round of division **(Fig. 1.4B)**.

Proliferation and morphogenesis of the vulval cells

Once the central cells of the VPC competence group (P5.p – P7.p) have acquired their differentiated vulval fate, the cell cycle progresses. The same pathways responsible for the fate acquisition and the *hox* gene *lin-39* seem to play important roles in the cell cycle activation of the vulval cells (Shemer and Podbilewicz, 2002). However their exact roles are not well understood. During the proliferation period the three vulval cells will complete three rounds of division, resulting in the 22 cells of the adult *C. elegans* vulva. P6.p gives rise to 8 descendants and the P5.p and p7.p to 7 descendants each **(Fig. 1.4C)**.

In parallel to the proliferation of the vulval cells, the AC invades the vulval epithelium (Sherwood, 2005) and the 1° lineage detaches from the cuticle, moving dorsally in a process transcriptionally controlled by the LIN-39 target gene *vab-23* (Pellegrino et al., 2011), to form an invagination. This invagination continues growing thanks to the push of the 2° lineage, which migrates towards the center of the invagination in a process transcriptionally controlled by the ETS LIN-1 (Farooqui et al., 2012) **(Fig. 1.4C)**. Finally, the so-called Christmas tree structure is formed as a result of the morphogenesis at the end of the L4 larval stage. The process finishes with the eversion of the Christmas tree after the vulval invagination and the uterus have connected.

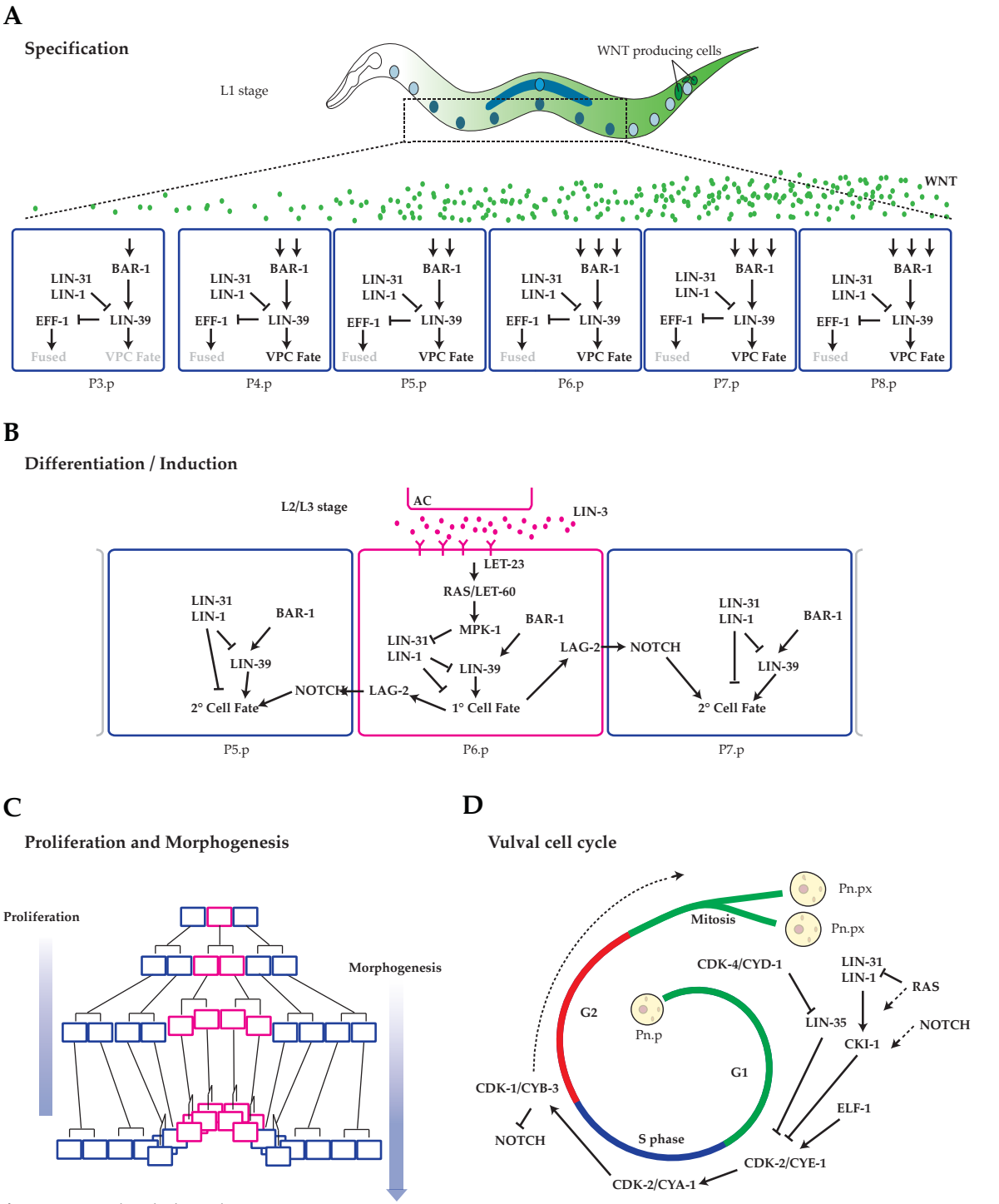

Fig. 1.4: Vulval development

(A) During the first larval stage (L1), the generation of an Anterior-Posterior gradient of WNT-ligands in the animal leads to the acquisition of the vulval precursor cell fate (VPCs). **(B)** The VPCs remain quiescent until late L2 when the Anchor Cell (AC) starts to release LIN-3. This will lead to the activation of RAS signaling in the closest VPC (P6.p) adopting the primary cell fate (1°). The activation of RAS results in the expression of the Notch ligand and the activation of Notch signaling in the neighbouring cells (P5.p & P7.p) adopting the secondary cell fate (2°). **(C)** Three rounds of division, coupled with morphogenesis of the tissue take place during L3 and L4 larval stages to form a vulva. **(D)** The cell cycle of the vulva.

The Cell Cycle in *C. elegans* vulval development

The mitotic cell cycle in *C. elegans* vulval development comprises the four known phases. At least three different parallel mechanisms repress the progression through the cell cycle during the long G1 phase that goes from the specification of the VPCs at the end of the L1 larval stage to the induction at the beginning of the L3 larval stage. First, the LIN-1/LIN-31 complex promotes the expression of the Cyclin dependent Kinase Inhibitor *cki-1* arresting the cell cycle in this phase (Clayton et al., 2008). Secondly, the heterochronic genes *lin-28* (Moss et al., 1997) and *lin-14* (Ruvkun et al., 1989) actively prolong this phase until the beginning of the L3 larval stage to achieve a total synchronization of the vulval development with the gonad/uterus development. Finally, LIN-35 –the *C. elegans* orthologous of Rb- inhibits the expression of *cye-1*.

After the heterochronic genes *lin-28* and *lin-14* levels decrease in the early L3 stage, and the AC has triggered the induction of the VPCs, the cell cycle proceeds into the S phase. This switch is the consequence of: the disruption in the primaries and modification in the secondaries of the LIN-1/LIN-31 complex after the vulval induction, leading to a reduction in the levels of *cki-1,* and the continuous inhibition of LIN-35 from the CDK-4/CYD-1 complex –the G1 CDK/Cyclin complex- (Boxem and van den Heuvel, 2001). The inhibition of LIN-35 allows *efl-11,* a E2F like protein, to promote the expression of *cye-1*, the *C. elegans* Cyclin E (Brodigan et al., 2003), and the progression into the S phase. Once the DNA has been duplicated, the CDK-2/CYA-1 complex guides the vulval cells throughout the G2 phase. Interestingly the transition between G2 and M phase, governed by the CDK-1/CYB-1/-2/-3 complexes, is necessary for the down-regulation of the NOTCH signaling in the 1° lineage. The CDK-1/CYB-3 complex phosphorylates the Intracellular Notch Cleavage Domain (NICD) leading to its degradation (Nusser-Stein et al., 2012) **(Fig. 1.4D)**.

1.3.2 The HOX gene *lin-39* as vulval development coordinator

The *C. elegans hox* gene *lin-39* (for HOX genes see above) plays a pivotal role in the development of the mid-body region and controls several aspects of vulval development (Clandinin et al., 1997; Clark et al., 1993; Maloof and Kenyon, 1998; Wang and Sternberg, 2000). Interestingly, beside that most *hox* genes are expressed following the order within the cluster, *lin-39* is expressed in the mid body when it is actually the first *hox* gene of the loosely organized *C. elegans hox* cluster (Aboobaker and Blaxter, 2003).

lin-39 expression is complexly regulated during vulval development by different pathways. At least the RAS, WNT, and Rb-related pathways coordinately regulate *lin-39* in the VPCs (Chen and Han, 2001; Eisenmann et al., 1998; Guerry et al., 2007). Even *lin-39* itself is

required to up-regulate *lin-39* expression in response to RAS signaling (Maloof and Kenyon, 1998; Wagmaister et al., 2006b)

As soon as the Pn.p cells are born in the early L1 larval stage, *lin-39* transcription is activated in response to WNT signaling (Eisenmann et al., 1998). At this point and together with the PBX protein CEH-20, LIN-39 is required to prevent the VPCs from fusing with the hypodermis by inhibiting the expression of the fusion gene *eff-1* (Shemer and Podbilewicz, 2002). It is not yet clear whether the control of *eff-1* expression is via a direct binding of LIN-39 in the promoter of *eff-1*, LIN-39 presents two weak binding peaks (Niu et al., 2011), or it is due to the regulation of *eff-1* expression through downstream targets such the transcription factors *egl-18 and elt-6* (Koh et al., 2002),or *vab-23* (Pellegrino et al., 2011). In addition, during this stage, LIN-39 promotes the expression of the NOTCH receptor *lin-12* (Takács-Vellai et al., 2007) and its ligand *lag-2* (Chen and Greenwald, 2004) in the VPCs.

During the first and second larval stage, the expression of *lin-39* is maintained in basal levels by the combined action of the WNT signaling and the repression of the Rb-related pathway and the LIN-1/LIN-31 complex (Wagmaister et al., 2006a). Once these inhibitory signals disappear after induction, the RAS signaling cascade promotes maximum expression level of *lin-39* in P6.p (Wagmaister et al., 2006b). Although the regulatory networks downstream of LIN-39 after induction are not well understood, it is clear that this switch, from basal to high expression levels, functions as a trigger for the next steps in vulval development. This switch leads to an increase of *lag-2* expression in P6.p resulting in the previously described activation of the 2° cell fate in the neighbouring cells.

In contrast with the well-understood control of expression of *lin-39* and a good understanding of how *lin-39* determinates cell fate, nothing is known about the implication of *lin-39* in the cell cycle of the VPCs and how it promotes proliferation. The only insight about a role of *lin-39* in the cell cycle is the observation that in the absence of the fusion gene *eff-1* in *lin-39* mutant animals, the VPCs do not fuse nor divide but adopt, at least in some cases, a "vulval like" fate (Shemer and Podbilewicz, 2002).

Finally, *lin-39* controls the 1° lineage morphogenesis through the expression of the transcription factor *vab-23*. Thus, LIN-39 binds to the promoter of *vab-23* activating its expression. VAB-23 will then remodel the transcriptional program needed for successful 1° lineage morphogenesis completion (Pellegrino et al., 2011).

In addition, of its role in vulval development, *lin-39* defines the fate of the VC neurons (Salser et al., 1993), and together with the other *hox* gene *mab-5,* controls the migration of the Q cell descendants. Thus, once the Q cell descendants are born the Q_R neuroblast expresses *lin-39* and migrates towards the anterior side of the animal, while the Q_L neuroblast expresses *mab-5* and therefore migrates towards the opposite direction (Maloof et al., 1999).

Moreover, *lin-39* expression can be observed in several ventral hypodermal cells in the embryo but its function at this stage is poorly understood.
As other *hox* genes described above, *lin-39* works together with two co-factors (Yang et al., 2005), the PBX gene *ceh-20* (Liu and Fire, 2000) and the *Meis* homologue *unc-62* (Van Auken et al., 2002). Interestingly, both overlap in time during vulval development and Q neuroblast migration but they seem to have slightly different roles. This suggests that in a given time point, in a VPC there are at least two pools of LIN-39 complexes with different functions.

2

Aim of this thesis

The HOX genes family is an important evolutionary conserved class of transcriptional regulators that control development of the animal body plan. Therefore the lack or reduction of their function can lead to severe diseases like cancer and syndromes such the synpolydactyly type II in humans (Lufkin, 2005).
However, we lack a complete picture of their role during the different phases of organogenesis and the mechanism of how *hox* genes link the different processes taking place during animal's development is still unknown.
Highly conserved pathways such RAS, WNT and Notch Signaling converge in a single *hox* gene, *lin-39,* to produce a completely functional organ, the vulva of *C. elegans.* This combination of simplicity and conservation makes of this system a great tool to study how *hox* genes coordinate the different phases during development.

Much is known about the role of *lin-39* in the acquisition of competence and fate during the development of the vulva of *C. elegans.* However, is still poorly understood if *lin-39* coordinates competence and fate acquisition with the cell proliferation and how is this achieved. Thus, the specific aim of this thesis was to elucidate the role of *lin-39* in the activation of the cell cycle of the vulval primordium.

3

Thesis projects

3.1 The *C. elegans hox* gene *lin-39* coordinates cell fate specification and cell cycle progression

Daniel Roiz[1,2], Juan Miguel Escobar-Restrepo[1], Philipp Leu[1,3], Alex Hajnal[1,*]

[1]Institute of Molecular Life Sciences, University of Zurich, Winterthurerstrasse 190, Zurich CH-8057, Switzerland.

[2]Molecular Life Science PhD Program – Life Science Zurich Graduate School

[3]Currently at Institute of Biochemistry, ETH Zurich, Otto-stern-weg 3

*Corresponding author: alex.hajnal@imls.uzh.ch

Key words: *C. elegans*, *hox* gene, NOTCH, organogenesis, cell cycle, Cyclin, Cdk kinase, proliferation.

3.1.1 Abstract

Cell fate specification during organogenesis is usually followed by cell proliferation to produce the appropriate number of differentiated cells. The *C. elegans* vulva is an excellent model to study how cell fate specification and cell proliferation are coordinated. The six vulval precursor cells (VPCs) are born at the first larval stage, but remain arrested in the G1 phase of the cell cycle until the beginning of the third larval stage when their fates are specified and the three proximal VPCs proliferate to generate 22 vulval cells. An epidermal growth factor (EGF) signal from the gonadal anchor cell combined with lateral DELTA/NOTCH signaling between the VPCs determine the primary (1°) and secondary (2°) fates, respectively. The *hox* gene *lin-39* plays a central role in integrating these spatial patterning signals and maintaining the VPCs as polarized epithelial cells. Using a fusion-defective *eff-1(lf)* mutation to keep the VPCs polarized, we find that VPCs lacking *lin-39* remain responsive to the inductive EGF signal, but can neither activate lateral NOTCH signaling nor proliferate. LIN-39 directly promotes G1/S-phase progression by inducing *cye-1 cyclinE* and *cdk-4* expression through a non-canonical HOX binding motif. The activation of NOTCH signaling or loss of the LIN-31 Forkhead transcription factor re-activates *cye-1* and *cdk-4* expression and restores VPC proliferation in the absence of LIN-39. The *hox* gene *lin-39* is therefore a central node in a regulatory network coordinating VPC differentiation and proliferation.

3.1.2 Introduction

During organogenesis, two-dimensional sheets of epithelial cells are remodeled into three-dimensional organs (Trinkaus 1969). This process is guided by soluble and membrane-associated ligand-receptor interactions that activate intracellular signaling pathways, which in turn control nuclear determinants such as HOX, *ETS, ZnF, bHLH* and *Forkhead* transcription factors. Organogenesis can be divided into four conceptual steps that are compartmentalized in time: (1) specification of the precursor cells that are competent to differentiate, (2) induction of distinct cell fates among the precursor cells, (3) proliferation of the precursor cells to generate the required number of cells of the different types and (4) terminal differentiation and spatial rearrangement of post-mitotic cells during the morphogenesis phase (Ackermann and Paw, 2003). Currently, we lack a clear understanding of the mechanisms and specific factors that coordinate these different aspects of organogenesis.

The *hox* genes encode homeobox domain-containing transcription factors that play diverse

roles during organogenesis (reviewed by (Rezsohazy et al., 2015)). Originally discovered as key determinants of segment identity in the *Drosophila* embryo (Lewis, 1978), *hox* genes control a broad range of cellular functions including cell proliferation and tissue morphogenesis. De-regulated expression of *hox* genes has also been linked to the formation of acute myeloid (AML) and lymphoid leukemia (ALL) in humans (Celetti et al., 1993). HOX proteins form heterodimers with their PBX or MEIS family co-factors to activate their target genes that carry distinct DNA motifs in their enhancers (Rezsohazy et al., 2015). However, there exists no comprehensive picture of the direct target genes that mediate the different aspects of *hox* gene function.

The development of the *C. elegans* vulva, the egg-laying organ of the hermaphrodite, is an excellent model to investigate how cell fate specification, cell proliferation and organ morphogenesis are coordinated in time and space (Schindler and Sherwood, 2012; Schmid and Hajnal, 2015; Sternberg, 2005). Vulval fate specification involves the combined action of the conserved Wingless (WNT), EGFR/RAS/MAPK and DELTA/NOTCH signaling pathways. Towards the end of the first larval stage (L1), twelve epidermal Pn.p cells align along the ventral midline of the animal. A WNT signal from a group of tail cells induces six Pn.p cells in the mid-body region (P3.p through P8.p) to become vulval precursor cells (VPCs) (Eisenmann, 2005; Eisenmann et al., 1998). These six VPCs are competent to differentiate into one of two alternate vulval cell fates. However, P3.p is furthest away from the source of the WNT signal and adopts a VPC fate only in around 50% of the animals. WNT signaling induces the expression of the *hox* gene *lin-39* in the VPCs, which is necessary to maintain the VPCs as polarized epithelial cells and to prevent them from fusing to the surrounding syncytial epidermis (hyp7) by repressing the expression of the *eff-1* fusogen (Eisenmann et al., 1998; Gleason et al., 2006; Salser et al., 1993; Shemer and Podbilewicz, 2002) (**Fig. 3.1.1A)**. Thereafter, the VPCs remain quiescent during most of the L2 stage, until an inductive signal from the gonadal anchor cell (AC) selects the nearest VPC (P6.p) to adopt a 1° vulval fate. The AC secretes the LIN-3 growth factor, which is homologous to the mammalian epidermal growth factor (EGF), and activates the EGF receptor homolog LET-23 in the VPCs (**Fig. 3.1.1A**). Downstream of LET-23, the canonical RAS/MAPK pathway controls the activity of nuclear determinants that specify the 1° and 2° cell fates (**Fig. 3.1.1A**) (Sundaram, 2006). Activated MAPK phosphorylates the LIN-1 ETS and LIN-31 Forkhead transcription factors, which in their un-phosphorylated state inhibit vulval differentiation by repressing, among others, *lin-39* transcription (Guerry et al., 2007; Wagmaister et al., 2006b). Since, the 1° VPC P6.p receives most of the inductive LIN-3 signal, it exhibits the highest LIN-39 activity. LIN-39 also plays an essential role during and after vulval fate specification (Maloof and Kenyon, 1998). For example, during fate specification LIN-39 induces the expression of *lag-2*, which encodes a DELTA family NOTCH ligand (Zhang and Greenwald,

2011), in P6.p (**Fig. 3.1.1A)**. Thus, a lateral DELTA signal from P6.p activates the LIN-12 NOTCH receptor, which specifies the 2° and inhibits the 1° fate (Berset et al., 2001; Sundaram, 2006; Yoo et al., 2004), in the adjacent VPCs P5.p and P7.p (**Fig. 3.1.1A)**. After vulval induction, LIN-39 promotes the proliferation of the vulval cells (Shemer and Podbilewicz, 2002) and activates the expression of *vab*-23 (Pellegrino et al., 2011) to control the formation of the vulval toroids during morphogenesis.

One poorly understood aspect of vulval development is the control of VPC proliferation. The heterochronic genes *lin-14* and *lin-28* are required to keep the VPCs quiescent during the L2 stage, in part by maintaining high levels of the CDK inhibitor CKI-1 (Euling and Ambros, 1996; Hong et al., 1998; van den Heuvel, 2005). The MAPK targets LIN-31 and LIN-1 are also required for the quiescence of the VPCs (Clayton et al., 2008), while LIN-39 is necessary for their proliferation after vulval fate specification (Shemer and Podbilewicz, 2002).

However, it is unclear how activation of the EGFR and NOTCH signaling pathways during vulval induction controls the activities of cell cycle regulators to induce cell cycle progression in the VPCs and maintain vulval cell proliferation. In this study, we show that the *hox* gene *lin-39* functions as a central node in a regulatory network coordinating VPC fate specification and proliferation. Furthermore, we have identified the cyclin E *cye-1* and the cyclin dependent kinase *cdk-4* as LIN-39 targets that promote the G1 to S phase transition of the VPCs during vulval induction.

3.1.3 Results

The VPCs do not adopt a defined cell fate and fail to proliferate in *lin-39* mutants.

Shemer et al. (Shemer and Podbilewicz, 2002) originally reported that in *lin-39(lf)* mutants carrying an *eff-1(lf)* mutation to prevent the fusion of the Pn.p cells with the hypodermis, the VPCs remained polarized but failed to proliferate. However, despite the lack of proliferation the proximal VPCs P5.p, P6.p and P7.p occasionally formed an invagination, indicating that VPCs lacking *lin-39* can adopt vulval cell fates and differentiate if maintained as polarized epithelial cells (Shemer and Podbilewicz, 2002). These observations indicated that *lin-39* plays a pivotal role as a regulator of cell cycle progression in the VPCs.

To extend these findings, we first examined the fates of the VPCs in *eff-1(lf); lin-39(lf)* double mutants using established cell fate reporters. The *ajm-1::gfp* reporter, which labels the cell junctions of polarized epithelial cells, was expressed in the VPCs of all *eff-1(lf); lin-39(lf)* double mutants examined, indicating the epithelial nature of the cells (**Fig. 3.1.1B, B', G**). However, at the late L2/early L3 stage, the VPCs in *eff-1(lf); lin-39(lf)* animals neither expressed the 1° fate-specific markers *Pegl-17::gfp* (Burdine et al., 1998) and *Plag-2::gfp* (Siegfried and Kimble, 2002) nor the *lin-12::gfp* reporter, which is normally up-regulated in

the 2° VPCs (Shaye and Greenwald, 2002) (**Fig. 3.1.1C-E', G**). By contrast, the expression of a reporter for the *let-23 egf* receptor (Haag et al., 2014) was detected in around 20% of the animals (**Fig. 3.1.1F, F', G**), indicating that the VPCs remain responsive to the inductive AC signal even in the absence of *lin-39*. In around 10% of *eff-1(lf); lin-39(lf)* mutants, the VPCs formed an invagination that contained on average four vulval cells (**Fig. 3.1.1H, I**). Interestingly, in those animals some of the invaginated cells did express the *Pegl-17::gfp* and *Plag-2::gfp* reporters (**Fig. 3.1.1J**). To test if these rare invaginations were induced by inductive *lin-3* signaling, we introduced the *lin-3(e1417)* allele, which specifically depletes *lin-3* expression in the AC (Hwang and Sternberg, 2004). None of the *eff-1(lf); lin-39(lf); lin-3(lf)* triple mutants examined, displayed and invagination (**Fig. 3.1.1H**).

We conclude that the unfused VPCs in *lin-39* mutants still sense the inductive LIN-3 EGF signal and occasionally form an invagination, but they cannot adopt a defined cell fate and therefore do not proliferate. These results are in line with previous reports showing that *lag-2* could be regulated by LIN-39 (Zhang and Greenwald, 2011; Takács-Vellai et al., 2007) and are further supported by the presence of a putative LIN-39 binding site in *lag-2* detected by the modENCODE project.

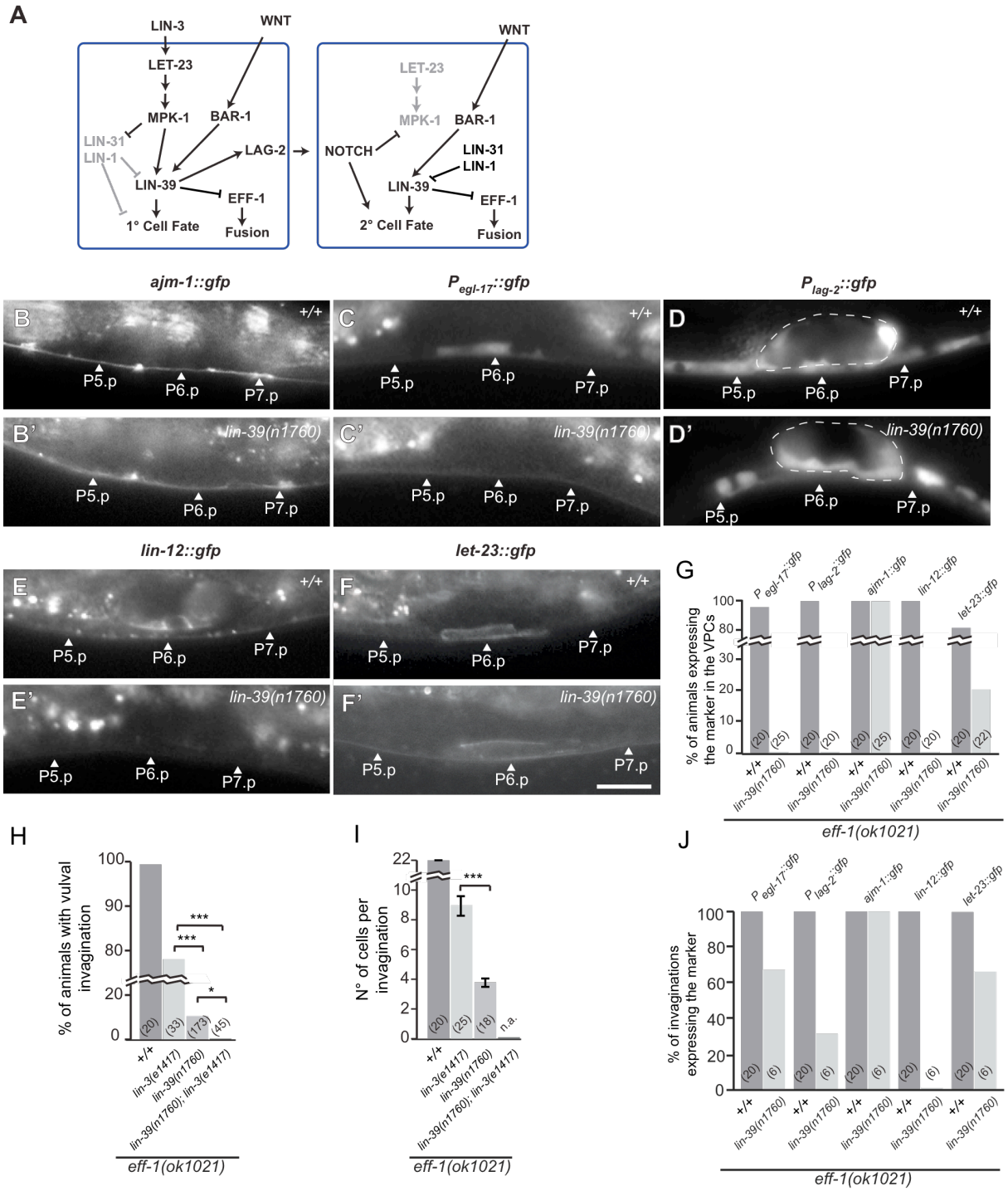

Figure 3.1.1. The VPCs in *lin-39* mutants sense the AC signal but do not adopt specific cell fates and fail to proliferate

(A) Model of the vulval fate specification pathways. LIN-3 EGF binds to LET-23 EGFR in P6.p to activate the RAS/MAPK signaling pathway. MAPK phosphorylation of the LIN-1 ETS/ LIN-31 Forkhead complex in P6.p de-represses the *lin-39 hox* gene. LIN-39 specifies the 1° cell fate and induces LAG-2 /DELTA expression to activate NOTCH signaling in the 2° VPCs P5.p and P7.p. **(B, B')** Expression of the adherens junction marker AJM-1::GFP and **(C, C')** the 1° cell fate markers *Pegl-17::gfp* and **(D, D')** *Plag-2::gfp* in *eff-1(ok1021)* single and *eff-1(ok1021); lin-39(n1760)* double mutants at the late L2/early L3 stage. **(E, E')** Expression of the translational LIN-

12::GFP and (**F, F′)** LET-23::GFP reporters in the VPCs at at the late L2/early L3 stage (all in the *eff-1(ok1021)* background). The arrowheads point at the positions of the VPC nuclei. The scale bar in (**F′**) is 10 μm. **(G)** Quantification of the cell fate reporters shown in (**B**) through (**F′**) at the late L2/early L3 stage. For each genotype, the percentage of animals expressing the indicated fate marker is shown. **(H)** Frequency of vulval invaginations and (**I**) average number of cells per invagination in *lin-3(e1417)* and *lin-39(n1760)* single and double mutants in an *eff-1(ok1021)* background. (**J**) Expression of the cell fate reporters in the vulval invaginations of *eff-1(ok1021)* single and *eff-1(ok1021); lin-39(n1760)* double mutants at the L4 stage. The number of animals analyzed for each genotype is shown in brackets. The error bars represent the standard error of the mean (s.e.m.). Statistical significance was analyzed with a Fisher's exact probability test; *** signifies $p<0.001$ and * $p<0.05$.

lin-39 induces the expression of the cell cycle regulators *cye-1*, *cki-1* and *cdk-4*

To characterize the role of LIN-39 in regulating the VPC cell cycle, we explored the modENOCODE data (Niu et al., 2011) by searching for putative LIN-39 binding sites in known cell cycle regulators. Several genes encoding regulators of the G1/S phase transition contain predicted LIN-39 binding sites, either in their 5′ promoter region or within an intron. Notably, we found strong LIN-39 binding sites in the genes encoding the CDK kinase CDK-4 (Park and Krause, 1999), the G1/S phase cyclin CYE-1 (Fay and Han, 2000), and the *cdc-14* gene, which encodes the activator of the cyclin-dependent kinase inhibitor CKI-1 (Saito et al., 2004). In addition, a weaker site was found in the *cki-1* locus itself (Hong et al., 1998) (**Fig. 3.1.S1** and **Fig. 3.1.3A)**.

To further investigate whether *lin-39* controls the expression of those genes, we compared the expression patterns of different cell cycle reporters in *eff-1(lf)* single versus *eff-1(lf); lin-39(lf)* double mutants that had been synchronized at the mid to late L2 stage, shortly before the VPCs normally begin to proliferate (see materials and methods). The expression of a transcriptional *cdk-4::gfp* reporter that includes the two alternative first exons and 1kb of 5′ regulatory sequences containing the predicted LIN-39 binding site was strongly reduced in *eff-1(lf); lin-39(lf)* double mutants (**Fig. 3.1.2A, A′, D**). Similarly, the expression of a *cki-1::gfp* reporter containing 8kb of 5′ regulatory sequences and the endogenous 3′ UTR (Hong et al., 1998) was down-regulated in *eff-1(lf); lin-39(lf)* double mutants (**Fig. 3.1.2B, B′, D**).

To analyze *cye-1* expression, we generated a *cye-1::gfp* reporter, in which a *gfp* cassette was fused in frame into the third exon, such that both predicted LIN-39 binding sites were included. Since *cye-1* is only transiently expressed in the VPCs at the late G1/early S-phase, we exposed late L2 larvae to hydroxyurea (Hu) for four hours to arrest their cell cycle in the early S-phase before analyzing *cye-1::gfp* expression (see materials and methods). With this procedure we were able to detect *cye-1::gfp* expression in around 20% of the VPCs of *eff-1(lf)* single mutants (**Fig. 3.1.2C, C′, D**). Similar to the other cell cycle regulators, *cye-1::gfp* expression was significantly reduced in *eff-1(lf); lin-39(lf)* double mutants (**Fig. 3.1.2D**). Finally, the expression of a translational *cdc-14::gfp* reporter (Saito et al., 2004) was only slightly reduced in *eff-1(lf); lin-39(lf)* mutants. (The frequency of CDC-14::GFP positive VPCs dropped from 60% (94/150) in *eff-1(lf)* single mutants to 40% (61/146) in *eff-1(lf); lin-39(lf)* double mutants.) Taken together, these experiments indicate that LIN-39 induces the expression of several cell cycle regulators that control the G1 to S phase transition.

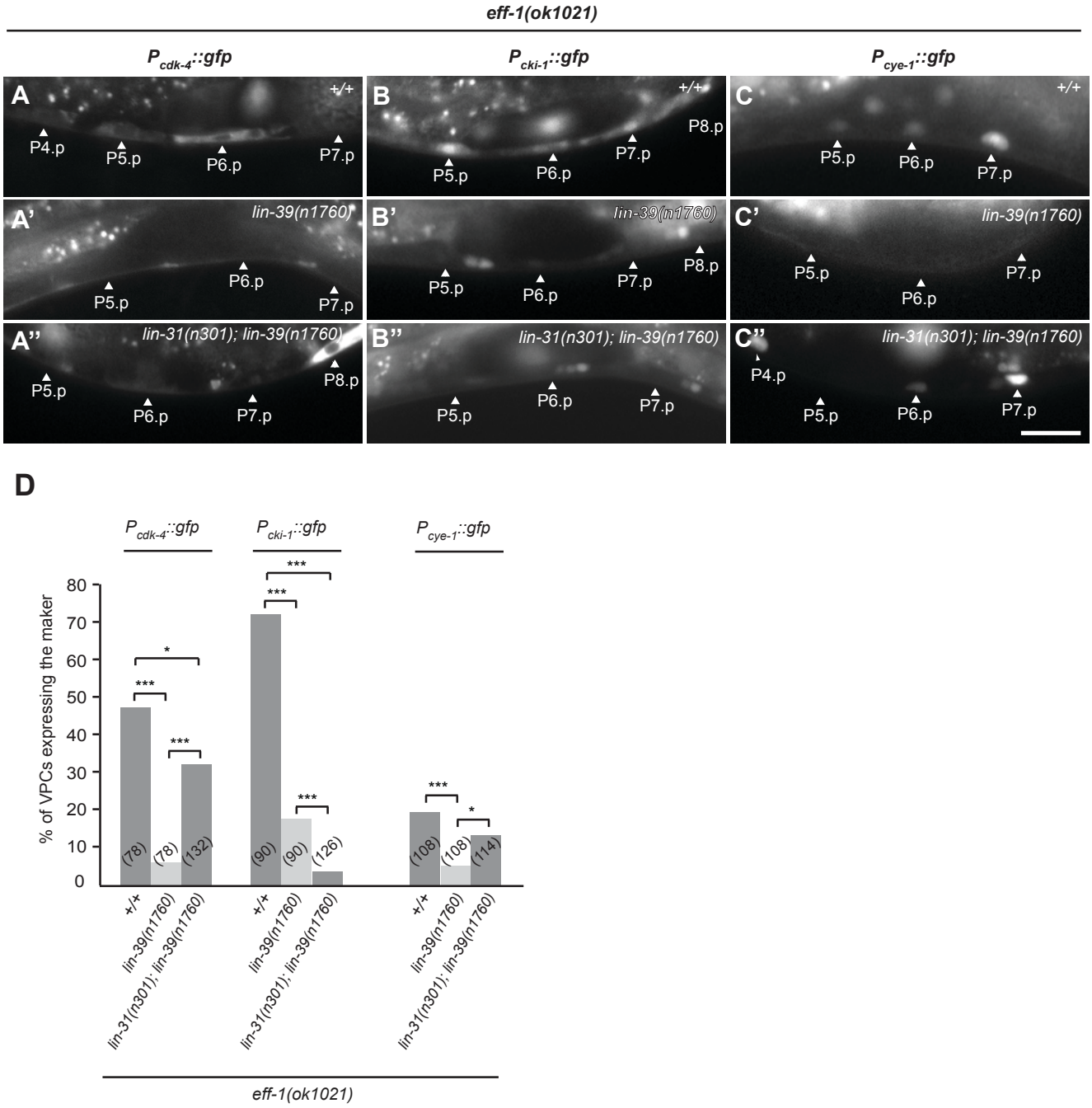

Figure 3.1.2. Reduced *cdk-4, cki-1* and *cye-1* reporter expression in *lin-39* mutants and re-activation in *lin-31* mutants

(A-A'') Expression of the transcriptional *Pcdk-4::gfp,* (**B-B''**) *Pcki-1::gfp* and (**C-C''**) *Pcye-1::gfp* reporters in mid L2 larvae. The first row shows *eff-1(ok1021)* single mutants, the second row *eff-1(ok1021); lin-39(n1760)* double mutants and the third row *lin-31(n301) eff-1(ok1021); lin-39(n1760)* triple mutants. *Pcye-1::gfp* expression was scored in S-phase arrested early L3 larvae by exposing mid L2 larvae synchronized 26 hours after L1 arrest for 4 hours to 40 mM hydroxyurea (see materials and methods). The arrowheads point at the positions of the VPC nuclei. The scale bar in (**C'**) is 10 μm. **(D)** Percentage of VPCs expressing the markers shown in (A) through (C'') in the different genetic backgrounds. The number of VPCs analyzed for each genotype is shown in brackets. Statistical significance was analyzed with a Fisher's exact probability test; * $p<0.05$ and *** signifies $p<0.001$.

LIN-39 induces *cye-1* expression through a non-canonical HOX Binding Site

Even though the modENCODE data indicated the presence of LIN-39 HOX binding sites (HBS) in several cell cycle regulators, we could not identify the canonical HOX/PBX consensus motif TGATNNAT (Mann and Affolter, 1998) within the predicted binding regions. However, by aligning the putative LIN-39 binding sites to the synthetic regions in the *C. briggsae* and *C. remanei* genomes, we identified conserved sequence blocks containing the motif TTTG(A/T)AT(T/C)T, which appears to be diverged from the canonical HOX/PBX binding motif TGATNNAT (**Fig. 3.1.3A** and **Fig. 3.1.S1**).

To test if LIN-39 directly activates *cye-1* expression through these non-canonical HBSs, we generated four variants of the *cye-1::gfp* reporter described above and integrated single copies of each reporter at a defined location on chromosome II using the *mosSCI* technique (Frøkjaer-Jensen et al., 2008): a wild-type reporter with both HBSs intact; the ΔHBS1 reporter, in which the HBS upstream of the promoter had been mutated from TTT**GAAT**CT to TTT**CCCC**CT; the ΔHBS2 reporter, in which the HBS in the second intron had been mutated from TTT**GTAT**TT to TTT**CCCC**TT; and the ΔHBS1ΔHBS2 reporter, in which both HBSs had been mutated (**Fig. 3.1.3B**). We then measured for each reporter the relative *cye-1::gfp* signal intensity in the VPCs of early L3 larvae. Expression of the wild-type reporter was significantly stronger in the 1° VPCs than in the 2° VPCs (**Fig. 3.1.3C, D** and **Tab. 3.1.S1** for statistical analysis). The ΔHBS1 reporter showed strongly reduced and equal expression levels in the 1° and 2° VPCs (**Fig. 3.1.3C', D**). By contrast, the ΔHBS2 reporter exhibited only a moderate reduction in the expression levels and maintained the bias towards 1°-specific expression (**Fig. 3.1.3C'', D**). Finally, the expression of the ΔHBS1ΔHBS2 reporter was even further reduced when compared to either single mutant ΔHBS reporter (**Fig. 3.1.3C''', D**). Thus, the two HBS cooperatively induce *cye-1* expression in the VPCs. Though, the HBS1 site introduces a 1° lineage-specific bias and overall contributes to a greater extent than the HBS2 site.

To confirm the modENCODE data and directly measure the binding of LIN-39 to the HBS motifs in the *cye-1* gene, we performed chromatin immunoprecipitation (ChIP) experiments combined with quantitative real-time PCR (Q-PCR) analysis as described previously (Pellegrino et al., 2011) **(**see also materials and methods). By using chromatin extracts of transgenic animals carrying a single copy of the ΔHBS1ΔHBS2 reporter integrated on chromosome II and a functional *lin-39::gfp* reporter, we could directly compare LIN-39 binding to the wild-type (endogenous) and the mutant (transgenic) HBS motifs in the same chromatin extracts. For this purpose, we designed PCR primer pairs specifically amplifying either of the two wild-type HBSs in endogenous *cye-1* on chromosome I or the mutant HBSs in the ΔHBS1ΔHBS2 reporter on chromosome II (**Fig. 3.1.3E** and **Tab 3.1.S2**). Q-PCR analysis of LIN-39::GFP ChIP revealed a nearly two-fold enrichment of LIN-39 binding at the wild-

type HBS1 site in the endogenous *cye-1* locus when compared to the precipitates from the animals lacking the *lin-39::gfp* transgene, while LIN-39 was only weakly (around 1.2-fold) enriched at the mutant ΔHBS1 site in the *cye-1* reporter (**Fig. 3.1.3F** shows the average values of three independent experiments). Despite the clear LIN-39 peak observed by modENCODE at the HBS2 site in the second intron of *cye-1*, we could not detect a significant enrichment of LIN-39::GFP at this site, which may be due to a much weaker or transient binding of LIN-39 (**Fig. 3.1.3F**). This result is consistent with the relatively mild effect of the ΔHBS2 mutation on the reporter expression.

Taken together, the *cye-1* reporter analysis and ChIP-Q-PCR experiments indicate that LIN-39 directly regulates the expression of *cye-1* by binding to the conserved HBS motif in the 5' regulatory region. The second HBS motif located in the second intron appears to play a minor role in activating *cye-1* expression. The higher *cye-1* reporter expression levels in the 1° compared to the 2° VPCs can be explained by the up-regulation of LIN-39 expression in 1° VPCs in response to the EGF signal from the AC (Wagmaister et al., 2006a). Given the sequence conservation in the LIN-39 binding sites detected by modENDODE in the *cki-1* and *cdk-4* genes, it seems likely that LIN-39 also activates the transcription of these cell cycle regulators to promote the G1/S phase transition of the VPCs.

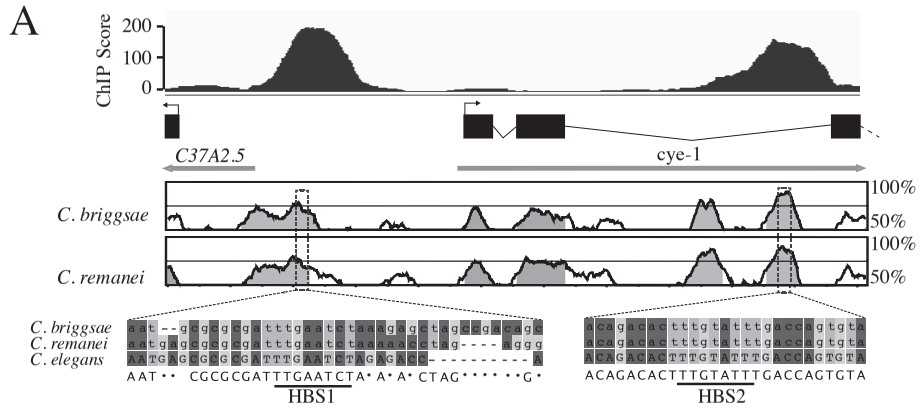
A
ChIP Score
200
100
0
C37A2.5
cye-1
C. briggsae
C. remanei
100%
50%
C. briggsae
C. remanei
C. elegans
HBS1
HBS2

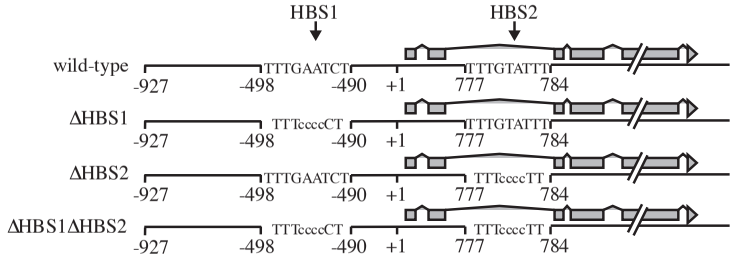
B
HBS1
HBS2
wild-type
ΔHBS1
ΔHBS2
ΔHBS1ΔHBS2
TTTGAATCT
TTTGTATTT
TTTccccCT
TTTccccTT
-927
-498
-490
+1
777
784

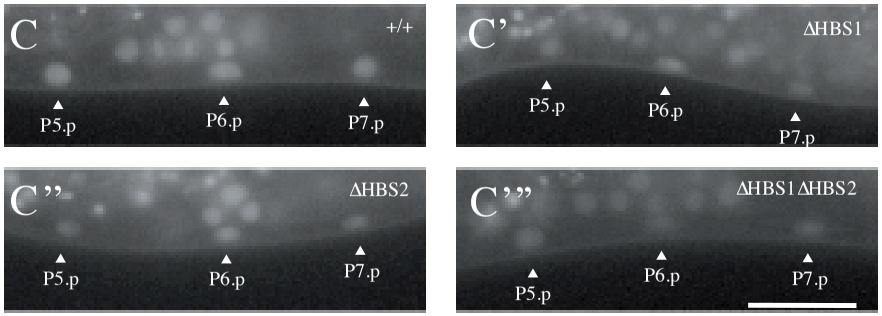
C
+/+
C'
ΔHBS1
C''
ΔHBS2
C'''
ΔHBS1ΔHBS2
P5.p
P6.p
P7.p

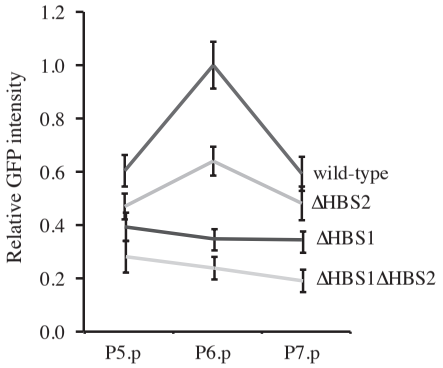
D
Relative GFP intensity
1.2
1.0
0.8
0.6
0.4
0.2
0.0
wild-type
ΔHBS2
ΔHBS1
ΔHBS1ΔHBS2
P5.p
P6.p
P7.p

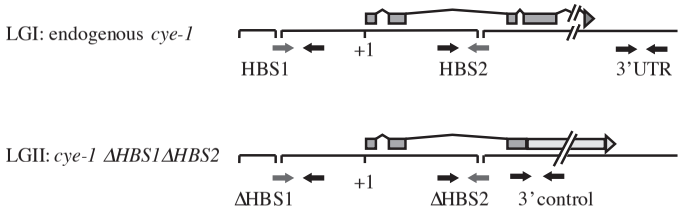
E
LGI: endogenous cye-1
HBS1
+1
HBS2
3'UTR
LGII: cye-1 ΔHBS1ΔHBS2
ΔHBS1
+1
ΔHBS2
3' control

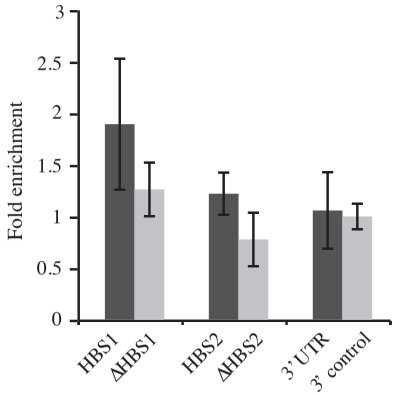
F
Fold enrichment
3
2.5
2
1.5
1
0.5
0
HBS1
ΔHBS1
HBS2
ΔHBS2
3'UTR
3' control

Figure 3.1.3. LIN-39 regulates *cye-1* expression via the HBS motifs

(A) The top graph shows the LIN-39 ChIP read counts in the *cye-1* genomic region as reported by modENCODE (Niu et al., 2011). The sequence conservation between the *C. elegans, C. briggsae* and *C. remanei cye-1* loci is shown in the graphs underneath (Couronne et al., 2003) with the sequence alignments of the two LIN-39 binding sites containing conserved HBS motifs. **(B)** Structure of the wild-type *cye-1* locus and the mutations in the two HBS motifs. (C-C'') Expression pattern of the wild-type *cye-1::gfp* reporter and the HBS1&2 single and double mutants in the VPCs of early L3 larvae. The arrowheads point at the positions of the VPC nuclei and the scale bar in (**C'''**) is 10 μm. (**D**) Quantification of wild-type and mutant *cye-1::gfp* reporter expression in P5.p through P7.p in early L3 larvae. All values were normalized to the average GFP intensity measured with the wild-type reporter in P6.p. A statistical analysis of the data is shown in suppl. Table 1. **(E**) Location of the PCR primers used for ChIP-Q-PCR analysis of endogenous *cye-1* on LGI and the *cye-1ΔHBS1ΔHBS2* reporter on LGII. **(F)** Enrichment of LIN-39::GFP at the HBS sites of endogenous *cye-1* (dark grey columns) and the ΔHBS1ΔHBS2 reporter (light grey columns). The specific enrichment was calculated as described in materials and methods, and the average values obtained in three independent experiments are shown. The error bars represent the standard error of the mean (s.e.m.).

The *lin-31 forkhead* transcription factor inhibits VPC proliferation

Since LIN-39 is expressed in the VPCs immediately after they are born at the late L1 stage (Clark et al., 1993; Wagmaister et al., 2006a), we reasoned that additional factors must exist that counteract LIN-39 function and block VPC proliferation until the vulval cell fates have been specified at the end of the L2 stage. The complex of the LIN-1 ETS and LIN-31 Forkhead transcription factors plays an important role in inhibiting vulval differentiation downstream of the EGFR/RAS/MAPK pathway (Jacobs et al., 1998; Tan et al., 1998). In particular, LIN-1 and LIN-31 repress the transcription of *lin-39* and promote the expression of *cki-1* (Clayton et al., 2008; Guerry et al., 2007; Wagmaister et al., 2006b). In order to test if LIN-31 or LIN-1 also repress the cell cycle of the VPCs, we examined VPC proliferation in *eff-1(lf) lin-31(lf); lin-39(lf)* and *eff-1(lf); lin-39(lf); lin-1(lf)* triple mutants. To quantify VPC proliferation, we counted the number of invaginations at the L4 stage as well as the average number of differentiated vulval cells per animal. Due to the variable position of the VPCs and their descendants in *eff-1(lf); lin-39(lf)* double mutants it was impossible to unambiguously identify the individual VPC lineages. We therefore segmented L4 animals into 6 zones that correspond to the areas where the VPCs are located in wild-type L4 larvae (**Fig. 3.1.4A** and **Table 3.1.1**). The first zone spans from the posterior pharynx to the turn of the anterior gonad arm, the second zone from the gonad turn to the distal tip of the anterior gonad, the third zone is between the anterior distal tip and the midline of the animal, the fourth zone from the midline to the posterior distal tip, the fifth zone between the posterior distal tip and the gonad turn and the sixth zone from the gonad turn to the anus.

A *lin-31(lf)* but not a *lin-1(lf)* mutation rescued the proliferation defect of *eff-1(lf); lin-39(lf)* double mutants (**Fig. 3.1.4C, D** and **Table 3.1.1**). In *eff-1(lf) lin-31(lf); lin-39(lf)* triple mutants, both the frequency of VPCs undergoing differentiation to form an invagination as well as the number of differentiated cells in the invaginations were increased (**Fig. 3.1.4C** and **Table 3.1.1**). Moreover, we observed no further increase in vulval induction or VPC proliferation in *eff-1(lf) lin-31(lf); lin-39(lf); lin-1(lf)* quadruple mutants (**Fig 3.1.4F** and **Table 3.1.1**). While in *eff-1(lf); lin-39(lf)* double mutants the invaginations were centered around the mid body region underneath the AC, the invaginations in the *eff-1(lf) lin-31(lf); lin-39(lf)* triple mutants were shifted towards the posterior body region, suggesting an AC-independent induction of vulval differentiation under these conditions (**Fig. 3.1.4C** and **Table 3.1.1**). An alternative explanation may be that a loss or posterior shift of the anterior Pn.p cells results in a posterior shift of the VPCs. However, analysis of a *Plin-31::nls::yfp* reporter (la Cova and Greenwald, 2012) did not indicate a loss or posterior shift of the Pn.p cells in the *eff-1(lf); lin-39(lf)* background (**Fig. 3.1.S2A**). Surprisingly, we observed Pn.p cell duplications in around 8% of *eff-1(lf); lin-39(lf)* animals (**Fig. 3.1.S2C**). Possibly, the early loss of *cki-1* expression

results in premature Pn.p cell divisions as previously reported (Saito et al., 2004).

The *lin-31(lf)* mutation not only restored VPC proliferation in the *eff-1(lf); lin-39(lf)* background but also re-activated *cye-1::gfp* and *cdk-4::gfp* expression in the VPCs (**Fig. 3.1.2A", C", D**). On the other hand, the expression of *cki-1::gfp* was not induced in the *eff-1(lf) lin-31(lf); lin-39(lf)* background (**Fig. 3.1.2B", D**) because LIN-31 positively regulates *cki-1* expression as reported previously (Clayton et al., 2008). We further tested if ectopic expression of *cye-1* or inactivation of *cki-1* may have the same effect as a *lin-31(lf)* mutation. However, neither the inactivation of CKI-1 through a *cdc-14(lf)* mutation (Roy et al., 2011; Saito et al., 2004) nor the forced expression of *cye-1* under control of the Pn.p cell-specific *lin-31* promoter were sufficient to induce VPC proliferation in the *eff-1(lf); lin-39(lf)* background (**Table 3.1.1**). These results indicate that LIN-31 opposes LIN-39 function independently of LIN-1 by repressing the expression of *cdk-4* and *cye-1* and possibly also other cell cycle regulators.

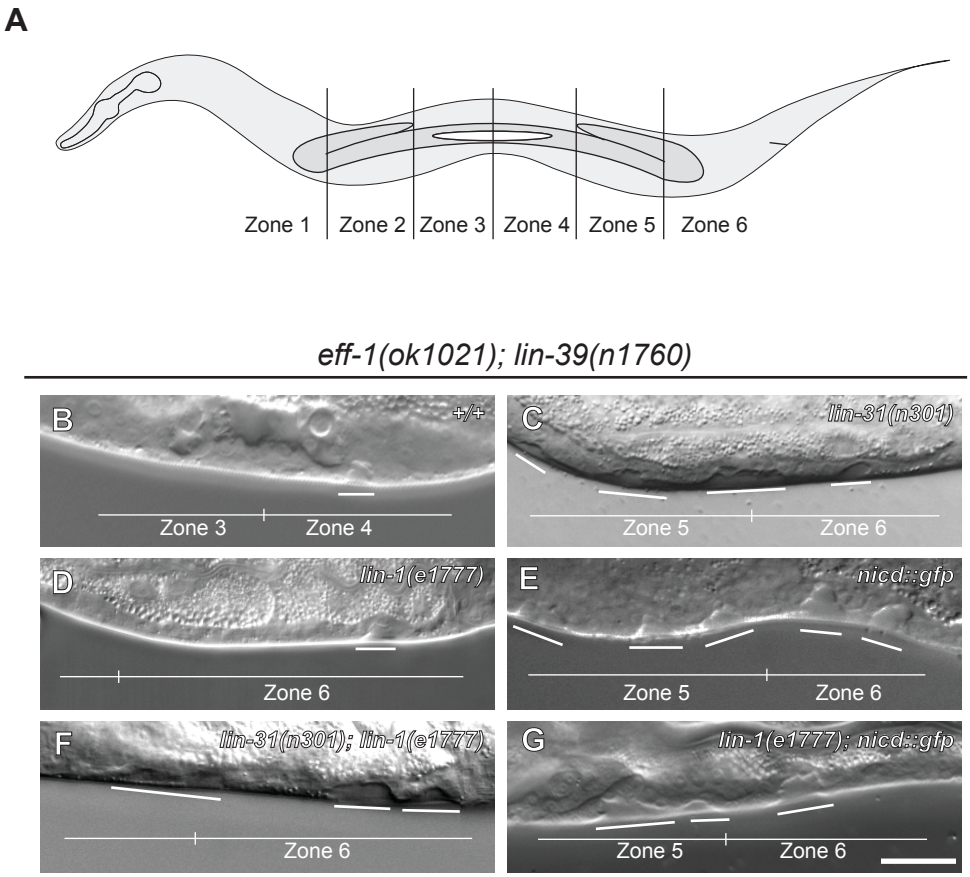

Figure 3.1.4. Suppression of the *lin-39* proliferation defect by *lin-31(lf)* mutations or by activation of NOTCH signaling

(A) The six zones in an L4 larva used to determine the position of the vulval invaginations in the different backgrounds shown below. **(B)** Normarski images of an *eff-1(lok1021); lin-39(n1760)* L4 larva, **(C)** combined with the *lin-31(n301)* mutation, **(D)** with the *lin-1(n1777)* mutation, **(E)** together with the *Pbar-1::nicd::gfp* transgene (*zhEx500*), (**F**) with the *lin-1(n1777)* and *lin-31(n301)* mutations and (**G**) in combination with the *lin-1(n1777)* mutation and the *Pbar-1::nicd::gfp* transgene. The vulval invaginations are marked with solid white lines and the zones are indicated below. For quantification of the phenotypes, see **Table 3.1.1**. The scale bar in (**G**) is 10 μm.

Genotype (all in the *eff-1(lf) background*)	% of animals with invagination per zone						induction (s.e.m.) (n)	vulval cells (s.e.m) (n)	% animals with invaginations
	1	2	3	4	5	6			
	0	0	0	100	0	0	3.00 (0) (20)	22 (0) (20)	100
lin-39(n1760)	0	0	0	11	0	0	0.06 (0.1) (173)	3.8 (0.3) (18)	11
lin-31(n301)	0	13	66	100	73	0	3.1 (0.3) (15)	23.7 (2.2) (15)	100
lin-31(n301); lin-39(n1760)	0	0	13	44	56	75	1.4 (0.2) (16)	11.1 (1.5) (15)	94
lin-1(e1777)	0	30	85	100	80	20	4.0 (0.2) (20)	29.9 (1.5) (20)	100
lin-39(n1760); lin-1(e1777)	0	0	0	3	8	11	0.08 (0.04) (37)	4.7 (1.0) (6)	16
lin-31(n301); lin-1(e1777)	92	100	100	100	100	91	n.s.	70.7 (4.4) (12)	100
lin-31(n301); lin-39(n1760); lin-1(e1777)	0	5	15	60	55	65	1.6 (0.3) (20)	15.4 (1.1) (16)	80
cdc-14(he141); lin-39(n1760)	0	0	0	7	0	0	0.04 (0.01) (169)	4.8 (0.4) (11)	7
lin-39(n1760); zhEx536[P_{lin-31}::cye-1]	0	0	0	19	0	0	0.07 (0.4) (21)	3.0 (0.7) (4)	19
zhEx500[P_{bar-1}::nicd::gfp]	0	33	67	92	67	42	4.2 (0.5) (12)	34.8 (2.6) (11)	91
lin-39(n1760); zhEx500[P_{bar-1}::nicd::gfp]	0	0	11	44	55	72	1.6 (0.3) (18)	13.9 (1.9) (15)	83
lin-39(n1760); lin-1(e1777); zhEx500[P_{bar-1}::nicd::gfp]	0	0	0	50	60	45	1.2 (0.2) (20)	9.2 (1.6) (15)	75

Table 3.1.1. Suppression of the *lin-39* proliferation defect by *lin-31(lf)* mutations or by activation of NOTCH signaling

For each genotype, the frequency of vulval invaginations in each of the six zones, the average number of induced VPCs per animal, the average number of differentiated vulval cells per animal and the percentage of animals developing at least one vulval invagination are shown. Nomarski images of selected examples are shown in **Fig. 3.1.4**. s.e.m indicates the standard error of the mean and n the number of animals analyzed.

Ectopic activation of LIN-12 NOTCH signaling restores VPC proliferation

Since neither *lin-12 notch* nor *lag-2 delta* were expressed in the VPCs of *eff-1(lf); lin-39(lf)* double mutants (**Fig. 3.1.1D', E', G** and (Regős et al., 2013)), we tested whether the VPC proliferation defect of *eff-1(lf); lin-39(lf)* double mutants could be rescued by forced activation of the NOTCH signaling pathway. For this purpose, we introduced a transgene expressing the intracellular LIN-12 domain (NICD) under the control of the *bar-1* promoter, which is active in all VPCs (*bar-1::nicd::gfp*) (Nusser-Stein et al., 2012). In the *eff-1(lf)* background, the *bar-1::nicd::gfp* transgene caused ectopic 2° fate specification in all VPCs except for P6.p, which was induced by the AC signal to adopt a 1° fate (Nusser-Stein et al., 2012). Similar to *lin-31(lf)*, the *bar-1::nicd::gfp* transgene induced VPC proliferation and the formation of ectopic vulval invaginations in the *eff-1(lf); lin-39(lf)* background (**Fig. 3.1.4E** and **Table 3.1.1**). We again observed a shift of the vulval invaginations towards the posterior body region as described above for the *lin-31(lf)* mutation (**Fig. 3.1.4C, E** and **Table 3.1.1**).

We have previously reported that the non-phosphorylated form of *lin-1* is required for certain aspects of 2° cell fate execution by acting downstream of the NOTCH pathway during vulval morphogenesis (Farooqui et al., 2012). To examine if LIN-1 also acts downstream of NOTCH to promote VPC proliferation, we crossed the *lin-1(lf)* mutation into the *eff-1(lf); lin-39(lf); bar-1::nicd::gfp* strain (**Fig. 3.1.4G** and **Table 3.1.1**). However, *lin-1(lf)* did not suppress the VPC proliferation induced by the *bar-1::nicd::gfp* transgene. Thus, NOTCH signaling promotes VPC proliferation in a LIN-1-independent manner (**Fig. 3.1.4G** and **Table 3.1.1**).

LIN-31 acts downstream of or in parallel to LIN-12 NOTCH to block 2° VPC proliferation

One possible scenario is that NOTCH signaling promotes VPC proliferation by preventing the LIN-31-mediated repression of cell cycle regulators. To investigate this possibility, we examined the epistatic relationship between LIN-12 NOTCH and LIN-31. We used a dominant *lin-31* mutant (*lin-31phd*), in which the MAPK phosphorylation sites that are required for transcriptional activation had been deleted to convert LIN-31 into a constitutive repressor (Tan et al., 1998). A transgene expressing the *lin-31phd* mutant efficiently suppressed the ectopic vulval induction of the distal VPCs (P3.p, P4.p and P8.p) caused by the *bar-1::nicd::gfp* transgene in a *lin-31(lf)* background (**Table 3.1.2**). In particular, the vulval induction index in *bar-1::nicd::gfp; lin-31phd* double transgenic animals was comparable to the induction index in *lin-31phd* single transgenic animals, indicating that *lin-31phd* is epistatic and hence likely acts downstream of the NOTCH signaling pathway to repress VPC induction. For example, LIN-12 NOTCH signaling may inactivate LIN-31 in the 2° VPCs to relieve the cell cycle arrest and permit the execution of the 2° lineage. Alternatively, LIN-31

and LIN-12 NOTCH may act in parallel pathways, and activation of NOTCH signaling overcomes the LIN-31-mediated repression of its target genes.

		% of induced VPCs						induction	
	Genotype	P3.p	P4.p	P5.p	P6.p	P7.p	P8.p	(s.e.m.)	(n)
unc-29(lf); lin-31(lf)	*P_{bar-1}::nicd::gfp*	47	63	100	100	100	79	4.6 (0.2)	(19)
	-	35	55	95	95	85	35	3.2 (0.2)	(20)
	gaEx69[lin-31(PhD)]	16	16	92	100	84	8	2.9 (0.1)	(25)
	zhEx542[P_{bar-1}::nicd::gfp]	54	92	100	100	91	86	4.5 (0.2)	(22)
	gaEx69[lin-31(PhD)]; zhEx542[P_{bar-1}::nicd::gfp]	5	35	90	100	95	45	3.2 (0.2)	(20)

Table 2. NOTCH signaling acts upstream of or in parallel with LIN-31 Forkhead

For each genotype, the frequency of induced VPCs and the average number of induced VPCs per animal are shown. s.e.m indicates the standard error of the mean and n the number of animals analyzed.

3.1.4 Discussion

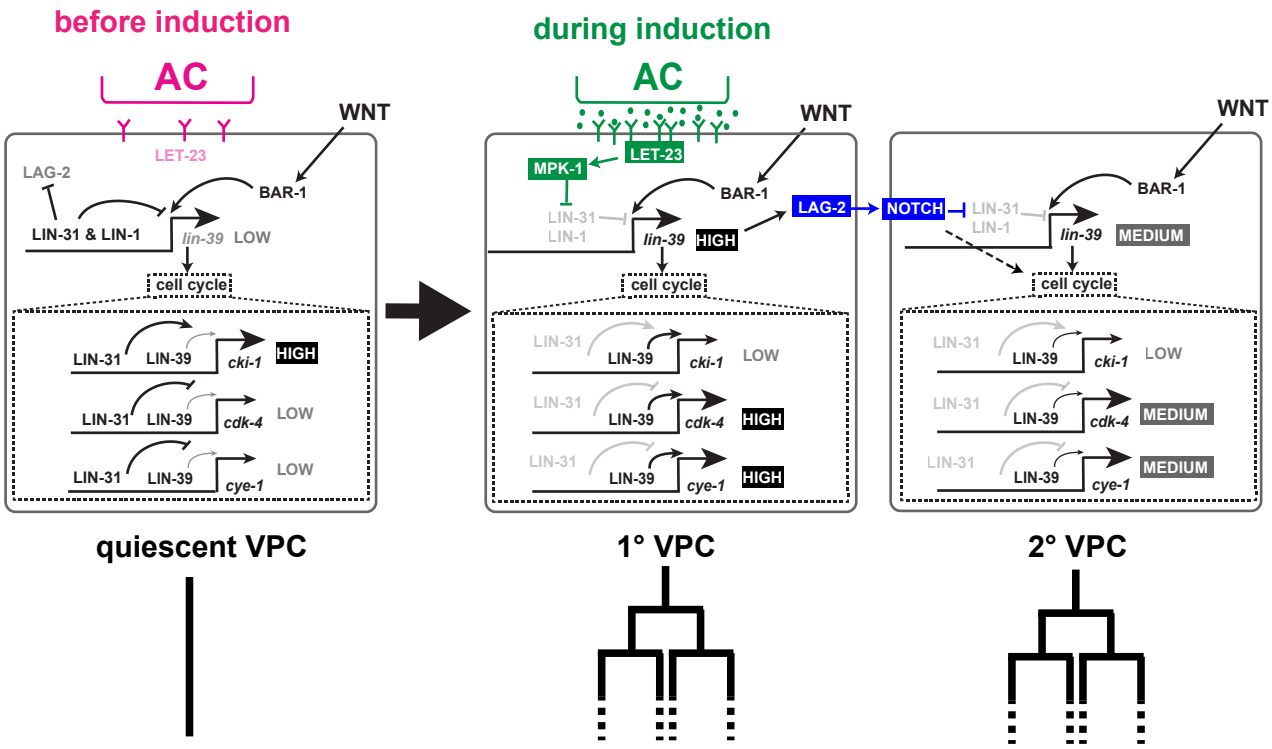

Figure 3.1.5. Regulation of VPC proliferation by LIN-39

Left cell: Before vulval induction, LIN-1 and LIN-31 repress *lin-39* and *lag-2* expression, while WNT signaling maintains low LIN-39 levels in all VPCs. In addition, LIN-31 promotes *cki-1* and represses *cye-1* and *cdk-4* expression to maintain VPC quiescence. Middle cell: During vulval induction, strong RAS/MAPK signaling in the 1° VPC (P6.p) results in the inactivation of the LIN-1/LIN-31 complex and de-repression of *lin-39*. High LIN-39 levels induce *cdk-4* and *cye-1* expression to permit S-phase entry. In addition, the up-regulation of *lag-2* activates lateral NOTCH signaling in the adjacent 2° VPCs P5.p and P7.p. Right cell: Activation of NOTCH signaling in the 2° VPCs P5.p and P7.p counteracts LIN-31 activity. This results in the up-regulation of LIN-39 and induction of *cye-1* and *cdk-4* expression to permit S-phase entry.

The *hox* gene *lin-39* links cell fate specification and cell cycle progression

lin-39 plays several essential roles during vulval development by specifying the vulval equivalence group, maintaining the VPCs as polarized epithelial cells and promoting VPC proliferation (Shemer and Podbilewicz, 2002). Here, we have investigated the mechanism by which *lin-39* coordinates VPC fate specification and proliferation. Based on our data, we propose the following model linking the spatial patterning pathways to the control of VPC proliferation (**Fig. 3.1.5**): Before the inductive AC signal activates RAS/MAPK signaling, basal *lin-39* expression levels are maintained by WNT signaling, which opposes the activity of the LIN-1/LIN-31 repressor complex (Wagmaister et al., 2006b) (**Fig. 3.1.5**). The basal *lin-*

39 expression is sufficient to inhibit the fusion of the VPCs with hyp7 (Eisenmann et al., 1998) and sustain low expression levels of the G1 phase cell cycle components, which may be necessary to prevent an irreversible cell cycle exit of the VPCs. At the same time, LIN-31 enhances *cki-1* (Clayton et al., 2008) and represses *cye-1* and *cdk-4* expression in order to arrest the VPC cell cycle in the early G1 phase.

As the RAS/MAPK pathway is activated by the inductive AC signal in late L2 larvae (**Fig. 3.1.5**), LIN-31 and LIN-1 are inactivated through MAPK phosphorylation (Tan et al., 1998), *lin-39* is de-repressed and its levels increase in the 1° lineage (Eisenmann et al., 1998; Wagmaister et al., 2006a). At the same time, the expression of the CDK inhibitor *cki-1* decreases due to reduced LIN-31 and LIN-1 activity (Clayton et al., 2008), while *cye-1* and *cdk-4* expression increase in response to raising LIN-39 levels. Interestingly, the activation of a single cell cycle component, for example the ectopic expression of *cye-1* or a mutation in the CKI-1 activator *cdc-14*, is not sufficient to restore VPC proliferation in the absence of LIN-39. This observation indicates that LIN-39 facilitates cell cycle progression by inducing the expression of multiple core cell cycle regulators. Along these lines, LIN-39 also seems to stimulate the transcription of the cell cycle inhibitor *cki-1*. This observation may appear contradictory to the role of LIN-39 in promoting VPC proliferation. However, the relationship between positive and negative cell cycle regulators is complex. The mammalian CDK-4/Cyclin D complex sequesters the CKI-1 homolog p27/KIP1, which in turn stabilizes the CDK-4/Cyclin D complex (Cheng et al., 1999; LaBaer et al., 1997). Thus, LIN-39 may activate the entire cell cycle machinery, rather than individual components, to ensure a regulated G1/S phase transition of the VPCs upon vulval induction.

NOTCH signaling promotes cell cycle progression by counteracting LIN-31

Before vulval induction, LIN-1 ETS represses the transcription of the delta ligand *lag-2*, thereby blocking the activation of the lateral LIN-12 NOTCH signaling pathway (Zhang and Greenwald, 2011). Once the LIN-1 repressor activity has been relieved through MAPK phosphorylation, LIN-39 can up-regulate LAG-2 expression in the 1° VPCs to induce LIN-12 NOTCH signaling in the 2° lineage (Chen and Greenwald, 2004). Thus, in *lin-39(lf)* mutants the NOTCH pathway is not activated and *lin-12 notch* expression drops to undetectable levels because the auto-regulatory positive feedback loop is broken (Nusser-Stein et al., 2012; Shaye and Greenwald, 2002). We have found that forced activation of the NOTCH pathway restores VPC proliferation in the *lin-39(lf)* background, indicating that NOTCH signaling promotes VPC cell cycle progression independently of LIN-39. Since lateral NOTCH signaling effectively blocks RAS/MAPK signaling in the 2° lineage (Berset et al., 2001; Yoo et al., 2004), NOTCH probably promotes cell cycle progression in a MAPK-independent fashion. Our epistasis analysis further indicates that NOTCH acts upstream of or in parallel

with LIN-31. Activation of the NOTCH pathway may inhibit LIN-31 protein function in the 2° lineage, similar to the inhibitory effect RAS/MAPK signaling exerts on LIN-31 in the 1° lineage. For example, NOTCH signaling may induce the phosphorylation of LIN-31 by a kinase other than MAPK to block the repressive function of LIN-31. Alternatively, NOTCH activity may overcome the LIN-31-mediated transcriptional repression of cell cycle regulators at the target gene level. Our present data cannot distinguish between these two scenarios. However, since the forced expression of NICD did not completely rescue the *lin-39(lf)* proliferation defect, LIN-39 and NOTCH signaling likely need to cooperate in the 2° VPCs. Thus, the basal LIN-39 levels induced by WNT signaling as well as the inhibition of LIN-31 function by the lateral NOTCH signal are required for normal cell cycle progression in the 2° VPCs.

Cell cycle control by *hox* genes

hox genes have been implicated in the control of cell proliferation in a wide variety of tissues in different organisms (Hombría and Lovegrove, 2003; Rezsohazy et al., 2015). For example, *hox* genes promote cell proliferation during insect and vertebrate limb development (Cohn et al., 1997; Mahfooz et al., 2004), tail regeneration in the zebrafish (Thummel et al., 2007) and hematopoietic stem cell expansion (Schiedlmeier et al., 2007). Moreover, de-regulated *hox* gene expression caused by chromosomal translocations or other mutations has been observed in different types of leukemia (Schiedlmeier et al., 2007). However, in most of these cases the HOX proteins are thought to control proliferation indirectly by inducing secondary targets that act as cell fate determinants or signaling molecules, which in turn control proliferation. A notable exception is the regulation of the CDK inhibitor p21 by HOXA10 in myelomonocytic cells, where a direct binding of the HOXA10 protein to the enhancer region has been demonstrated (Bromleigh and Freedman, 2000). Our data indicate a direct function of the *C. elegans* HOX protein LIN-39 in the control of cell proliferation. LIN-39 binds to a conserved sequence motif in the G1 cyclin gene *cye-1* and possibly also in other genes encoding regulators of the G1 to S-phase transition. Interestingly, the LIN-39 binding sites in these genes contain a non-canonical motif that appears to be derived from the canonical HOX/PBX binding site TGATNNAT (Mann and Affolter, 1998). This observation may point at the existence of a subgroup of HOX target genes with specialized functions in proliferation control. The type of co-factor present in the specific cellular context may largely determine the choice of HOX binding sites. However, the two known HOX co-factors CEH-20 PBX and UNC-62 MEIS play different, partially LIN-39 independent roles during vulval development and they have so far not been implicated in controlling VPC proliferation (Yang, 2005). Moreover, the existing ChIPseq data do not indicate an obvious enrichment of UNC-62 at the

HBSs in the *cye-1* and *cdk-4* genes (Niu et al., 2011). It thus seems likely that LIN-39 utilizes another, yet to be identified co-factor to promote VPC proliferation.

Global versus local cell cycle control

Towards the end of the first larval (L1) stage, the P cells migrate from the lateral sides to the ventral midline where P3 through P8 divide to produce the VPCs P3.p through P8.p and their sister Pn.a cells. Thereafter, the VPCs arrest their cell cycle in the G1 phase until the end of the L2 stage, when their cell fates are specified and the VPCs begin to proliferate. The early heterochronic genes *lin-28* and *lin-14* impose a global cell cycle block on the VPCs, probably by up-regulating *cki-1* expression (Hong et al., 1998). However, the VPCs in *lin-28(lf)* mutants not only proliferate precociously, but they also adopt the correct fate pattern at the beginning instead of the end of the L2 stage. Hence, VPC fate specification and cell cycle progression remain coupled in heterochronic mutants. Nevertheless, the precocious vulval differentiation in *lin-28* mutants results in the formation of a non-functional vulva because the uterus has not yet reached the correct developmental stage when vulval morphogenesis takes place and therefore no proper uterine-vulval connection can be established (Moss et al., 1997). By contrast, the regulatory mechanism we have described here links VPC proliferation to the input from the spatial patterning signals. This local control mechanism ensures that the VPCs only resume proliferation once their fates have been defined and after the somatic gonad has reached the proper developmental stage to ensure that the development of the uterus and vulva progress in synchrony.

In conclusion, we have shown that the HOX protein LIN-39 controls the expression of multiple cell cycle components that are necessary for the G1 to S-phase transition of the VPCs. LIN-39 promotes VPC proliferation through two distinct mechanisms; it induces the expression of core cell cycle components in 1° VPCs, and activates lateral NOTCH signaling in the 2° VPCs to relieve the cell cycle inhibition imposed by the LIN-31 Forkhead transcription factor. LIN-39 thus coordinates VPC proliferation and fate specification.

3.1.5 Materials and methods

C. elegans methods and strains

The strains used for the experiments and crosses were derivates of Bristol strain N2 of *Caenorhabditis elegans*. The animals were cultivated under standard conditions at 20°C as described in (Brenner, 1974) unless specified. The mutations used in this study have been previously described and are listed below according to their linkage group. To construct the different mutant combinations standard genetic methods were used.

Alleles used: LGI: *lin-31(n301, n1053)* (Ferguson and Horvitz, 1985), *unc-29(e1072)* (Tan et al., 1998), *eff-1(ok1021)* (Sapir et al., 2007); LGII: *cdc-14(he141)* (Saito et al., 2004); LGIII: *lin-39(n1760)* (Clark et al., 1993); LGIV: *lin-3(e1417)* (Hwang and Sternberg, 2004), *lin-1(e1777)* (Ferguson and Horvitz, 1985).

Transgenes used: *maIs113[cki-1::gfp, dpy-20(+)]* (Hong et al., 1998), *ayIs4[Pegl-17::gfp]* (Burdine et al., 1998), *qIs56[Pcye-1::gfp, unc-119(+)]* (Kostic et al., 2003); *arIs82[lin-12::gfp; unc-4(+); Pegl-17::lacZ]* (Shaye and Greenwald, 2002), *zhIs1[lin-39::gfp]* (Szabó et al., 2009), *zhIs038[let-23::gfp, unc-119(+)]* (Haag et al., 2014), *zhIs80[Pcye-1::gfp], zhIs86[Pcye-1::gfp, unc-119(+)], zhIs87[Pcye-1ΔHBS1::gfp, unc-119(+)], zhIs88[Pcye-1ΔHBS2::gfp, unc-119(+)], zhIs89[Pcye-1ΔHBS1ΔHBS2::gfp, unc-119(+)], zhEx500[Pbar-1::nicd::gfp, unc-119(+)]* (Nusser-Stein et al., 2012), *arEx1541[Plin-31::2nls::yfp]* (la Cova and Greenwald, 2012), *gaEx69[lin-31(PhD); unc-29(+)]* (Tan et al., 1998), *zhEx530[cdc-14::gfp], zhEx535[Pcdk-4::gfp], zhEx536[Plin-31::cye-1], zhEx542[Pbar-1::nicd::gfp, unc-119(+)].*

Plasmids and transgenic lines

Plasmid pDR8 (*Pcye-1::gfp*) was made by cloning the promoter and the first part of the coding region (-942 to +1375) in frame with the *gfp* cassette into the HindIII and SalI sites of plasmid pPD95.75 (a gift from Andrew Fire). pDR9 (*Plin-31::cye-1)* was built by cloning full length *cye-1* cDNA into the NotI and SalI sites of plasmid pB253 (Tan et al., 1998). pDR10 (*Pcdk-4::gfp*) was made by introducing the *cdk-4* promoter region including the two annotated isoforms (-800 to +1588) into the BamHI and SphI sites of plasmid pPD96.04 (a gift from Andrew Fire). pMS253 *(cdc-14c::gfp)* was a kind gift from Saito et al. (Saito et al., 2004). pDR11 (*Pcye-1::gfp, unc-119(+)*) was built by cloning a 4 kb SpeI fragment containing the *Pcye-1::gfp* reporter from the plasmid pDR8 into the SpeI site of the *mosSCI* vector pCFJ151 (Frøkjaer-Jensen et al., 2008). pDR12 (*Pcye-1ΔHBS1::gfp, unc-119(+)*), pDR13 (*Pcye-1ΔHBS2::gfp, unc-119(+)*) and pDR15 (*Pcye-1ΔHBS1ΔHBS2::gfp, unc-119(+)*) were obtained by site-directed mutagenesis of the plasmid pDR11 introducing the mutations described in the results section. The primers used for plasmid constructions are listed in **Table 3.1.S2**.

Worms carrying extra-chromosomal arrays were generated by microinjection of purified plasmid DNA into the syncytial gonads of young adult worms (Mello et al., 1991). All constructs were injected at a concentration of 50 ng/µl. For *zhIs80*, *zhEx530*, *zhEx535* and *zhEx542* we used pCFJ90 (*Pmyo-2::mcherry)* as transformation marker at a concentration of 2.5 ng/µl (Frøkjaer-Jensen et al., 2008). The total concentration of injected DNA was adjusted to 150 ng/µl by adding the plasmid pBluescript-KS. For the generation of the *mosSCI* lines (Frøkjaer-Jensen et al., 2008), *zhIs86* to *zhIs89*, we injected the plasmids pDR11, pDR12, pDR13 or pDR15 together with the markers pCFJ90 (*Pmyo-2::mcherry)* at a concentration of 2.5 ng/µl, pCFJ104 (*Pmyo-3::mcherry)* at a concentration of 5 ng/µl and pGH8 (*Ppan.::mcherry)* at a concentration of 10 ng/µl, together with the *Mos1* transposase plasmid pJL43.1 at a concentration of 50 ng/µl (Frøkjaer-Jensen et al., 2008).

Microscopy and data analysis

Animals were mounted on 4% agarose pads in 20mM tetramisole hydrochloride in aqueous solution. The vulval induction index was scored as described in (Berset et al., 2001). To obtain synchronized late L2 larvae, oocytes were isolated by hypochlorite treatment of gravid adults, allowed to hatch in the absence of food for 24 hours to obtain arrested L1 larvae that were transferred to plates containing OP50 bacteria and grown until they had reached the late L2/early L3 stage. For S-phase arrest, hydroxyurea was added to synchronized L2 larvae at a concentration of 40mM as described in (Ambros, 1999). The location of the vulval invaginations and the number of cells per invagination were counted using Nomarski optics in a Leica DMRA microscope equipped with a cooled CCD camera (Hamamatsu ORCA-ER) controlled by the Openlab 5 software (Improvision). To quantify GFP reporter expression, a calibrated fluorescent light source (X-Cite exacte, Excelitas Technologies Corp) was used on the same microscope. To compare GFP expression levels in the *eff-1(lf)* and *eff-1(lf); lin-39(lf)* backgrounds, images were acquired under the same illumination conditions and acquisition settings. Fluorescent signal intensities in the VPC nuclei were quantified using the Fiji software as described (Schindelin et al., 2012).

ChIP Q-PCR Analysis

Chromatin extracts were prepared from 100 ml mixed-stage liquid cultures of animals carrying the *zhIs1[lin-39::gfp]* and *zhIs89[Pcye-1ΔHBS1ΔHBS2::gfp]* arrays. As negative controls, extract from animals carrying only *zhIs89[Pcye-1ΔHBS1ΔHBS2::gfp]* were prepared and processed in parallel. Cross-linking was done with 1% paraformaldehyde for 20 minutes at room temperature. LIN-39::GFP bound chromatin was precipitated using GFP-Trap® antibodies (Chromotek) as described in Pellegrino et al. (Pellegrino et al., 2011) and following the protocol by (Mukhopadhyay et al., 2008) with the following modification:

Extracts were pre-cleared by incubation with Dynabeads (10 µl of stock solution per sample) before adding GFP-Trap® beads (20µl of stock solution per 4-5 mg/ml of total protein in the samples). After reverse cross-linking, the binding of LIN-39::GFP to the different sites was quantified by performing Q-PCR using an ABI Prism 7900HT thermocycler with the MESA Green mastermix plus (Eurogentec) and primers specific for the wild-type HBS in endogenous *cye-1* and the mutant HBS in the *zhIs89* reporter (**Fig. 3.1.3E**, for the sequences of the primer used see **Table 3.1.S2**). For each measurement, the signal was first normalised to the signal obtained from the input DNA (% input). To calculate the specific enrichment, the % input value obtained with each Q-PCR assay from the *zhIs1[lin-39::gfp]*; *zhIs89[Pcye-1ΔHBS1ΔHBS2::gfp]* strain was divided by the % input value obtained from the *zhIs89[Pcye-1ΔHBS1ΔHBS2::gfp]* negative control strain. In addition to the Q-PCR assays in the HBS regions, we used a primer pair in the 3' UTR of *cye-1* and a primer pair spanning the *cye-1-gfp* fusion in the *zhIs89* reporter. The data in figure 3F show the average ratios obtained in three independent experiments.

Statistical analysis

t-tests for independent samples were used to determine the statistical significance of differences in fluorescence intensity values (**Fig. 3.1.3D**). To test the statistical significance of all other data, the Fisher's exact probability test was performed. In all figures, * indicates $p<0.05$, ** $p<0.005$ and *** $p<0.001$.

3.1.6 Acknowledgements

We wish to thank all past and present members of the Hajnal lab for their inputs and comments throughout this work. We are grateful to Erika Fröhli for her technical support. We are also grateful to the Saito and Kim labs for sharing reagents and to the *C. elegans* genetics center for providing strains. This work was supported by grants from the Swiss National Fond SNF to A.H. and the Kanton Zürich.

3.1.7 References

Ackermann, G. E. and Paw, B. H. (2003). Zebrafish: a genetic model for vertebrate organogenesis and human disorders. *Frontiers in Bioscience* **8**, d1227–53.

Ambros, V. (1999). Cell cycle-dependent sequencing of cell fate decisions in Caenorhabditis elegans vulva precursor cells. *Development* **126**, 1947–1956.

Berset, T., Hoier, E. F., Battu, G., Canevascini, S. and Hajnal, A. (2001). Notch Inhibition of RAS Signaling Through MAP Kinase Phosphatase LIP-1 During C. elegans Vulval Development. *Science* **291**, 1055–1058.

Bromleigh, V. C. and Freedman, L. P. (2000). p21 is a transcriptional target of HOXA10 in differentiating myelomonocytic cells. *genes & Development* **14**, 2581–2586.

Burdine, R. D., Branda, C. S. and Stern, M. J. (1998). EGL-17(FGF) expression coordinates the attraction of the migrating sex myoblasts with vulval induction in C. elegans. *Development* **125**, 1083–1093.

Celetti, A., Barba, P., Cillo, C. and Rotoli, B. (1993). Characteristic patterns of HOX gene expression in different types of human leukemia. *International Journal of Cancer* **53**, 237–244.

Chen, N. and Greenwald, I. (2004). The Lateral Signal for LIN-12/Notch in C. elegans Vulval Development Comprises Redundant Secreted and Transmembrane DSL Proteins. *Developmental Cell* **6**, 183–192.

Cheng, M., Olivier, P., Diehl, J. A. and Fero, M. (1999). The p21Cip1 and p27Kip1 CDK "inhibitors" are essential activators of cyclin D-dependent kinases in murine fibroblasts. *The EMBO Journal* **18**, 1571–1583.

Clark, S. G., Chisholm, A. D. and Horvitz, H. R. (1993). Control of Cell Fates in the Central Body Region of C. elegans by the Homeobox Gene /in-39. *Cell* **74**, 43–55.

Clayton, J. E., van den Heuvel, S. J. L. and Saito, R. M. (2008). Transcriptional control of cell-cycle quiescence during C. elegans development. *developmental biology* **313**, 603–613.

Cohn, M. J., Patel, K., Krumlauf, R., Wilkinson, D. G., Clarke, J. D. and Tickle, C. (1997). Hox9 genes and vertebrate limb specification. *Nature* **387**, 97–101.

Couronne, O., Poliakov, A., Bray, N., Ishkhanov, T., Ryaboy, D., Rubin, E., Pachter, L. and Dubchak, I. (2003). Strategies and tools for whole-genome alignments. *Genome Research* **13**, 73–80.

Eisenmann, D. M. (2005). Wnt signaling. *WormBook* 1–17.

Eisenmann, D. M., Maloof, J. N., Simske, J. S., Kenyon, C. and Kim, S. K. (1998). The β-catenin homolog BAR-1 and LET-60 Ras coordinately regulate the Hox gene lin-39 during Caenorhabditis elegans vulval development. *Development* **125**, 3667–3680.

Euling, S. and Ambros, V. (1996). Heterochronic genes control cell cycle progress and developmental competence of C. elegans vulva precursor cells. *Cell* **84**, 667–676.

Farooqui, S., Pellegrino, M. W., Rimann, I., Morf, M. K., Müller, L., Fröhli, E. and Hajnal, A. (2012). Coordinated Lumen Contraction and Expansion during Vulval Tube Morphogenesisin Caenorhabditis elegans. *Developmental Cell* **23**, 494–506.

Fay, D. S. and Han, M. (2000). Mutations in cye-1, a Caenorhabditis elegans cyclin E homolog, reveal coordination between cell-cycle control and vulval development. *Development* 1–12.

Ferguson, E. L. and Horvitz, H. R. (1985). Identification and characterization of 22 genes that affect the vulval cell lineages of the nematode Caenorhabditis elegans. *Genetics* **110**, 17–72.

Frøkjaer-Jensen, C., Davis, M. W., Hopkins, C. E., Newman, B. J., Thummel, J. M., Olesen, S.-P., Grunnet, M. and Jorgensen, E. M. (2008). Single-copy insertion of transgenes in Caenorhabditis elegans. *Nature genetics* **40**, 1375–1383.

Gleason, J. E., Szyleyko, E. A. and Eisenmann, D. M. (2006). Multiple redundant Wnt signaling components function in two processes during C. elegans vulval development. *developmental biology* **298**, 442–457.

Guerry, F., Marti, C.-O., Zhang, Y., Moroni, P. S., Jaquiery, E. and Muller, F. (2007). The Mi-2 nucleosome-remodeling protein LET-418 is targeted via LIN-1/ETS to the promoter of lin-39/Hox during vulval development in C. elegans. *developmental biology* **306**, 469–479.

Haag, A., Gutierrez, P., Bühler, A., Walser, M., Yang, Q., Langouët, M., Kradolfer, D., Fröhli, E., Herrmann, C. J., Hajnal, A., et al. (2014). An in vivo EGF receptor localization screen in C. elegans Identifies the Ezrin homolog ERM-1 as a temporal regulator of signaling. *PLoS Genet.* **10**, e1004341.

Hombría, J. C.-G. and Lovegrove, B. (2003). Beyond homeosis--HOX function in morphogenesis and organogenesis. *Differentiation* **71**, 461–476.

Hong, Y., Roy, R. and Ambros, V. (1998). Developmental regulation of a cyclin-dependent kinase inhibitor controls postembryonic cell cycle progression in Caenorhabditis elegans. *Development* **125**, 3585–3597.

Hwang, B. J. and Sternberg, P. W. (2004). A cell-specific enhancer that specifies lin-3 expression in the C. elegans anchor cell for vulval development. *Development* **131**, 143–151.

Jacobs, D., Beitel, G. J., Clark, S. G., Horvitz, H. R. and Kornfeld, K. (1998). Gain-of-function mutations in the Caenorhabditis elegans lin-1 ETS gene identify a C-terminal regulatory domain phosphorylated by ERK MAP kinase. *Genetics* **149**, 1809–1822.

Kostic, I., Li, S. and Roy, R. (2003). cki-1 links cell division and cell fate acquisition in the C. elegans somatic gonad. *developmental biology* 1–11.

la Cova, de, C. and Greenwald, I. (2012). SEL-10/Fbw7-dependent negative feedback regulation of LIN-45/Braf signaling in C. elegans via a conserved phosphodegron. *genes & Development* **26**, 2524–2535.

LaBaer, J., Garrett, M. D. and Stevenson, L. F. (1997). New functional activities for the p21 family of CDK inhibitors. *genes & Development* **11**, 847–862.

Lewis, E. B. (1978). A gene complex controlling segmentation in Drosophila. *Nature* **276**, 565–570.

Mahfooz, N. S., Li, H. and Popadić, A. (2004). Differential expression patterns of the hox gene are associated with differential growth of insect hind legs. *PNAS* **101**, 4877–4882.

Maloof, J. N. and Kenyon, C. (1998). The Hox gene lin-39 is required during C. elegans vulval induction to select the outcome of Ras signaling. *Development* **125**, 180–191.

Mann, R. S. and Affolter, M. (1998). Hox proteins meet more partners. *Curr. Opin. Genet. Dev.* **8**, 423–429.

Mello, C. C., Kramer, J. M., Stinchcomb, D. and Ambros, V. (1991). Efficient gene transfer in C. elegans: extrachromosomal maintenance and integration of transforming sequences. *The EMBO Journal* **10**, 3959–3970.

Moss, E.G., Lee, R.C. and Ambros, V. (1997). The cold shock domain protein LIN-28 controls developmental timing in C. elegans and is regulated by the *lin-4* RNA. *Cell* **88**, 637–646.

Mukhopadhyay, A., Deplancke, B., Walhout, A. J. M. and Tissenbaum, H. A. (2008). Chromatin immunoprecipitation (ChIP) coupled to detection by quantitative real-time PCR to study transcription factor binding to DNA in Caenorhabditis elegans. *Nat Protoc* **3**, 698–709.

Niu, W., Lu, Z. J., Zhong, M., Sarov, M., Murray, J. I., Brdlik, C. M., Janette, J., Chen, C., Alves, P., Preston, E., et al. (2011). Diverse transcription factor binding features revealed by genome-wide ChIP-seq in C. elegans. *Genome Research* **21**, 245–254.

Nusser-Stein, S., Beyer, A., Rimann, I., Adamczyk, M., Piterman, N., Hajnal, A. and Fisher, J. (2012). Cell-cycle regulation of NOTCH signaling during C. elegans vulval development. *Molecular Systems Biology* **8**, 1–14.

Park, M. and Krause, M. W. (1999). Regulation of postembryonic G(1) cell cycle progression in Caenorhabditis elegans by a cyclin D/CDK-like complex. *Development* **126**, 4849–4860.

Pellegrino, M. W., Farooqui, S., Fröhli, E., Rehrauer, H., Kaeser-Pebernard, S., Muller, F., Gasser, R. B. and Hajnal, A. (2011). LIN-39 and the EGFR/RAS/MAPK pathway regulate C. elegans vulval morphogenesis via the VAB-23 zinc finger protein. *Development* **138**, 4649–4660.

Regős, Á., Lengyel, K., Takács-Vellai, K. and Vellai, T. (2013). Identification of novel cis-regulatory regions from the Notch receptor genes lin-12 and glp-1 of Caenorhabditis elegans. *Gene Expression Patterns* **13**, 66–77.

Rezsohazy, R., Saurin, A. J., Maurel-Zaffran, C. and Graba, Y. (2015). Cellular and molecular insights into Hox protein action. *Development* 142, 1212–1227.

Roy, S. H., Clayton, J. E., Holmen, J., Beltz, E. and Saito, R. M. (2011). Control of Cdc14 activity coordinates cell cycle and development in Caenorhabditis elegans. *Mechanisms of Development* **128**, 317–326.

Saito, R. M., Perreault, A., Peach, B., Satterlee, J. S. and van den Heuvel, S. (2004). The CDC-14 phosphatase controls developmental cell-cycle arrest in C. elegans. *Nat Cell Biol* **6**, 777–783.

Salser, S. J., Loer, C. M. and Kenyon, C. (1993). Multiple HOM-C gene interactions specify cell fates in the nematode central nervous system. *genes & Development* **7**, 1714–1724.

Sapir, A., Choi, J., Leikina, E., Avinoam, O. and Valansi, C. (2007). AFF-1, a FOS-1-regulated fusogen, mediates fusion of the anchor cell in C. elegans. *Developmental Cell* **12**, 683–698.

Schiedlmeier, B., Santos, A. C. and Ribeiro, A. (2007). HOXB4's road map to stem cell expansion.pp. 16952–16957.

Schindelin, J., Arganda-Carreras, I., Frise, E., Kaynig, V., Longair, M., Pietzsch, T., Preibisch, S., Rueden, C., Saalfeld, S., Schmid, B., et al. (2012). Fiji: an open-source platform for biological-image analysis. *Nat. Methods* **9**, 676–682.

Schindler, A. J. and Sherwood, D. R. (2012). Morphogenesis of the Caenorhabditis elegans vulva. *WIREs Dev Biol* **2**, 75–95.

Schmid, T. and Hajnal, A. (2015). Signal transduction during C. elegans vulval development: a NeverEnding story. *Curr. Opin. Genet. Dev.* **32**, 1–9.

Shaye, D. D. and Greenwald, I. (2002). Endocytosis-mediated downregulation of LIN-12/Notch upon Ras activation in Caenorhabditis elegans. *Nature* **420**, 686–690.

Shemer, G. and Podbilewicz, B. (2002). LIN-39/Hox triggers cell division and represses EFF-1/fusogen-dependent vulval cell fusion. *genes & Development* **16**, 3136–3141.

Siegfried, K. R. and Kimble, J. (2002). POP-1 controls axis formation during early gonadogenesis in C. elegans. *Development* **129**, 443–453.

Sternberg, P. W. (2005). Vulval development. *WormBook*.

Sundaram, M. V. (2006). RTK/Ras/MAPK signaling. *WormBook* 1–19.

Szabó, E., Hargitai, B., Regős, Á., Tihanyi, B. and Barna, J. (2009). TRA-1/GLI controls the expression of the Hox gene lin-39 during C. elegans vulval development. *developmental biology* **330**, 339–348.

Takács-Vellai, K., Vellai, T., Chen, E. B., Zhang, Y., Guerry, F., Stern, M. J. and Müller, F. (2007). Transcriptional control of Notch signaling by a HOX and a PBX/EXD protein during vulval development in C. elegans. *Dev Biol* **302**, 661–669.

Tan, P. B., Lackner, M. R. and Kim, S. K. (1998). MAP Kinase Signaling Specificity Mediated by the LIN-1 Ets/LIN-31 WH Transcription Factor Complex during C. elegans Vulval Induction. *Cell* **93**, 569–580.

Thummel, R., Ju, M., Sarras, M. P. and Godwin, A. R. (2007). Both Hoxc13 orthologs are functionally important for zebrafish tail fin regeneration. *Dev Genes Evol* **217**, 413–420.

Trinkaus, J. P. (1969). Cells into organs: the forces that shape the embryo. *Foundations of Developmental Biology*.

van den Heuvel, S. (2005). Cell-cycle regulation. *WormBook* 1–16.

Wagmaister, J. A., Gleason, J. E. and Eisenmann, D. M. (2006a). Transcriptional upregulation of the C. elegans Hox gene lin-39 during vulval cell fate specification. *Mechanisms of Development* **123**, 135–150.

Wagmaister, J. A., Miley, G. R., Morris, C. A., Gleason, J. E., Miller, L. M., Kornfeld, K. and Eisenmann, D. M. (2006b). Identification of cis-regulatory elements from the C. elegans Hox gene lin-39 required for embryonic expression and for regulation by the transcription factors LIN-1, LIN-31 and LIN-39. *developmental biology* **297**, 550–565.

Yang, L. (2005). The roles of two C. elegans HOX co-factor orthologs in cell migration and vulva development. *Development* **132**, 1413–1428.

Yoo, A. S., Bais, C. and Greenwald, I. (2004). Crosstalk between the EGFR and LIN-12/Notch pathways in C. elegans vulval development. *Science* **303**, 663–666.

Zhang, X. and Greenwald, I. (2011). Spatial Regulation of lag-2 Transcription During Vulval Precursor Cell Fate Patterning in Caenorhabditis eleganslag-2. *Genetics* **188**, 847–858.

3.1.8 Supplementary Material

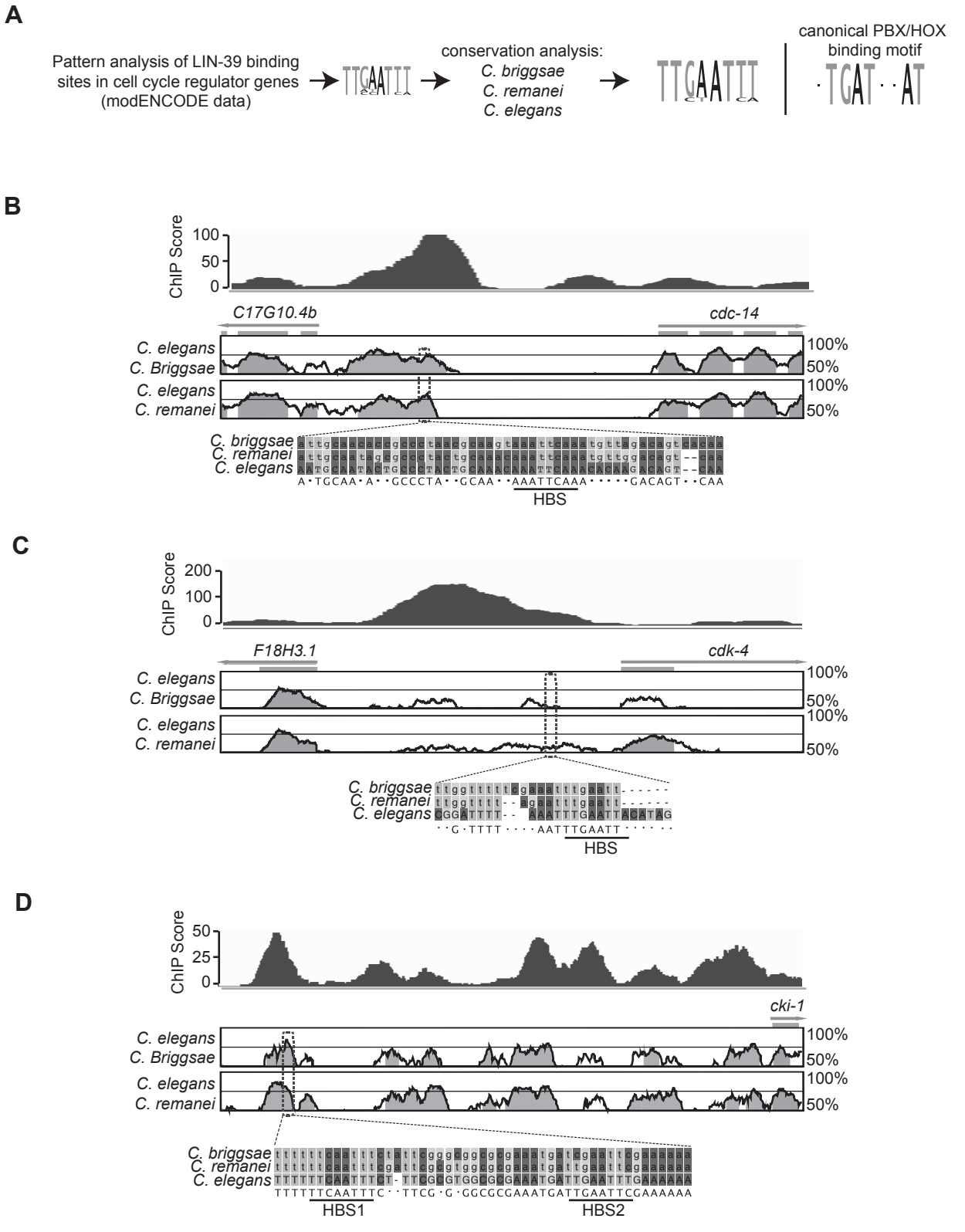

Supplementary Figure 3.1.S1

(A) Strategy used for the identification of the HBS motif. The DNA sequences in the LIN-39 binding regions the cell cycle regulator genes *cki-1*, *cdk-4*, *cye-1*, *cdc-14*, *cdk-1*, *cdk-7*, *lin-35*, *efl-1*, *lin-9*, *mat-1*, *mrt-2*, *cul-1*, *san-1*, *mdf-1*, *wee-1.3*, *lin-23* and *lin-36* that had been identified by modENCODE were searched for common motifs using the pattern finder tool in the CLC Main Workbench software package (http://www.clcbio.com). Alignment of the predicted binding regions with the *C. briggsae* and *C. remanei* syntenic regions was used to exclude non-conserved patterns. This lead to the identification of the motif as a putative HBS. **(B-D)** Analysis of the *cdc-14*, *cdk-4* and *cki-1* genomic regions. For each locus, the modENCODE LIN-39 ChIP peaks (Niu et al., 2011) are shown above the gene structure, and the conservation plots with the syntenic *C. briggsae* and *C. remanei* regions provided by (Couronne et al., 2003) and the sequence alignments of the regions containing the predicted HBS motifs are shown underneath.

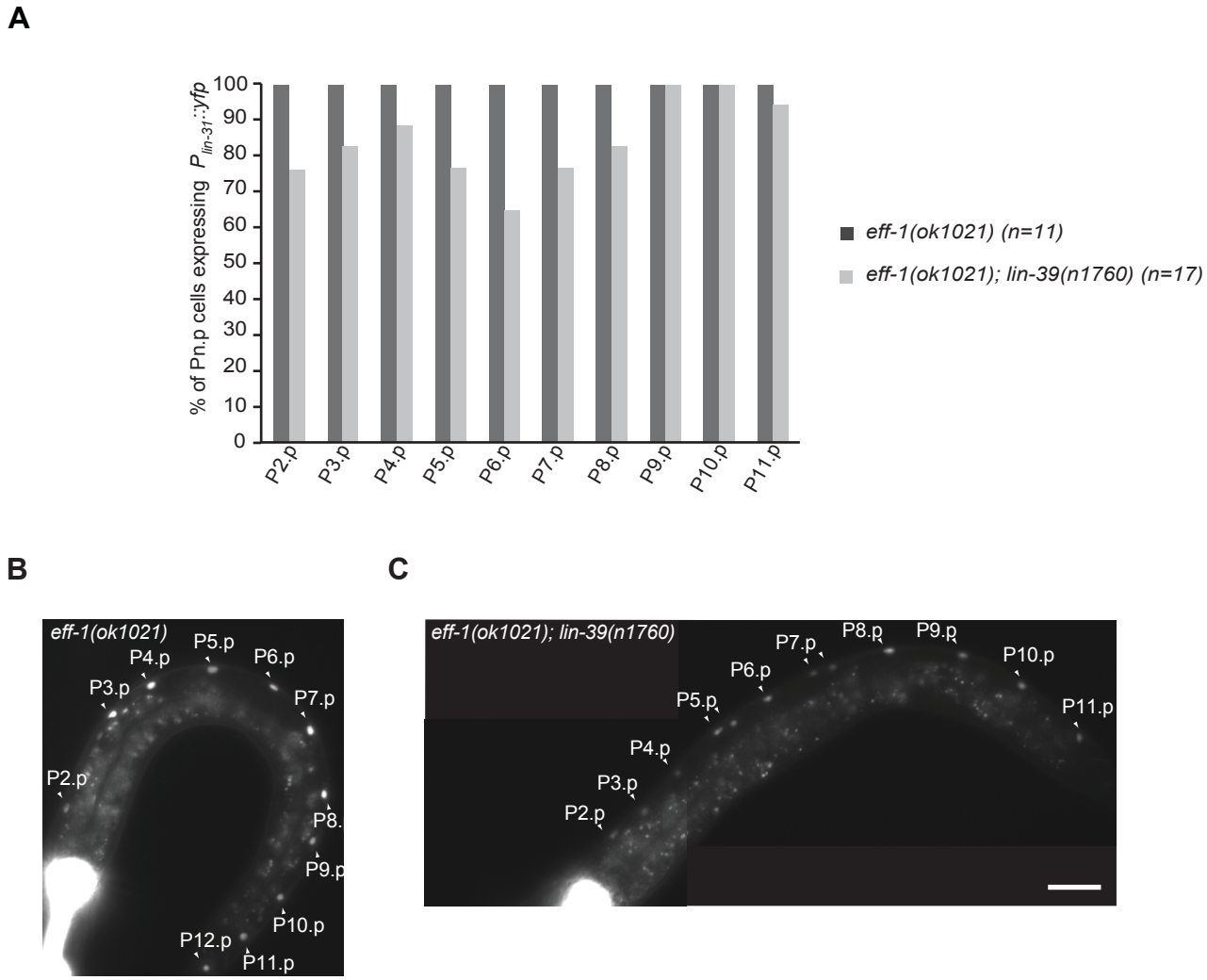

Supplementary Figure 3.1.S2

(A) Expression of the *Plin-31::yfp* reporter in the Pn.p cells P2.p through P11.p in *eff-1(lf)* single and *eff-1(lf); lin-39(lf)* double mutants. Even though some of the anterior Pn.p cells occasionally appeared to be missing, this phenotype cannot explain the posterior shift of the vulval invaginations shown in **Fig. 3.1.4** and **Table 3.1.1**. **(B)** *Plin-31::yfp* expression in a *eff-1(lf)* single and **(C)** an *eff-1(lf); lin-39(lf)* double mutant. Note the occasional duplication of Pn.p cells such as P5.p and P7.p in the example shown in (**C**). The scale bar in (**C**) is 10 μm.

P5.p

Reporter	ΔHBS1	ΔHBS2	ΔHBS1ΔHBS2
wild-type	0.0125050	0.0889219	0.0006429
ΔHBS1	NA	0.0000733	0.1703919
ΔHBS2	NA	NA	0.0212756

P6.p

Reporter	ΔHBS1	ΔHBS2	ΔHBS1ΔHBS2
wild-type	0.0000007	0.0017253	0.0000001
ΔHBS1	NA	0.0000733	0.0681572
ΔHBS2	NA	NA	0.0000008

P7.p

Reporter	ΔHBS1	ΔHBS2	ΔHBS1ΔHBS2
wild-type	0.0018787	0.2251436	0.0000089
ΔHBS1	NA	0.0000733	0.0160185
ΔHBS2	NA	NA	0.0004727

≤0.05
≤0.005
≤0.001

Supplementary Table 3.1.S1 Statistical analysis of *cye-1::gfp* expression

p-values of the statistical analysis (t-test) of the differences between the gfp intensities in the vulval cells between the four cye-1 reporters analyzed in **Fig. 3.1.3**. White indicates no significant difference. Light grey indicates $p<0.05$; medium grey $p<0.005$ and dark grey $p<0.001$.

Plasmid construction

ODR-85	agtcgacctgcaggcatgcaagctctcaggcatagctggaagtggttg	*Pcye-1* in pPD95.75 (Rev)
ODR-222	tttaagcttgaccctcgtcctcatcgtctg	*Pcye-1* in pPD95.75 (Fwd)
ODR-241	tttgtcgacatggctggaagaaagtcatc	*cye-1 cdna* (Fwd)
ODR-242	aaagcggccgcttagaaaagtcgttgcggatg	*cye-1 cdna* (Rev)
ODR-243	aaaggatcccctccataggcgccttttccaag	*Pcdk-4* in pPD96.04 (Rev)
ODR-244	tttgcatgcccaaacatgaaaaccaaccacg	*Pcdk-4* in pPD96.04 (Fwd)
ODR-259	cgcgattt**cccc**ctagagaccatatgacg	Mutagenesis HBS1
ODR-260	tctcta**gggg**gaaatcgcgcgctcatttc	Mutagenesis HBS1
ODR-263	cagacactt**cccc**ttgaccagtgtaatag	Mutagenesis HBS2
ODR-264	ctggtcaa**gggg**aaagtgtctgtttctcag	Mutagenesis HBS2

Q-PCR experiments

ODR-286	gtcatatggtctctaggggg	Δ1HBS RT-PCR
ODR-290	gtcatatggtctctagattc	1HBS RT-PCR
ODR-292	gagaaacagacactttgtat	2HBS RT-PCR
ODR-288b	aaacagacactttcccc	Δ2HBS RT-PCR
ODR-262	agttgctgtgccctctattg	Δ1HBS/1HBS RT-PCR
ODR-265	gatgtctgcgtcttattttc	Δ2HBS/2HBS RT-PCR
ODR-294	ccccggaaaatatcaaaaac	RT-PCR control (UTR)
ODR-295	caaagtaagaaggggaagtg	RT-PCR control (UTR)
ODR-302	cattcgaaacatacctttggg	RT-PCR control (*gfp*)
ODR-303	cgtgaagttggatcttcatc	RT-PCR control (*gfp*)

Supplementary Table 3.1.S2

Primers used for plasmid constructs described in materials and methods and the Q-PCR analysis of the ChIP experiments in **Fig. 3.1.3**.

3.2 Additional experiments

3.2.1 The modification of single components of the cell cycle does not suppress the lack of proliferation in *lin-39* mutants

To assess whether *lin-39* is a general regulator of the cell cycle and necessary for cell cycle components expression or it plays a secondary role by enhancing the expression of those components, we looked for the rescue of the proliferation phenotype of *eff-1(lf); lin-39(lf)* animals in two different ways:
First, we tried to rescue this phenotype by knocking out *cdc-14* -the *cki-1* phosphatase- using a null allele *he141*. If *lin-39* does not play a major role in the regulation of the expression of the cell cycle components, we would expect more proliferation when knocking out *cdc-14*. Thus, *cdc-14(lf); eff-1(lf); lin-39(lf)* animals would accumulate phosphorylated/inactive CKI-1 and therefore would be more prompt to proceed with the cell cycle. We observed no significant differences either in the number of invaginations nor in the number of cells per invagination between the *cdc-14(lf); eff-1(lf); lin-39(lf) and the eff-1(lf); lin-39(lf)* **(Table 3.1.1)**.
Second, we tried to promote cell cycle progression by over-expressing *cye-1* with the *lin-31* promoter in all the VPCs. Similarly to the previous experiment; if *lin-39* was playing only a role as an enhancer we expect proliferation upon the over-expression of *cye-1.* We observed no differences between those animals carrying the *Plin-31::cye-1* construct and those without it **(Table 3.1.1)**.
Taken together, we conclude that the modification of a single component of the pathway did not alter the output and therefore *lin-39* may play a general role controlling the activation of the expression of at least several cell cycle components.

3.2.2 The Pn.p cells are present in *lin-39(lf)* mutants

The phenotype observed in the *lin-39* mutants could be also due to the lack or defective formation of the Pn.p lineage. We used *Plin-31::yfp* as a marker to analyze whether the Pn.p were formed and distributed along the anterior-posterior axis in the ventral side of the animal.
In both, the *eff-1(lf)* mutants and the *eff-1(lf); lin-39(lf)* mutants, we could clearly identify the Pn.p lineage in the ventral side of the animal distributed along the anterior-posterior axis of the animal. Yet, in some *eff-1(lf); lin-39(lf)* we could observe that some Pn.p cells were

mislocalized or duplicated. Often, two Pn.p cells were located close to each other in the middle region of the animal, while one of the anterior Pn.p cells was missing. This phenotype could be due to a failure in the migration of the P progenitors, the duplication of some of the Pn.p lineages or a combination of both. On the other hand, we could identify always 11 Pn.p cells. P12.p does not express *lin-31* **(Table 3.1.1)**.
Altough *lin-39(lf)* animals have defects in the Pn.p lineage formation, these could not explain the phenotypes observed in subsequent steps during vulval development. Therefore, the phenotype observed during vulval development must be due to other roles of *lin-39* during the cell fate acquisition and cell cycle progression.

3.2.3 The ablation of the AC does not phenocopy the lack of *lin-39*

The AC releases LIN-3, which activates RAS signaling in the 1° cells, enhancing the expression of *lin-39*. Thus, mutants that cannot transcribe *lin-3* in the AC lead to an under induction of the vulval tissue. This effect is more severe when the early gonad is ablated and no gonad tissue is formed. Therefore, we tested whether the VPCs of gonad ablated *eff-1(lf)* animals was similar to those of *eff-1(lf); lin-39(lf).*
The *eff-1(lf)* ablated animals did not form any type of invagination, and at the L4 stage the VPCs could be still clearly identified in the ventral side. In addition, in most cases, these VPCs acquired the 3° cell fate, dividing once. On the other hand, the *eff-1(lf); lin-39(lf)* animals rarely showed a 3° cell fate and, as previously described, in some cases they formed an invagination. Therefore, we conclude that the secretion of LIN-3 still influences the behavior of the VPCs in the absence of *lin-39*.

3.2.4 *lin-39(ts)* partially resemble the phenotype observed with the cell cycle reporters in the *lin-39(lf)*

To verify the results observed with the *loss-of-function* allele of *lin-39*, we decided to test our cell cycle reporters for *cki-1, cdk-4* and *cye-1* in the previously described *temperature sensitive* allele of *lin-39 n709* (Clark et al., 1993). Furthermore, first to avoid possible fusions to the hypodermis and second to reproduce the set-up of previous experiments as closely as possible, we made all our experiments in the *eff-1(ok1021)* background. For this purpose we grew animals for 20 hours at 20°C for the *cki-1* and *cdk-4* reporters and for 25 hours at 20°C for the *cye-1* reporter. After this standard phase of growth a sample of the population was switch to 25°C for 4 hours while the rest was kept at 20°C for the same period. Finally the animals were analyzed under fluorescence microscopy and the expression of the reporters

quantified. In addition, and as previously described, the animals carrying the *cye-1* reporter were incubated with Hydroxiurea to enhance the chance to observe the reporter expression in the VPCs.

For the *cki-1* reporter we observed a strong reduction of VPCs expressing the reporter. Thus, while the animals growing at permissive temperature showed on average expression in 81% of their VPCs, those that suffered the heat shock only presented expression in 55% of their VPCs **(Fig. 3.2.1)**. This result supports the direct role of *lin-39* as regulator of *cki-1* expression. Unfortunately we did not observe a reduction in the number of animals expressing *cdk-4* reporter (60% at permissive temperature *versus* 69% after the heat shock) or in those carrying the *cye-1* reporter (29% at permissive temperature *versus* 34% after the heat shock) **(Fig. 3.2.1)**. Both led to a slight and probably not biologically significant change in their expression. One possibility to explain those results is the low efficiency of the heat shock to remove all functional *lin-39*. In addition, the results for the *cdk-4* reporter are very preliminary since they were only analyzed in one experiment without replicas.

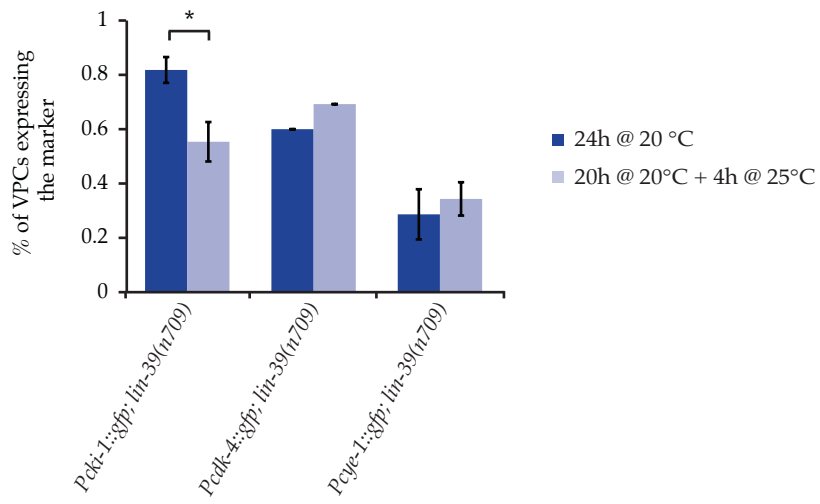

Fig. 3.2.1: *lin-39(ts)* partially resembles the phenotype observed in *lin-39(lf)*

lin-39(n709) animals carrying the transcriptional reporter for *cki-1*, *cdk-4* and *cye-1* were grown at 20°C for 20 hours and then switched to 25°C, temperature in which the allele *n709* is unstable and therefore not functional. Only *cki-1* reporter shows an effect after 4 hours in the restrictive temperature (25°C). The animals carrying the *cye-1* reporter were incubated for 25h at 20°C and afterwards switched to 25°C and exposed to Hidroxyurea. The error bars represent the s.e.m of the three replicates. For the *cdk-4* reporter only one replicate was quantified.

3.2.5 CKI-1 abundance in the nucleus indicates the lack of cell cycle in the *lin-39(lf)*

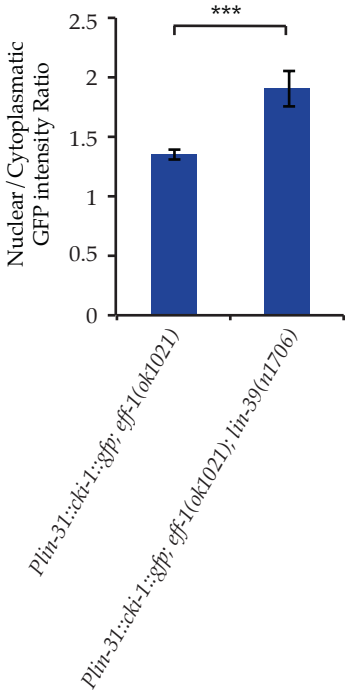

Fig. 3.2.2: CKI-1 is stabilized in the nucleus of *lin-39(lf)* mutants
GFP intensity quantification of a CKI-1 translational reporter driven by the promoter of the Pn.p specific gene *lin-31*. The ratio was calculated dividing the intensity value obtained per cell in the cytoplasm by the value obtained in the nucleus of the same cell. Plotted is the mean value of the ratio and the error bars represent the SEM. The *lin-39(lf)* animals show an enrichment in the nuclear pool of CKI-1.

The VPCs are arrested in G1 during the L2 larval stage. This is due to the expression and activation of CKI-1, which represses the CDK-2/CYE-1 complex and therefore the transition into S phase. Active CKI-1 is localized in the nucleus and upon phosphorylation by the CDK-4/CYD-1 complex is excluded to the cytoplasm.

Our previous experiments indicated that the cell cycle in the VPCs of the *eff-1(lf); lin-39(lf)* is not active as opposed to the wild-type animals or *eff-1(lf)* where the cell cycle before induction is simply arrested. These two conditions, even when they may appear similar are indeed different. In the first one, none of the components of the cell cycle are expressed and the cell is in a G0 phase where proliferative stimuli are not taken into account. In the second one, the cell has the cell cycle components ready to proceed, but certain factors like CKI-1 arrest the cell in a *gap* phase until the proliferative stimuli arrive.

Taking this into account we used a *gfp* translational reporter of CKI-1 driven by the *lin-31* promoter (*cki-1* expression is strongly reduced in *lin-39(lf)* mutants) to further verify the stage of the cell cycle in the VPCs of *eff-1(lf); lin-39(lf) versus eff-1(lf)* animals.

On control animals the GFP intensity ratio between the nucleus and the cytoplasm of the VPCs was 1.35, indicating that even when more CKI-1 was active an probably arresting the cell cycle in G1, there was an equilibrium between the active and inactive pool of CKI-1. On the contrary, the intensity ratio for the *eff-1(lf); lin-39(lf)* animals was on average 1.9, indicating that most of the CKI-1 pool was not phosphorylated and ready to arrest the cell cycle, probably due to the absence of *cdk-4* expression among others factors **(Fig. 3.2.2)**.

These results together with our transcriptional reporter data and the finding that LIN-39 directly binds the promoter of several cell cycle components support the idea of a complete shut-down of the cell cycle in the VPCs of *lin-39(lf)* mutants (see section 3.1).

3.2.6 Expression of *lin-1(gf)* does not show a clear effect in the expression of the cell cycle components

To test whether *lin-1* plays a positive role by promoting the expression of *cki-1, cdk-4* and *cye-1,* we analyzed the expression of transcriptional reporters of the genes under the influence of a truncated version of LIN-1 lacking the C terminus domain, *lin-1(ΔCT)*, analogous to the gain of function allele of *lin-1 e1790* (Jacobs et al., 1998). This allele is thought to function independently of LIN-31. We drove the expression of this *lin-1 gain of function* with a Heat shock promoter allowing us to restrict the effect of this allele to a time point of interest.
To perform this analysis we grew animals carrying each one of the cell cycle reporters and an extra chromosomal array of the *HS::lin-1(ΔTC)* at 20°C for 24 hours, followed by a heat shock treatment at 33°C for 30 minutes. Animals were incubated for 90 minutes at 20°C before analyzing the expression under the microscope. The control animals did not suffer heat shock. The array carrying the heat shock construct was extra chromosomal, therefore within the same population we analyzed transgenic animals carrying the *lin-1(gf)* array and the cell cycle reporter and transgenic animals without the array.
We observed a slight decrease in the expression of *cki-1* after the heat shock, indicating a possible role of LIN-1 promoting the cell cycle after its dissociation of LIN-31 upon induction, while could not quantify any significant differences for the *cdk-4* reporter **(Fig. 3.2.3)**. This result contradicts the findings of (Clayton et al., 2008). In their publication, Clayton and colleagues suggested that *lin-31* promotes the expression of *cki-1* independently of *lin-1,* but the lack of the last one showed also a slight reduction in the intensity of the reporter. Thus, *lin-1* could have a secondary role in promoting the expression of *cki-1,* perhaps helping *lin-31.* Taken together *lin-1* may repress the cell cycle by cooperating with *lin-31* prior to induction and as a promoter of cell cycle once it has dissociated from LIN-31. Yet, our results must be taken carefully since we observed that the levels of the *cki-1* reporter in the presence of the heat shock construct on the control animals (without heat shock) were extremely high in comparison with those observed in the control animals not carrying the heat shock construct.
The opposite effect was observed when studying the expression of *cdk-4*. We observed a slight increase in the expression of the *cdk-4* reporter, pointing in the same direction, yet the increase was not significant, due in part to the high variability observed among the VPCs of the same animals (Fig. 3.2.3). In addition, we observed a reduction in the expression of the *cdk-4* reporter upon heat shock in animals not carrying the *lin-1(gf)* construct **(Fig. 3.2.3)**. Taken together, we have observed that the *lin-1(gf)* could slightly influence the cell cycle of the VPCs by at least inhibiting the expression of *cki-1* and promoting the expression of *cdk-4.* These results, although weak, support that *lin-1* could play a secondary role in the cell cycle

of the VPCs promoting the progression as opposed to the primary role of *lin-31* promoting the arrest of the cell cycle (see section 3.1).

Finally we could not investigate the effect of the *lin-1(gf)* construct into the *cye-1* reporter given technical difficulties to quantify enough animals.

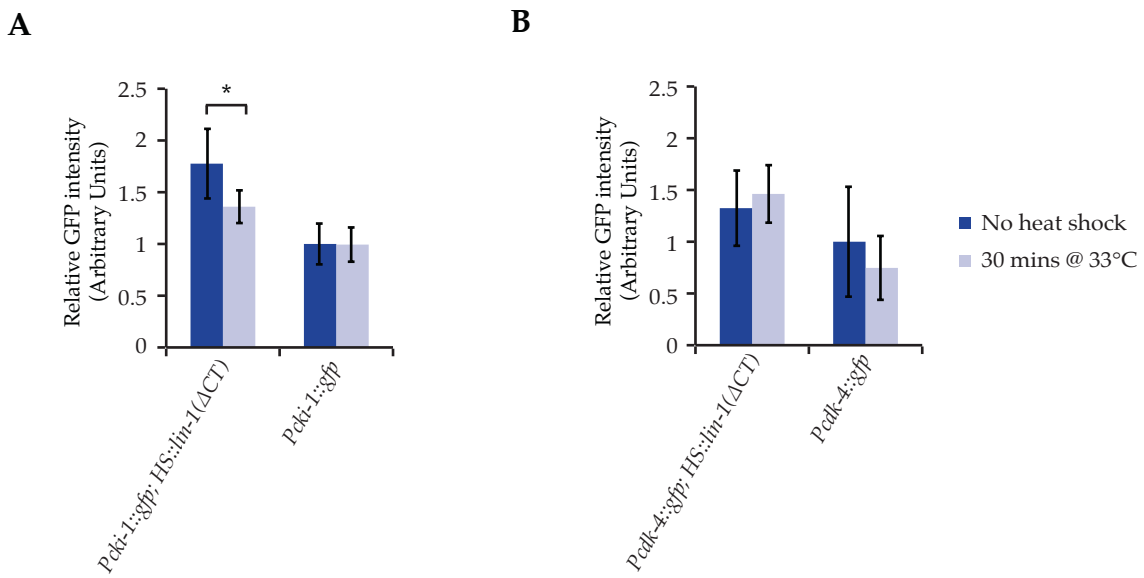

Fig. 3.2.3: The expression of *lin-1(gf)* does not show a clear effect in the expression of the cell cycle components

(A) Relative GFP intensity of the *Pcki-1::gfp* reporter under the influence of a heat shock construct expressing a truncated version of *lin-1* that acts as *gain of function*. A slight reduction upon heat shock can be observed **(B)** Relative GFP intensity of the *Pcdk-4::gfp* reporter under the influence of a heat shock construct expressing a truncated version of *lin-1* that acts as *gain of function*. A very slight increase in the intensity of the reporter can be observed after heat shock treatment. In both (A&B) the mean values are plotted and the error bars represent the SEM.

3.3 *chd-7* may control WNT signaling

3.3.1 Introduction

An important goal in developmental biology is to understand how organ development is controlled by several non-autonomous signals coming from other tissues. Those non-autonomous signals work in coordination to define cell fates, migration patterns and body location forming a functional organ.

WNT signaling and vulval precursor cells specification

The WNT signaling pathway is highly conserved among the bilateral group and plays a major role in the organization of their body plan (Nalbantoglu, 2011). In *C. elegans*, it controls many different aspects that go from the positioning of neurons to the specification of the vulval competence group (Gleason et al., 2006; Korswagen, 2002). This signaling cascade can be usually subdivided in two major steps, the production and release of the ligands by the producing cells, which are generally allocated in the posterior side of the developing animal, and the activation of intracellular factors in the receiving cells that are distributed a long the body axis. Both steps have been deeply studied, but is not clearly understood how the ligand production at the transcriptional level is controlled and how the pathway leads to a transcriptional switch in the receiving cells.

C. elegans expresses five different ligands –*cwn-1, egl-20, cwn-2, mom-2* and *lin-44*-, all of them are mostly expressed in different cells of the animal's tail, with the exception of *mon-2* that presents a broader expression pattern and *cwn-2* that is also expressed in the head (Gleason et al., 2006). In addition, the pathway can activate 5 different receptors that coexist in some tissues. This variety of ligands and receptors lead to 2 different outcomes in the receiving cell: the canonical WNT pathway **(Fig. 3.3.1A)**, where ß-catenin is released from the membrane complex translocating to the nucleus and switching transcription; and the non-canonical pathway **(Fig. 3.3.1B)**, where other factors like *pop-1* are the executers (Dale, 1998; Korswagen, 2002; Whangbo and Kenyon, 2010).

In the *C. elegans* vulva, WNT signaling is responsible for the specification of the vulval competence group. At the early L1 larval stage, the WNT ligands generate a gradient from tail to head activating the transcription of different *hox* genes along the anterior-posterior axis. Among those genes is *lin-39*. Its transcription is promoted in the mid-body Pn.p cells (P3.p-P8.p) constituting the vulval precursor cells (Koh et al., 2002; Wagmaister et al., 2006a). The ligands *cwn-1* and *egl-20* play a major role, being the loss of function of *cwn-1* the only

one that shows a phenotype in the competence of the VPCs by itself. Yet, the combination of mutants of the different ligands leads to similar phenotypes indicating that most of them contribute to the acquisition of the competence group (Gleason et al., 2006).

CHD-7 a chromo-helicase domain protein required during vulval development

chd-7 was identified in our lab by a screen designed to find genes implicated in 2° cell fate acquisition. *lip-1* is a notch target phosphatase that inhibits RAS signaling in 2° fate cells. *lip-1(lf)* animals expressing a 2° cell fate market, which is normally expressed in the VulC and VulD lineages at the L4 vulva (*Pegl-17::gfp*), were treated with ethane methyl sulfonate (EMS). 184 F2 mutant animals showing a change in the *Pegl-17::gfp* expression and morphological defects where isolated. Of those, 10 were analyzed. One of them, *zh52*, showed asymmetric loss of expression. Using genetic mapping and genome sequencing, a point mutation in the *chd-7* coding sequence was found. This SNP is a C to T transition that leads to a premature stop codon in the mRNA (CAG to TAG; Gln515 to Amber). The predicted mutant protein lacks all the functional domains and therefore may be non-functional **(Fig. 3.3.1C)**.

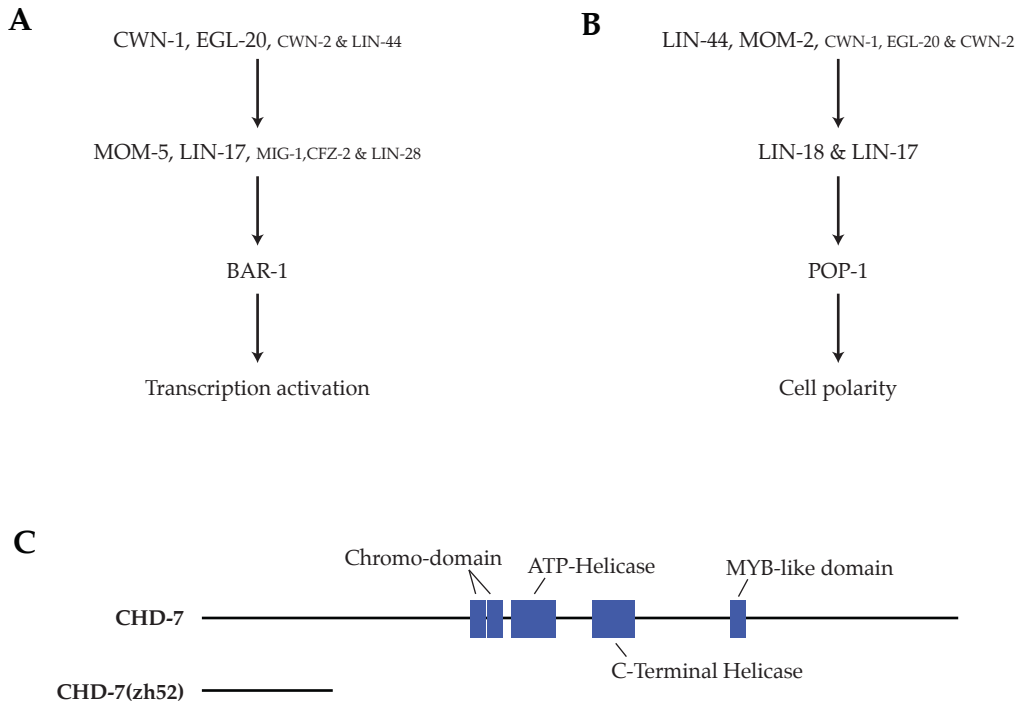

Fig. 3.3.1: WNT pathway in vulval development and the CHD-7 protein in *C. elegans*.
(A) The WNT ligands CWN-1 and EGL-20 are the major contributors to the activation of the WNT pathway in the VPCs, mainly through the activation of MOM-5 and LIN-17 (Gleason et al., 2006). The activation of the canonical WNT pathway leads to the release of BAR-1 and a general transcriptional activation of genes implicated in vulval development. **(B)** The polarity of the developing vulval cells is mainly defined by the WNT ligands LIN-44 and MOM-2 through the receptors LIN-18 and LIN-17 that will lead to the redistribution of POP-1 and the cellular asymmetry (Green et al., 2010). **(C)** Representation of the CHD-7 protein in *C. elegans* and its functional domains as well as the truncated protein resulting from the allele *zh52*.

CHD-7 is a putative chromo-helicase domain protein which has high similarity to the *Drosophila melanogaster* helicase Kismet and to the human helicase CHD7, whose mutants show Charge syndrome (Vissers et al., 2004) among others (Bouazoune and Kingston, 2012), and CHD8, which has been shown to control β-catenin target genes (Thompson et al., 2008). *chd-7* function in *C. elegans* is completely unknown, but it may have a similar function to the human homolog, which works as a nucleosome remodelling factor involved in a diverse range of developmental processes (Bouazoune and Kingston, 2012). In addition, studies with the *Drosophila* homolog *Kismet* showed that it activates transcription and counteracts PcG-dependent silencing by guiding other transcriptional activators to their targets (Srinivasan et al., 2008). Those experiments were validated in humans by Paredes *et al* ((Rodriguez-Paredes et al., 2009)) that described how CHD-8 controls the expression of Cyclin E2 through an interaction with the RNA polymerase II. In other cases, CHD-7 has been described to down regulate expression of certain factors such cell specific genes in mouse ES cells (Schnetz et al., 2010). In summary, CHD-7 function seems to be highly dependent of the target gene, the complex it belongs to and the cell type.
The *C. elegans* CHD-7 protein is 2967 amino acids long and contains two Chromo domains, one ATP-dependent Helicase domain, one C-terminal Helicase like domain and a Myb-like domain. The Chromo domains are thought to bind certain histones patterns providing the environment to a group of proteins to form a stable and functional complex (Eissenberg, 2001). The Helicase domains remodel the Nucleosomes to control the interaction of proteins with the DNA. Finally the Myb-like domain and other less conserved domains of CHD-7, may function to target its regulatory function to only certain genes by specific binding to particular DNA sequences.

3.3.2 Results

Loss of epithelial fate of the anterior VPCs in *chd-7* mutants.

To investigate the cause of the asymmetrical phenotype detected in the screen, we analyzed the *chd-7* mutant under Nomarski optics. We observed that around 70% of the animals lost the anterior secondary lineage (P5.p lineage) while the other 30% was phenotypically wild type **(Fig. 3.3.2A&B).** To confirm this result, we stained wild-type animals and *chd-7(zh52)* mutants using AJM-1 –an junction market– to check whether the lack of the P5.p lineage was due to early fusion to the hypodermis. This experiment revealed that not only P5.p but also all the anterior VPCs –P3.p to P5.p- fused to the hypodermis during the 2nd larval stage **(Fig. 3.3.2C&D)**.

Taken together, we conclude that the phenotype observed in the *chd-7(zh52)* mutants is due a failure to maintain the VPC cell fate in the anterior VPCs. Moreover, the A-P penetrance of the phenotype **(Fig. 3.3.2C)** could indicate dysfunctional WNT signaling.

chd-7 is expressed in a group of cells in the tail region

To further investigate the role of *chd-7* during vulval development, we constructed a transcriptional reporter using a 3kb fragment upstream of the annotated ATG (-3000 to +1) fused to GFP. Interestingly, the transcriptional reporter could be observed in the intestinal, anal and sphincter muscles –all of them non-striated muscles–, as well as in two anal ganglia cells (PHB and PHA), all of them in the tail region **(Fig. 3.3.3A)**. In addition, we observed expression in a head neuron and in the vulval muscles at the L4 larval stage (data no shown). We could not detect expression of our construct in the vulva epithelia.

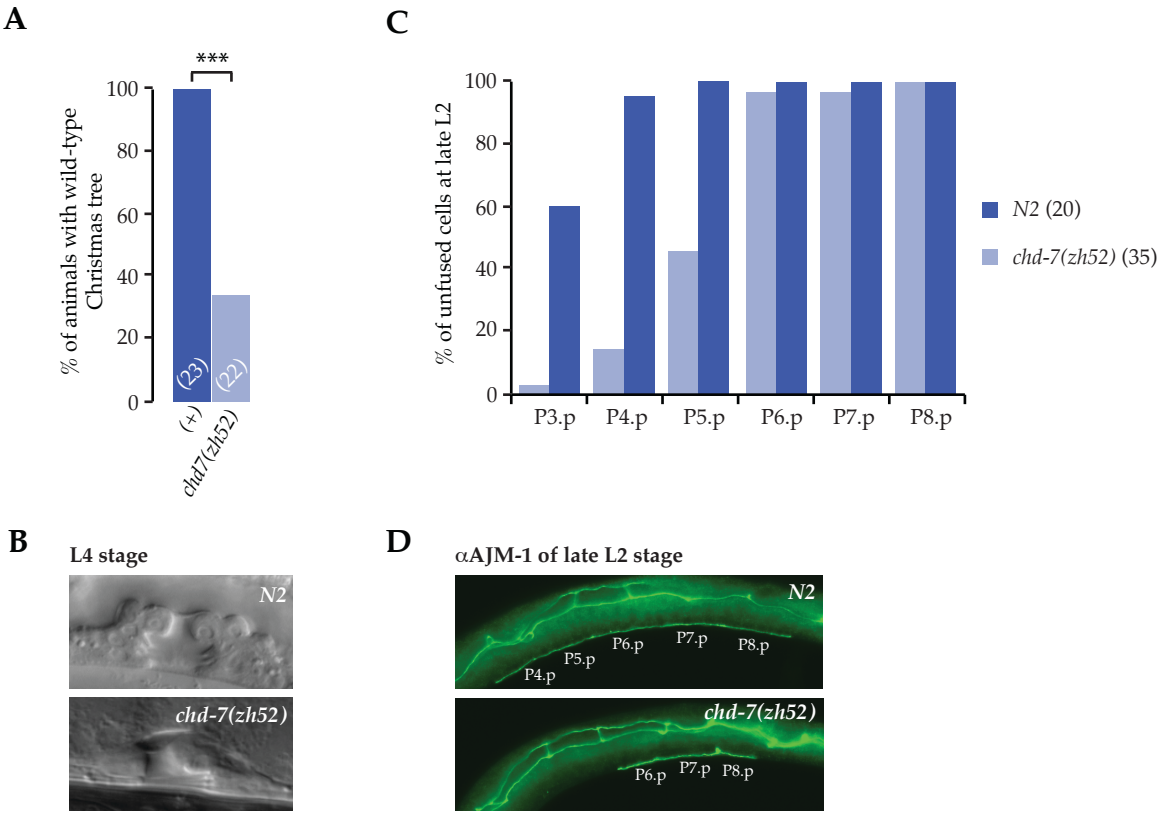

Fig. 3.3.2: Anterior VPCs lose their epithelial fate in the *chd-7(zh52)*

(A) Quantification of the *chd-7* phenotype at the Christmas tree stage using Nomarski optics. Statistical significance was tested with the Fisher Exact Probability Test, p<0.001=***. **(B)** *chd-7(zh52)* loses the anterior lineage of the developing vulva leading to an asymmetric Christmas tree structure. **(C)** Quantification of the AJM-1 staining in wild-type and *chd-7* animals before induction. The anterior lineages lose their epithelial fate and fuse with the hypodermis. **(D)** While the VPCs of wild-type animals maintain their epithelial fate and can be stained with AJM-1, the anterior VPCs of *chd-7(zh52)* fuse to the hypodermis.

chd-7(zh52) mutants resemble WNT-ligand reduction of function

The phenotype described above, which resembles previously described vulval phenotypes for the WNT-ligands, together with the expression pattern observed with our transcriptional reporter suggested that *chd-7* could be co-expressed in time and space with the WNT-ligands and therefore could control their expression (Gleason et al., 2006).

To verify this hypothesis we first built transcriptional reporters for four of the WNT-ligands (*cwn-1, egl-20, cwn-2, and lin-44)* and characterized their exact expression **(Fig. 3.3.3A)**. We observed *cwn-1* reporter expression in the ventral cord until the middle body, the anal, the sphincter and the intestinal muscles, as well as in the anal ganglia and the anus epithelial cells U and F. *egl-20* reporter expression was detected in the anal, the sphincter and the intestinal muscles, the anus epithelial cells U and F and other cells in the tail most likely somatic muscles. *cwn-2* reporter expression was observed through the whole animal, specially in undefined cells around the pharynx and the anterior part of the gut, and a group of cells in the tail including the anal and the intestinal muscles, in addition to the U and F cells. Finally *lin-44* reporter expression could only be detected in the Hypodermal cells 10 and 11.

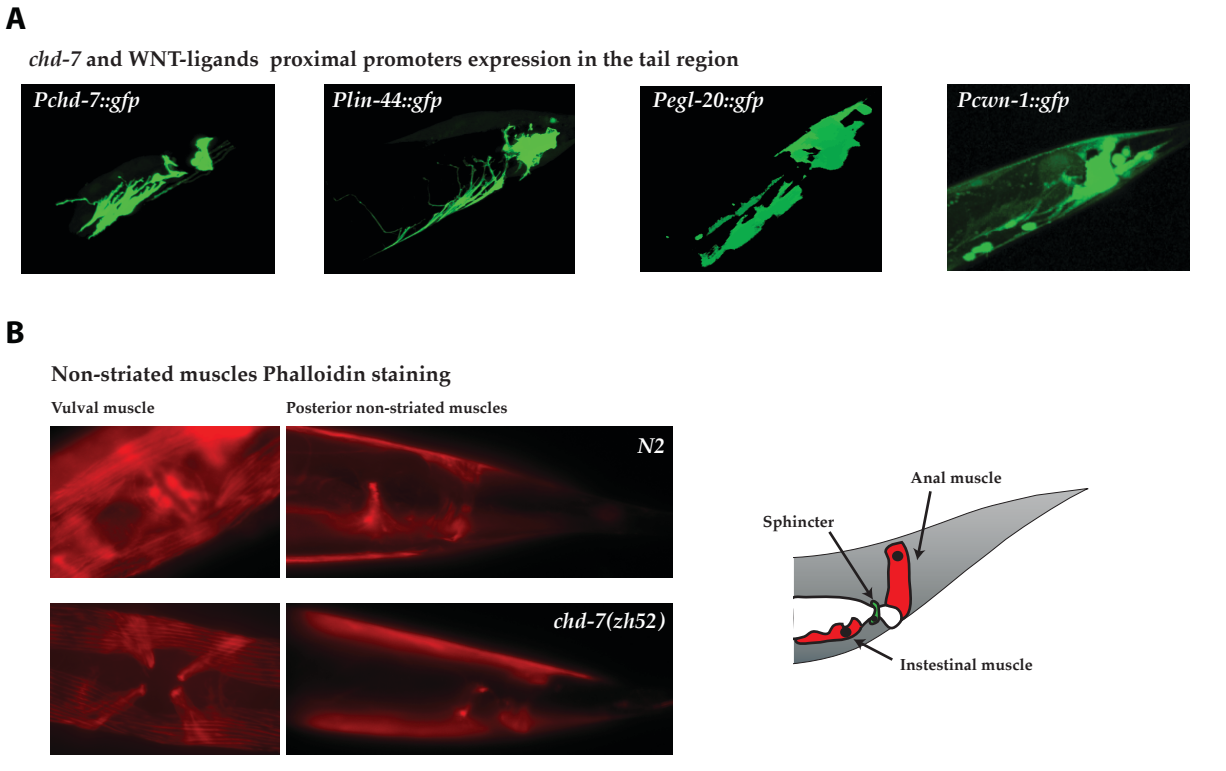

Fig. 3.3.3: *chd-7* proximal promoter drives its expression in the WNT Producing cells and is not required for their fate

(A) Expression patterns of GFP constructs driven by the proximal promoters of *chd-7, lin-44, egl-20* and *cwn-1*. **(B)** Phalloidin staining of the non-striated muscles in wild-type and *chd-7(zh52)* animals. Differences in the number of muscles or the structure of them cannot be appreciated.

Taken together, the expression of *chd-7* greatly overlapped with that previously shown for *cwn-1, cwn-2 and egl-20*, suggesting that *chd-7* could control their expression. Yet, the WNT-ligands were expressed in cells where we could not detect *chd-7*, which was mostly expressed in the non-striated muscles. A possible explanation is the lack or fate failure of the non-striated muscles in the *chd-7* mutant. CHD-7 in Xenopus is essential for the activation of Twist (Bajpai et al., 2010), which is necessary for non-striated muscle development in *C. elegans* (Corsi et al., 2000). Since both of those possibilities lead to a reduction in the absolute expression of the WNT-ligands, could therefore explain the phenotype previously described.

Non-striated muscles develop and function normally in *chd-7(zh52)* mutants

Following the results showed above, we hypothesized that the phenotype of *chd-7* could be due to the absence of some of the WNT-producing cells; the non-striated muscles present in the posterior part of the animal. To test this hypothesis we stained wild-type and *chd-7* animals with pDY-547-Phalloidin (Corsi et al., 2000), which binds to the F-actin allowing us to analyze the presence and morphology of all the non-striated muscle with the exception of the intestinal muscles, which can only be visualized using antibody staining.

We could not observe any different in the development or morphology of the non-striated muscles between the wild-type and *chd-7(lf)*. This indicates that, if *chd-7* has an effect in WNT-ligands production is not due to the lack of the WNT-producing cells **(Fig. 3.3.3)**.

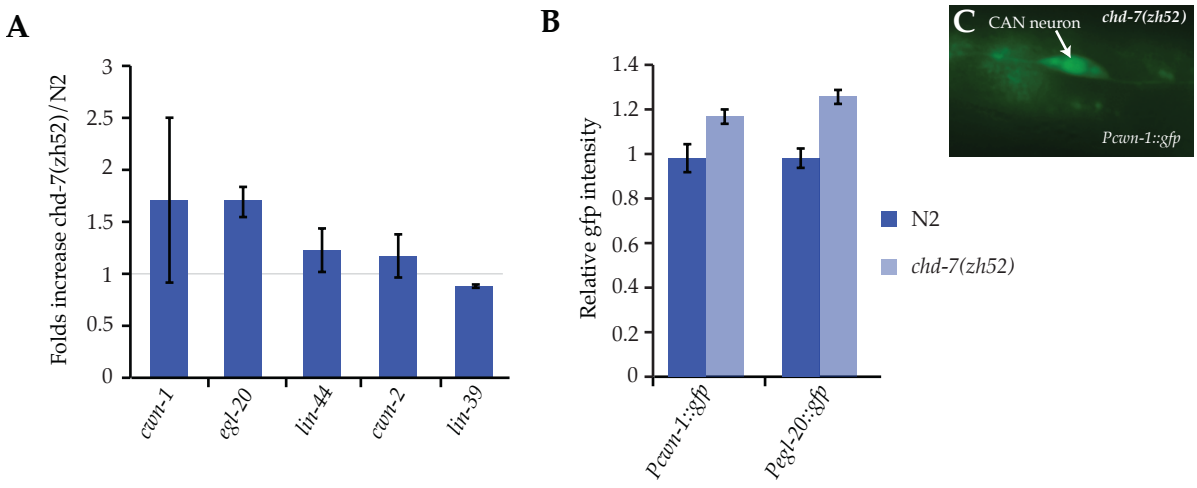

Fig. 3.3.4: WNT ligands expression is slightly up-regulated in the *chd-7(zh52)*

(A) RT-PCR experiments targeting the WNT-ligands (*cwn-1, egl-20, lin-44* and *cwn-2)* and *lin-39* show a slight increase in WNT ligands transcription couple to a decrease in the levels of *lin-39* in the *chd-7(zh52)* vs wild-type animals (N2) **(B)** Quantification of GFP intensity as a measure of transcriptional levels for the main WNT ligands (*cwn-1, egl-20)* in wild-type and mutant animals confirms the up-regulation detected using RT-PCR methods. **(C)** *cwn-1* expression detected in the CAN neurons of *chd-7(zh252).*

Several WNT-ligands are upregulated in *chd-7(zh52)* mutants

Next, using the transcriptional reporter of the WNT-ligands, we tested whether the major WNT-ligands –*cwn-1 & egl-20-* showed differential expression between the wild-type animals and the *chd-7* mutants. We observed no change in the pattern of expression (data no shown), but both transcriptional reporters were slightly up-regulated in *chd-7(lf)* **(Fig. 3.3.4B).** In addition, we could observe *cwn-1* expression in the CAN neurons in the mutant strain **(Fig. 3.3.4C)**. Interestingly the expression of *cwn-1* in the CAN neurons has only previously been shown using mFISH technology (Harterink et al., 2011) and was never detected on our wild-type animals carrying the *cwn-1* construct. Taken together, those results are contradictory with the phenotype observed in the vulva, which indicates a possible reduction of the ligand. Therefore, we verified our observations using RT-PCR for the WNT-ligands and *lin-39.* The results obtained supported both, an up-regulation of the WNT-ligands, in particular of *cwn-1* and *egl-20,* and a down-regulation of *lin-39,* which could explain the fusing phenotype in the vulva **(Fig. 3.3.4A)**. These two, *a priori,* opposite results could be due to different functions of *chd-7* in the WNT producing cells and the vulva. Yet, if this hypothesis is correct, *chd-7* should be expressed in the vulva through an enhancer not present in our reporter.

CHD-7 is expressed ubiquitously and localizes to the nucleous in *C. elegans*

The results above indicate that *chd-7* could have opposite roles in the WNT-producing cells and in the VPCs. In addition, this could also indicate, that if the effect of *chd-7* in the vulva is non-autonomous, most likely would not be through the expression of the WNT-ligands. Yet, our transcriptional reporter did not show expression of *chd-7* in the vulva.

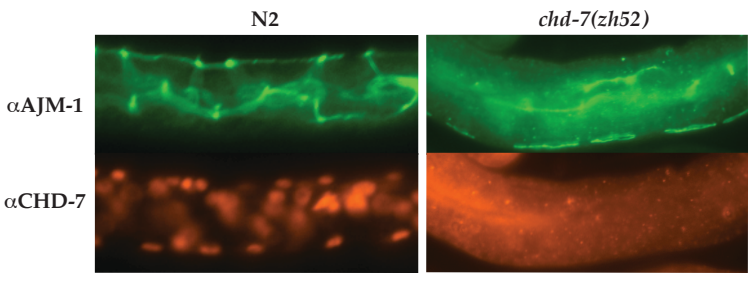

Figure 3.3.5: CHD-7 staining reveals ubiquitous expression and nuclear localization
CHD-7 antibodies specifically stain most of the nuclei in wild type animals while its presence can not be detected in the *chd-7(zh52)* mutants. As a control, AJM-1 antibodies staining the cellular junctions.

At this point, a plausible possibility could be that our *chd-7* reporter lacked enhancers allocated outside the 3Kb fragment used. For this reason we decided to use available antibodies for CHD-7. We stained wild-type animals and *chd-7(zh52)* mutants, as specificity control, with the *C. elegans* specific antibodies for CHD-7 (NovusBiologicals). Surprisingly, we could detect CHD-7 in every nucleus of the body in the wild-type animals, while a

complete absence in the *chd-7(zh52)*, indicating first the specificity of the anti-bodies and second the ubiquitous expression of CHD-7 **(Fig. 3.3.5)**.

Human gene	*C. elegans gene*	*Phenotype*
baf47	*R07E5.3*	*Vul, A-Rvl, Str*
brd7	*tag-298*	*wt*
brg1	*lin-35*	*wt*
baf60c	*tag-246*	*wt*
setdb1	*met-2*	*wt*
nlk	*lit-1*	*Expl, Str*
sox2	*sox-2*	*Pvl; Expl*
pb1	*pbrm-1*	*A-Rvl, P-Rvl, Vul*
p300	*cbp-1*	*Let, Str*
nanog	*tab-1*	*Str*
baf60c	*C18E3.2*	*NC*
ppar-g	*nhr-85*	*NC*
baf170	*psa-1*	*NC*
baf155	*psa-1*	*NC*
parp1	*pme-1*	*NC*
baf57	*swsn-3*	*NC*
smad1	*NF*	*NC*
oct4	*NF*	*NC*
baf60b	*NF*	*NC*
baf60a	*NF*	*NC*

Table 3.3.1: RNAi screen for putative CHD-7 partners

First column shows human genes previously described in a complex with CHD-7. The second columns present the *C. elegans* homologs. The third one describes the different phenotypes observed upon RNAi treatment against genes in wild-type animals. *wt* indicates wild-type; *Vul* is vulvaless (<3 VPCs induced); *A-Rvl* is anterior reversed vulva and *P-Rvl* is posterior reversed vulva; *Str* is sterile; *Expl* indicates that the animals explode during development; *Pvl* is protruding vulva; *Let* is Lethal indicating that animals die before they can be analysed.

chd-7 may work together with other DNA modifier genes

Human's CHD-7 function in complexes with other proteins. The components of these complexes are different according to the function and tissue ((Bajpai et al., 2010; Schnetz et al., 2010; Takada et al., 2007)). Therefore, we decided to test whether *chd-7* in *C. elegans* is working in a complex that could be homologous to those previously described in humans and mice. We performed an RNAi screen against the *C. elegans* homologs and observed that *pbrm-1* Polibromo-1 and R07E5.3 the BAF47 *C. elegans* homologs, showed a similar vulval phenotype to *chd-7(zh52)* (Table 3.3.1). In addition *pbrm-1*, The polibromo-1 homolog in *C. elegans*, has similar expression pattern as those observed with the transcriptional reporter of *chd-7* (Hunt-Newbury et al., 2007). On the other hand, neither *pbrm-1* nor R07E5.3 loss of function mutants reproduced the vulval phenotype observed in the *chd-7* background (data no shown).

3.3.3 Discussion

We have described a possible dual role of *chd-7* controlling the production of WNT-ligands in the tail and possibly promoting the sensitivity to the WNT signaling in the VPCs. A plausible model for this dual function could imply two independent functions. First, CHD-7 could promote the expression of *lin-39* in the VPCs. LET-418, a CHD family protein, negatively regulates *lin-39* expression in the vulva (Guerry et al., 2007). Perhaps, the

observed vulval phenotype can be the direct consequence of the low *lin-39* levels detected. Second, CHD-7 may repress globally the expression of the WNT-ligands to ensure their expression only in certain tissues. While this could well be the case, given that CHD-7 in other organism controls a variety of genes either promoting or repressing their expression depending on the associated proteins, a more in depth analysis of the genetic interactions of *chd-7* and the WNT pathway is necessary.

To further understand the role of *chd-7*, we tried, without any success, to cross the *zh52* allele with: first, several WNT-ligands to study possible epistatic interactions; second, previously published translational reporters of the WNT-ligands *cwn-1* and *egl-20* to check whether the WNT-gradients were affected; and third, a transcriptional reporter of *mec-4* previously used to study possible defects in the migration of the mechanosensory neurons, a process controlled by WNT-signaling (Prasad and Clark, 2006). While the *mec-4* reporter was integrated in chromosome I as *chd-7* and that may have prevented recombination, the translational reporter of *cwn-1* and *egl-20* were an extra-chromosomal array and an integrated array in chromosome IV respectively, and therefore should have resulted in homozygous descendants for both genetic traits in *chd-7(zh52)*.

A possible explanation is a linked mutation affecting the phenotype of *chd-7*. This mutation together with *chd-7* may produce the phenotype described in *zh52* animals. Another possibility is that the associated mutation rescues a lethality conferred by the *zh52* allele. On the other hand, if this was the case, we should have not encountered problems to obtain those crosses when the constructs were extra-chromosomal arrays.

Finally, to test if an associated mutation was in the background and had been selected through several generations due to an enhancement in the viability or a more visible phenotype, we crossed the *zh52* mutant with the balancer HT2 to obtain three independent lines and analyze homozygous *zh52* descendants. Non-surprisingly, we obtained different results in each of the lines. The, first line was almost wild-type with only 10% of the animals showing the defect, the second showed defective vulva in around 37% of the animals and the third resembled the penetrance of our original strain showing the phenotype in around 70% of the animals.

Even when this may be an interesting characteristic of *chd-7,* since it had been described in human to have a wide range of phenotypical penetrance, its usage for genetics studies in *C. elegans* may be compromised. In addition, the *a priori* contradictory results described in the results section of this thesis may be due to the pleiotropic phenotypes caused in those strains. Taken together, we decided to give up this project to focus on other issues of the vulva development.

On the other hand and at the light of new technologies such CRISPR (Friedland et al., 2013), we could overcome the aberrant background of our strain producing a new *chd-7 loss-of-*

function allele in completely wild-type background. In addition, we could produce a translational reporter in the endogenous *locus* to perform biochemical studies. These tools would allow us: first, to confirm the previous results; second, to understand whether CHD-7 controls the sensitivity of the VPCs to the WNT-ligands by modulating the expression of *lin-39;* third, to test what is the role of CHD-7 in the WNT-ligands production; and forth to identify CHD-7 partners.

3.3.4 Reference

Bajpai, R., Chen, D. A., Rada-Iglesias, A., Zhang, J., Xiong, Y., Helms, J., Chang, C.-P., Zhao, Y., Swigut, T. and Wysocka, J. (2010). CHD7 cooperates with PBAF to control multipotent neural crest formation. **463**, 958–962.

Bouazoune, K. and Kingston, R. E. (2012). Chromatin remodeling by the CHD7 protein is impaired by mutations that cause human developmental disorders. *PNAS* **109**, 19238–19243.

Corsi, A. K., Kostas, S. A., Fire, A. and Krause, M. (2000). Caenorhabditis elegans Twist plays an essential role in non-striated muscle development. *Development* **127**, 2041–2061.

Dale, T. C. (1998). Signal transduction by the Wnt family of ligands. *Biochemistry Journal* **329**, 209–223.

Eisenmann, D. M., Maloof, J. N., Simske, J. S., Kenyon, C. and Kim, S. K. (1998). The β-catenin homolog BAR-1 and LET-60 Ras coordinately regulate the Hox gene lin-39 during Caenorhabditis elegans vulval development. *Development* **125**, 3667–3680.

Eissenberg, J. C. (2001). Molecular biology of the chromo domain: an ancient chromatin module comes of age. *Gene* **275**, 19–29.

Gleason, J. E., Szyleyko, E. A. and Eisenmann, D. M. (2006). Multiple redundant Wnt signaling components function in two processes during C. elegans vulval development. *developmental biology* **298**, 442–457.

Green, J. L., Inoue, T. and Sternberg, P. W. (2010). Opposing Wnt Pathways Orient Cell Polarity during Organogenesis. *Cell* **134**, 646–657.

Guerry, F., Marti, C.-O., Zhang, Y., Moroni, P. S., Jaquiery, E. and Muller, F. (2007). The Mi-2 nucleosome-remodeling protein LET-418 is targeted via LIN-1/ETS to the promoter of lin-39/Hox during vulval development in C. elegans. *developmental biology* **306**, 469–479.

Harterink, M., Kim, D. H., Middelkoop, T. C., Doan, T. D., Oudenaarden, A. V. and Korswagen, H. C. (2011). Neuroblast migration along the anteroposterior axis of C. elegans is controlled by opposing gradients of Wnts and a secreted Frizzled-related protein. *Development* **138**, 2915–2924.

Hunt-Newbury, R., Viveiros, R., Johnsen, R., Mah, A., Anastas, D., Fang, L., Halfnight, E., Lee, D., Lin, J., Lorch, A., et al. (2007). High-Throughput In Vivo Analysis of Gene Expression in Caenorhabditis elegans. *Plos Biology* **5**, 1981–1997.

Janssen, N., Bergman, J. E. H., Swertz, M. A., Tranebjaerg, L., Lodahl, M., Schoots, J., Hofstra, R. M. W., van Ravenswaaij-Arts, C. M. A. and Hoefsloot, L. H. (2012). Mutation update on the CHD7 gene involved in CHARGE syndrome. *Hum. Mutat.* **33**, 1149-1160.

Koh, K., Peyrot, S. M., Wood, C. G. and Wagmaister, J. A. (2002). Cell fates and fusion in the C. elegans vulval primordium are regulated by the EGL-18 and ELT-6 GATA factors—Apparent direct targets of the LIN-39 Hox protein. … 1–10.

Korswagen, H. C. (2002). Canonical and non-canonical Wnt signaling pathways in Caenorhabditis elegans: variations on a common signaling theme. *Bioessays* **24**, 801–810.

Nalbantoglu, B., Tekir, S., Ülgen, K. (2011) Wnt Signaling Network in Homo Sapiens. *Edited by Paula Bubulya.*

Prasad, B. C. and Clark, S. G. (2006). Wnt signaling establishes anteroposterior neuronal polarity and requires retromer in C. elegans. *Development* **133**, 1757–1766.

Rodriguez-Paredes, M., Ceballos-Chavez, M., Esteller, M., Garcia-Dominguez, M. and Reyes, J. C. (2009). The chromatin remodeling factor CHD8 interacts with elongating RNA polymerase II and controls expression of the cyclin E2 gene. *Nucleic Acids Research* **37**, 2449–2460.

Schnetz, M. P., Handoko, L., Akhtar-Zaidi, B., Bartels, C. F., Pereira, C. F., Fisher, A. G., Adams, D. J., Flicek, P., Crawford, G. E. and LaFramboise, T. (2010). CHD7 targets active gene enhancer elements to modulate ES cell-specific gene expression. *PLoS Genet.* **6**, e1001023.

Srinivasan, S., Dorighi, K. M. and Tamkun, J. W. (2008). Drosophila Kismet regulates histone H3 lysine 27 methylation and early elongation by RNA polymerase II. *PLoS Genet.*

Takada, I., Mihara, M., Suzawa, M., Ohtake, F., Kobayashi, S., Igarashi, M., Youn, M.-Y., Takeyama, K.-I., Nakamura, T., Mezaki, Y., et al. (2007). A histone lysine methyltransferase activated by non-canonical Wnt signaling suppresses PPAR-γ transactivation. *Nat Cell Biol* **9**, 1273–1285.

Thompson, B., Tremblay, V., Lin, G. and Bochar, D. (2008). CHD8 Is an ATP-Dependent Chromatin Remodeling Factor That Regulates {beta}-Catenin Target Genes. *Molecular and Cellular Biology* **28**, 3894–3904.

Vissers, L. E. L. M., Ravenswaaij, C. M. A. V., Admiraal, R., Hurst, J. A., Vries, B. B. A. de, Janssen, I. M., Vliet, W. A. V. D., Huys, E. H. L. P. G., Jong, P. J. de, Hamel, B. C. J., et al. (2004). Mutations in a new member of the chromodomain gene family cause CHARGE syndrome. *Nature genetics* **36**, 955–957.

Wagmaister, J. A., Gleason, J. E. and Eisenmann, D. M. (2006a). Transcriptional upregulation of the C. elegans Hox gene lin-39 during vulval cell fate specification. *Mechanisms of Development* **123**, 135–150.

Whangbo, J. and Kenyon, C. (2010). A Wnt Signaling System that Specifies Two Patterns of Cell Migration in C. elegans. *Molecular Cell* 851–858.

4

Materials and Methods

4.1 Animal methods

4.1.1 *C. elegans* methods and strains

The strains used for the experiments and crosses were derivates of Bristol strain N2 of *Caenorhabditis elegans.* The animals were cultivated under standard conditions at 20°C as described in (Brenner, 1974) unless specified. The mutations used in this study have been previously described, with the exception of the allele *zh52* that has been described in this work, and are listed below by their linkage group. To construct the different mutant combinations standard genetic methods were used.

The alleles used are:

LG I: *lin-31(n301* & *n1053)* (Ferguson and Horvitz, 1985)*; unc-29(e1072)* (Tan et al., 1998)*; eff-1(ok1021)* (Sapir et al., 2007)

LG II: cdc-14(he141) (Saito et al., 2004)*; chd-7(zh52)*

LG III: lin-39(n1760 & *n709)* (Clark et al., 1993)

LG IV: lin-3(e1417) (Hwang and Sternberg, 2004)*; lin-1(e1777)* (Ferguson and Horvitz, 1985)

Balancers: *hT2(I;III)*

The Constructs used are*:*

Previously published:

maIs113[Pcki-1::gfp::cki-1 3'UTR, dpy-20(+)] (Hong et al., 1998)
ayIs4 [Pegl-17::GFP] (Burdine et al., 1998)
qIs56[Plag-2p::gfp, unc-119(+)] (Kostic et al., 2003)
arIs82 [lin-12::gfp; unc-4(+); Pegl-17::LacZ] (Shaye and Greenwald, 2002)
gaEx69 [lin-31(PhD); unc-29(+)] (Tan et al., 1998)
zhIs1 [lin-39::gfp] (Szabó et al., 2009)
zhIs038 [let-23::gfp, unc-119(+)] (Haag et al., 2014)
arEx1541 [Plin-31::2nls::yfp] (la Cova and Greenwald, 2012)
gaEX69 [lin-31(PhD); unc-29(+)] (Tan et al., 1998)
zhEx500 [Pbar-1::nicd::gfp, unc-119(+)] (Nusser-Stein et al., 2012)

Non-Previously published:

zhIs80 [Pcye-1::gfp]
zhIs86 [Pcye-1::gfp, unc-119(+)]
zhIs87 [Pcye-1Δ1LBS::gfp, unc-119(+)]
zhIs88 [Pcye-1Δ2LBS::gfp, unc-119(+)]
zhIs89 [Pcye-1Δ1Δ2LBS::gfp, unc-119(+)]
zhEx352 [Pchd-7::gfp]
zhEx410 [Pcwn-1::gfp::cwn-1 3'utr]
zhEx411 [Pegl-20::gfp]
zhEx412 [Pcwn-2::gfp]
zhEx430 [Plin-44::gfp]
zhEx530 [cdc-14c::gfp]
zhEx535 [Pcdk-4::gfp]
zhEx536 [Plin-31::cye-1::gfp]
zhEx538 [HS::lin-1(ΔCT)]
zhEx542 [Pbar-1::nicd::gfp, unc-119(+)]

Transgenic worms were generated by microinjection of purified DNA into young adult worms (Mello et al., 1991). All the constructs were injected at a concentration of 50 ng/μl, using pCFJ90 (*Pmyo-2::mCherry)* as co-marker at a concentration of 2.5 ng/μl unless specified. The final concentration of injected DNA was filled up to 150 ng/μl using the plasmid pBluescript-KS. For the generation of the *mosSCI* lines (Frøkjaer-Jensen et al., 2008), *zhIs86* to *zhIs89*, we injected the plasmids pDR11, pDR12, pDR13 and pDR15 together with the

following markers: pCFJ90 (*Pmyo-2::mCherry)* at a concentration of 2.5 ng/µl, pCFJ104 (*Pmyo-3::mCherry)* at a concentration of 5 ng/µl, pGH8 (*Prap::mCherry)* at a concentration of 10 ng/µl, and with the germline expressed Mos 1 transposase from the plasmid pJL43.1 at a concentration of 50 ng/µl. *zhIs82* was integrated inducing double strand breaks with gamma irradiation. The plasmid pSF18 (Farooqui et al., 2012) was co-injected with pPD118.33 (*Pmyo-2::gfp)* at a concentration of 2.5 ng/µl.

4.1.2 Liquid cultures of worms and sucrose floating

Worms were grown for 4 to 5 days in liquid cultures of the bacterial strain *Na22* as described in *wormbook.org*. Once the desired concentration of animals was obtained, the culture was centrifuged at 1300 rpm for 1 minute. The supernatant was discarded and the animals were washed twice with ice-cold 0.1M NaCl. Finally, the worms were resuspended in an ice-cold solution 1:1 of 0.1M NaCl and 60% sucrose solution and centrifuged at 1100g for 5 mins.
The floating worms were transferred to a new tube and washed at least twice with 0.1M NaCl.

4.1.3 RNAi experiments

RNAi effects were induced using the method described by (Kamath et al., 2003). Bacterial clones containing the RNAi of interested were grown at 37°C over-night in 2xTY with 50µg/ml ampicillin. 200-300µl of those cultures were poured into NGM plates including 3mM IPTG, 50µg/ml ampicillin and 50µg/ml tetracycline and settle for 24 hours at room temperature. Finally animals were plated and allowed to grow at 20°C. Unless noted otherwise, the F1 generation was analyzed.

4.2 Protein methods

4.2.1 Chromatin Immunoprecipitation (ChIP) performance and analysis

Chromatin extracts were prepared from 100 ml mixed-stage liquid cultures of animals carrying the *zhIs1[lin-39::gfp]* and *zhIs89[Pcye-1ΔHBS1ΔHBS2::gfp]* arrays. As negative controls, extract from animals carrying only *zhIs89[Pcye-1ΔHBS1ΔHBS2::gfp]* were prepared

and processed in parallel. Cross-linking was done with 1% paraformaldehyde for 20 minutes at room temperature. LIN-39::GFP bound chromatin was precipitated using GFP-Trap® antibodies (Chromotek) as described in Pellegrino et al. (Pellegrino et al., 2011) and following the protocol by (Mukhopadhyay et al., 2008) with the following modification: Extracts were pre-cleared by incubation with Dynabeads (10 μl of stock solution per sample) before adding GFP-Trap® beads (20μl of stock solution per 4-5 mg/ml of total protein in the samples). After reverse cross-linking, the binding of LIN-39::GFP to the different sites was quantified by performing Q-PCR using an ABI Prism 7900HT thermocycler with the MESA Green mastermix plus (Eurogentec) and primers specific for the wild-type HBS in endogenous *cye-1* (ODR-290 and ODR-262 for the 1st putative binding, and ODR-292 and ODR-265 for the 2nd putative binding) and the mutant HBS in the *zhIs89* reporter (ODR-286 and ODR-262 for the 1st putative binding, and ODR-288 and ODR-265 for the 2nd putative binding). For each measurement, the signal was first normalised to the signal obtained from the input DNA (% input). To calculate the specific enrichment, the % input value obtained with each Q-PCR assay from the *zhIs1[lin-39::gfp]*; *zhIs89[Pcye-1ΔHBS1ΔHBS2::gfp]* strain was divided by the % input value obtained from the *zhIs89[Pcye-1ΔHBS1ΔHBS2::gfp]* negative control strain. In addition to the Q-PCR assays in the HBS regions, we used a primer pair in the 3' UTR of *cye-1* and a primer pair spanning the *cye-1-gfp* fusion in the *zhIs89* reporter. The data in figure 3F show the average ratios obtained in three independent experiments.

4.2.2 Antibody staining

Immunostaining was performed as described previously (Miller and Shakes, 1995). The worms were permeabilized using the freeze-crack method, by placing them in a Poly-lysine pretreated slide and freezing them in liquid N2. They were fixed in methanol at -20°C Immediately after for 10 minutes. Following fixation the samples were blocked with 3% bovine serum albumin for 30 minutes and incubated with primary antibody (1:25 MH27 and/or 1:500 anti-CHD-7) for 2 hr at room temperature in a humid chamber. Finally they were washed 3 times with PBS-T, incubated for 1-2 hours with the corresponding secondary antibody (1:100 anti-mouse TRITC and anti-rabbit CY-5), washed and mounted in Mowiol.

4.2.3 Phalloidin staining

Animals were stained with Phalloidin following the method previously described in (Corsi et al., 2000), with the following modifications: the animals were lyophilized in a vacuum centrifuge at 45°C and fixed in ice cold acetone for 5 minutes at room temperature. Next, the

acetone was removed by speed vacuum and 0.007U of Phalloidin conjugated added to the worms. These were incubated in the dark for 1 hour at room temperature. Finally the worms were washed with PBS-T and mounted with Moviol.

4.2.4 Western Blot

Polyacrylamide gels were prepared according to standard protocols and placed in fresh SDS running buffer. At the same time, the desired amount of animals was boiled in 2xSDS solution for 5 minutes at 95°C, and loaded into the gel. The SDS gels were run at 100 V until the leader marker arrived to the lower part of the gel. The proteins previously separated by SDS-PAGE were blotted for 1 hour at 4°C and 100V into a PVDF membrane using the MiniProtean® Electrophoresis System from BioRad. Thereafter, the membrane was blocked with TBS-T milk for 4 hours and incubated with the primary anti-bodies over-night at 4°C. Next, the membrane was washed with TBS-T and incubated with Horseradish peroxidase (HRP) conjugated antibodies for 1h at 4°C. Finally Amersham ECL Western Blotting detection reagents (GE Healthcare) was used to reveal the membrane.

4.3 DNA methods

4.3.1 Worm Lysis and PCR techniques

Prior to the amplification of PCR fragments, genomic DNA samples were prepared by dissolving worms into a Protease K solution for 1h at 60°C, and then inactivated for 10 minutes at 95°C.This DNA solution was used unless specified as DNA template for PCR amplification. The amplification was following the manufacturer's protocols provided with the different Polymerase used in this work (Phusion® High-Fidelity DNA Polymerase (NEB), Taq DNA Polymerase (Invitrogen), LongAmp® Taq DNA Polymerase PfuUltra HF® Polymerase (Agilent).
The PCRs were run in 0.2ml MultiplyPro Tubes (Sarstedt) in a BioRad MyCycler TermoCycler. Finally the PCR products were checked using 0.8% agarose gels containing 50μl of 2μg/ml Ethidium bromide per 50ml agarose solution.
When further steps required PCR purification or gel extraction of the desire band, the GenElute PCR Clean-Up Kit or the GenElute GelExtraction Kit (Sigma-Aldrich) were used.

4.3.2 Oligonucleotides

cdc-14

ODR-233	aaattctaagtttctgcggg	Genotyping he141
ODR-234	atcggtatatgaaggggaca	Genotyping he141

cdk-4

ODR-244	tttgcatgcccaaacatgaaaaccaaccacg	Fwd promoter
ODR-243	aaaggatcccctccataggcgccttttccaag	Rev transcriptional

chd-7

ODR-131	gagccaactccgtctatgcaagaatc	Genotyping zh52
ODR-132	ccactgattgtgatggttccattg	Genotyping zh52
OSN-179	atgagttccttctttgcgcacac	Fwd promoter
OSN-180	gctcacacagaaaaagaggtctg	Nested Fwd promoter
OSN-195	agtcgacctgcaggcatgcaagctcattttgtgtgtttggttatgtggttataatg	Fusion Promoter GFP

cwn-1

ODR-11	gcatgaatgaatgagatggcag	Fwd promoter
ODR-12	ggcagcatttgtgcttttc	Nested Fwd promoter
ODR-23	cgtgccctaccatgtagaag	Rev UTR reporter
ODR-24	catgtagaagtaatatcttg	Nested Rev 3'UTR
ODR-25	gaacttctatcgtcttttc	Fwd 3'UTR
ODR-109	tcgtcgagaatgcaagtgtc	RT-PCR
ODR-110	gctccatcgaacttatccttg	RT-PCR
ODR-57	agtcgacctgcaggcatgcaagcttcgattggagagaagaaaaatgga	Fusion Promoter GFP
ODR-58	gaaaaagacgatagaagttcctatttgtatagttcatccatg	Fusion 3'UTR GFP

cwn-2

ODR-14	gcaaatttcctttaatgggctc	Nested Fwd promoter
ODR-15	caatcttgtagcaaatttcc	Fwd Promoter
ODR-59	agtcgacctgcaggcatgcaagctcaaagagtgacaactttcac	Fusion Promoter GFP
ODR-111	catcggagcacaaaatgc	RT-PCR
ODR-112	gaatgcagcttctcgtgttg	RT-PCR

cye-1

ODR-85	agtcgacctgcaggcatgcaagctctcaggcatagctggaagtggttg	Fusion Promoter GFP
ODR-222	tttaagcttgaccctcgtcctcatcgtctg	Fwd promoter
ODR-242	aaagcggccgcttagaaaagtcgttgcggatg	Rev transcriptional
ODR-241	tttgtcgacatggctggaagaaagtcatc	Fwd translational
ODR-259	cgcgatttccccctagagaccatatgacg	Mutagenesis 1LBS
ODR-260	tctctagggggaaatcgcgcgctcatttc	Mutagenesis 1LBS
ODR-263	cagacactttcccctttgaccagtgtaatag	Mutagenesis 2LBS
ODR-264	ctggtcaaggggaaagtgtctgtttctcag	Mutagenesis 2LBS
ODR-286	gtcatatggtctctaggggg	Δ1LBS RT-PCR
ODR-290	gtcatatggtctctagattc	1LBS RT-PCR
ODR-292	gagaaacagacactttgtat	2LBS RT-PCR
ODR-288	aaacagacactttcccc	Δ2LBS RT-PCR
ODR-262	agttgctgtgccctctattg	Δ1LBS/1LBS RT-PCR
ODR-265	gatgtctgcgtcttattttc	Δ2LBS/2LBS RT-PCR
ODR-302	cattcgaaacatacctttggg	RT-PCR control
ODR-303	cgtgaagttggatcttcatc	RT-PCR control

egl-20

ODR-18	gctgaccaatccaattcctc	Fwd promoter
ODR-19	cagcctttcggaacctgaag	Nested Fwd promoter
ODR-64	gcgtttatatattcgtcaggctatttgtatagttcatccatg	Fusion Promoter GFP
ODR-113	gggcaatattctcctccatc	RT-PCR
ODR-114	tggtaatgaggtcgtggaag	RT-PCR

lin-1

ODR-250	ctgactctcgccaagaccgg	Genotyping e1777
ODR-251	gtgtgctccccgtcaagcag	Genotyping e1777

lin-3

OJE-129	gactaacaaccaatctacag	genotyping e1417
OJE-130	gattgaagctgttcgggag	genotyping e1417

lin-39

OMP-70	ctgagactccacccttcgtc	Genotyping n709
OMP-71	tcccagtccttgacttgagg	Genotyping n709
ODR-121	gacaagaaaggcatcagtgg	RT-PCR
ODR-122	gattccttgtgtatgctgttcg	RT-PCR
ODR-245	cacgcggcgagaagcgacaac	Genotyping n1760
ODR-246	catcatcggaggtgtcattgg	Genotyping n1760

lin-44

ODR-104	agtcgacctgcaggcatgcaagctgacgctgacgctgtgtcacctcgaaaag	Fusion Promoter GFP
ODR-105	ctgactctcgccaagaccgg	Nested Fwd promoter
ODR-106	acgtgtctatacaagcttctg	Fwd promoter
ODR-119	ttcgaaggagttcaggaagg	RT-PCR
ODR-120	acgcccaaatcagagaagac	RT-PCR

other primers

C	agcttgcatgcctgcaggtcgact	Fwd GFP
D	aagggcccgtacggccgactagtagg	Rev unc-54-3'UTR
D*	ggaaacagttatgtttggtatattggg	Nested Rev unc-54

4.3.3 Cloning into plasmid vector

Vector DNA and DNA fragment of interest were digested with the desire restriction enzyme following the instruction of the manufacturer. After digestion, cut vector was dephosphorylated adding Antartic Phosphatase and its buffer (NEB) and incubated at 37°C for 1 hour. Thereafter, the linearized vector and fragment were purified using the GenElute PCR Clean-Up Kit and ligated using T4 DNA Ligase (Roche) as described by the manufacturer in a ratio of 3:1 between the Fragment and the vector. Finally, the resulting DNA sample was transformed into pre-treated *E. coli* using the 5-5-3-5 method, and plated in agar plates with the corresponding resistance.

To screen for the successful cloning, single colonies of the previously plated bacteria were isolated and grown in liquid culture with the corresponding resistance for 12 to 24 hours. Next, the bacterial pellet was treated with lysozyme and STET buffer to destroy the cell membrane. After this step, the samples were centrifuged and the supernatant was collected to proceed with an Ethanol/Acetate DNA precipitation. Finally the isolated DNA was tested using restriction enzymes and confirmed by sequencing. For bigger yields of the desired DNA, the QIAfilter Plasmid Midi Kit (Qiagen) was used.

The plasmid and PCR fusions presented in this study were constructed as follow: Plasmid pDR8 (*Pcye-1::gfp*) was made by cloning the promoter and the first part of the coding region (-942 to +1375) in frame with the *gfp* cassette into the HindIII and SalI sites of plasmid pPD95.75 (a gift from Andrew Fire). pDR9 (*Plin-31::cye-1)* was built by cloning full length *cye-1* cDNA into the NotI and SalI sites of plasmid pB253 (Tan et al., 1998). pDR10 (*Pcdk-4::gfp*) was made by introducing the *cdk-4* promoter region including the two annotated isoforms (-800 to +1588) into the BamHI and SphI sites of plasmid pPD96.04 (a gift from Andrew Fire). pMS253 *(cdc-14c::gfp)* was a kind gift from Saito et al. (Saito et al., 2004). pDR11 (*Pcye-1::gfp, unc-119(+)*) was built by cloning a 4 kb SpeI fragment containing the *Pcye-1::gfp* reporter from the plasmid pDR8 into the SpeI site of the *mosSCI* vector pCFJ151 (Frøkjaer-Jensen et al., 2008). pDR12 (*Pcye-1ΔHBS1::gfp, unc-119(+)*), pDR13 (*Pcye-ΔHBS2::gfp, unc-119(+)*) and pDR15 (*Pcye-ΔHBS1ΔHBS2::gfp, unc-119(+)*) were obtained by site-directed mutagenesis of the plasmid pDR11 introducing the mutations described in the results section. The *chd-7, cwn-1, egl-20, cwn-2* and *lin-44* transcriptional reporters were constructed by fusing the promoter regions to the *gfp* cassette of the pPD95.75. The primers used for plasmid and Fusion constructions are listed in **the section 4.3.2.**

4.3.4 Site directed mutagenesis

To mutate up to 4 nucleotides in a specific location of a plasmid, ~40bp long primers overlapping in 80% of their length and including the desired mutation in the middle were designed. Then, those primers were used to perform a PCR using the PfuUltra HF polymerase and the target plasmid as template. After the amplification, 1μl of DpnI (NEB) was added to the mix and incubated at 37°C for 1 hour to eliminated the plasmid template. Finally, the resulting PCR products were transformed and screened as mention above using DNA sequencing

4.4 Microscopy methods

4.4.1 Microscopy and data analysis

Animals were mounted on 4% agarose pads in 20mM tetramisole hydrochloride in aqueous solution. The vulval induction index was scored as described in (Berset et al., 2001). To obtain synchronized late L2 larvae, oocytes were isolated by hypochlorite treatment of gravid adults, allowed to hatch in the absence of food for 24 hours to obtain arrested L1 larvae that were transferred to plates containing OP50 bacteria and grown until they had reached the late L2/early L3 stage. For S-phase arrest, hydroxyurea was added to synchronized L2 larvae at a concentration of 40mM as described in (Ambros, 1999). The location of the vulval invaginations and the number of cells per invagination were counted using Nomarski optics in a Leica DMRA microscope equipped with a cooled CCD camera (Hamamatsu ORCA-ER) controlled by the Openlab 5 software (Improvision). To image GFP reporter expression, a calibrated fluorescent light source (X-Cite exacte, Excelitas Technologies Corp) was used on the same microscope. To compare GFP expression levels, images were acquired under the same illumination conditions and acquisition settings. Fluorescent signal intensities in were quantified using the Fiji software as described (Schindelin et al., 2012).

4.4.2 Laser ablation

Laser ablation and cutting experiments were performed with a micropoint dye laser (Photonics Instruments) attenuated to around 70% maximal intensity at a pulse rate of 10 Hz aimed at the nucleoli of the AC for cell ablations. Animals were recovered with M9 and plated in a NGM plate for recovery until further analysis.

4.5 Statistical methods

t-tests for independent samples were used to determine the statistical significance of differences in fluorescence intensity values. To test the statistical significance of all other data, the Fisher's exact probability test was performed. In all figures, * indicates $p<0.05$, ** $p<0.005$ and *** $p<0.001$.

5

General discussion

5.1 Vulva: a model to study *hox* gene regulatory networks

Deregulation of *hox* genes results in a variety of developmental disorders and diseases in mammals (Collins and Hess, 2015). For example, the HOXA9 is over-expressed in more than 50% of the acute myeloid leukemias and is a sign of poor prognosis (Andreeff et al., 2008;). In addition, in many superior animals, the complexity of the networks controlling the development makes it difficult to study them directly. For example, in healthy uterus at least four different *hox* genes can be detected (HOXA7, HOXA9, HOXA10 and HOXA11). In this case, HOXA7 is necessary for the expression of the other three in their corresponding segments. Misregulation leads to segment transformation and in many cases to cancer (Cheng et al., 2005). Unfortunately, in many cases, it is unclear whether the HOX de-regulation is the cause or the consequence. More importantly, the downstream networks and the processes directly governed by the *hox* genes are not well understood.

The vulva of *C. elegans* is the perfect model to gain a basic understanding of: the complexity of the *in vivo* interaction between the HOX and its targets; how the specificity is maintained; and how are the effectors networks that the *hox* genes directly influence to execute the different cell programs. As mention previously in this work, the vulval development is a very well understood process with very clear read out to detect dysfunctionality. Furthermore, it is exclusively governed by the *hox* gene *lin-39*. The regulation of *lin-39* expression is very well understood and therefore allows us to focus in the less well-known areas of the HOX biology. In addition, previous work by the modENCODE consortium (Niu et al., 2011) has revealed the *in vivo* binding profile of *lin-39*. All together, makes *lin-39* and the vulva a very strong model to understand *hox* gene function.

Using this model, I have been able to show that the *hox lin-39* controls the activation of the cell cycle in the vulval precursor cells, allowing the expression of the cell cycle machinery. In addition, I have identified two different mechanisms to achieve this goal. First, LIN-39 activates the transcription of the secondary cell fate key components, the NOTCH ligand *lag-2* and the NOTCH receptor *lin-12*. The last one, upon activation by the ligand, promotes the cell cycle progression in the secondary lineage. Second, *lin-39* binds the promoter of several cell cycle regulators promoting their expression. However, this study has opened up new important questions about the co-factors that may be working with LIN-39 to control cell cycle activation. It is likely that in this case LIN-39 works with in an unknown complex, since the binding pattern identified in this work does not resemble the PBX-HOX binding previously described (Mann and Affolter, 1998). Understanding these differences could help us to elucidate the mechanism underneath the HOX specificity *in vivo*.

5.2 Vulva: a model to study cell cycle regulatory networks

This study has allowed us to draw a solid model for cell cycle regulation. I have been able to establish the first model of the activation of the cell cycle in the VPCs by incorporating the findings of this work in the well-established vulval system.

I have shown, that in addition to *lin-39*, the Forkhead protein LIN-31 independently of LIN-1 acts as a cell cycle repressor. In addition to its already known role promoting the expression of the cell cycle inhibitor *cki-1* (Clayton et al., 2008), I have shown that LIN-31 repressed the expression of at least two cell cycle components, *cdk-4* and *cye-1*. Moreover, I was able to rescue the lack of proliferation of the *lin-39* loss of function mutants by adding a second mutation in the *lin-31 locus*. Therefore, LIN-31 could act as a general repressor of the cell cycle balancing the function of LIN-39.

Interestingly, my results also suggest that the role of LIN-31 in the cell cycle does not need of the ETS LIN-1, as oppose to its role in the inhibition of the vulval induction (Tan et al., 1998). I have shown that LIN-1 plays a cooperative and secondary role inhibiting the cell cycle probably stabilizing LIN-31 repressor status.

Finally, I have shown that NOTCH signaling can promote the cell cycle of the vulval secondary lineage in the absence of *lin-39*. Moreover, doing epistatic analysis with a negative dominant form of *lin-31*, I have shown that NOTCH signaling may inhibit LIN-31 in the secondary lineage.

5.3 Vulva: new perspectives and open questions

This work has connected cell fate and cell cycle in a functional model that includes RAS, WNT and NOTCH signaling and the transcription factors HOX LIN-39 and Forkhead LIN-31. However, very interesting questions have emerged. In this last part I will list several open questions and possible approached to tackle them.

The first question that arises is whether LIN-39 acts alone or with a novel co-factor to activate the cell cycle of the VPCs. As mention previously, the binding pattern identified in this study does not resemble the TGATNNAT consensus binding proposed for the PBX-HOX complex (Mann and Affolter, 1998). On the other hand, it appears to be a condensed form of it. A possible explanation is that LIN-39 indeed works with CEH-20, the *C. elegans* PBX homologue, in a tripartite together with other co-factors like the Meis homologue UNC-62. This association PBX/HOX/MEIS has been previously observed in Hindbrain development (Jacobs et al., 1999) and proposed for some aspects of vulval development (Yang and Kenyon, 2005). Unfortunately, how this tripartite modifies the consensus binding of the PBX-Hox binding is completely unknown. Although the answer to this question seems complex, using the vulval development we could identify whether CEH-20 and UNC-62 are needed for LIN-39 function in the cell cycle. Following experiments shown in this work, we could test whether the levels of *cye-1* are affected in any or both of the mutants. Another approach that could elegantly identify new LIN-39 co-factors is the combination of ChIP techniques with Mass spectrometry.

Second, how LIN-31 inhibits the expression of several cell cycle components is sill unknown. Forkhead proteins DNA binding sequences are very loose and there is not ChIP data available from LIN-31. ChIP data would allow us to identify binding regions and possibly a consensus sequence throughout the *C. elegans* genome. This information could not only help us to answer the question about the cell cycle regulation but to learn more about the biology of LIN-31 and its targets.

Third, what are the differences underlying the function of LIN-31, LIN-1 and the complex of both is not yet understood. Perhaps, as discussed previously for the HOX genes, the complex of LIN-1/LIN-31 may have different DNA binding specificity and therefore different targets. To test that a comparative study of the bindings of LIN-1, LIN-31 and the LIN-1/LIN-31 may be necessary.

Finally, how NOTCH signaling interacts with LIN-31 remains elusive. One possibility could be that, as RAS signaling does in the 1° lineage (Tan et al., 1998), NOTCH could activate a kinase in the secondary lineage. To test this hypothesis we could use two approaches: a forward genetic screen using *Pbar-1::nicd::gfp; eff-1(lf); lin-39(lf)* or NICD ChIP data. The first approach could identify regulators that are control transcriptionally or at the protein level

while the second one only those that are strictly regulated at the transcriptional level. The identification of this factor could close a recurring question in the field of vulval development. In addition, whether NOTCH would activate the cell cycle exclusively through the inhibition of LIN-31 remains elusive. In other systems NOTCH signaling has been shown to control cell cycle through the transcription of Cyclins (Joshi et al., 2009). Therefore, it is a possibility that NOTCH signaling in parallel to the inhibition of LIN-31 directly promotes the transcription of the G1/S phase machinery.

It seems clear to me that the classical view of one transcription factor and one binding sequence is not longer valid. On the contrary, my work and the previous work of others indicate that transcription factor binding is far more complex. I believe that in a given time and cell a transcription factor is part of different pools of complexes, each of them regulated in different manners and with different specificities. Given the complexity of the matter, *C. elegans* and its vulval development can be the perfect model to elucidate the mechanisms underneath these open questions.

6

References

Ackermann, G. E. and Paw, B. H. (2003). Zebrafish: a genetic model for vertebrate organogenesis and human disorders. *Frontiers in Bioscience* **8**, d1227–53.

Aktas, H., Cai, H. and Cooper, G. M. (1997). Ras links growth factor signaling to the cell cycle machinery via regulation of cyclin D1 and the Cdk inhibitor p27KIP1. *Molecular and cellular biology* **17**, 3850–3857.

Ambros, V. (1999). Cell cycle-dependent sequencing of cell fate decisions in Caenorhabditis elegans vulva precursor cells. *Development* **126**, 1947–1956.

Andreeff, M., Ruvolo, V., Gadgil, S., Zeng, C., Coombes, K., Chen, W., Kornblau, S., Barón, A. E. and Drabkin, H. A. (2008). HOX expression patterns identify a common signature for favorable AML. *Leukemia* **22**, 2041–2047.

Attwooll, C., Lazzerini Denchi, E. and Helin, K. (2004). The E2F family: specific functions and overlapping interests. *The EMBO journal* **23**, 4709–4716.

Aubin, J., Déry, U., Lemieux, M. and Chailler, P. (2002). Stomach regional specification requires Hoxa5-driven mesenchymal-epithelial signaling. *Development* **129**, 4075–4087.

Bajpai, R., Chen, D. A., Rada-Iglesias, A., Zhang, J., Xiong, Y., Helms, J., Chang, C.-P., Zhao, Y., Swigut, T. and Wysocka, J. (2010). CHD7 cooperates with PBAF to control multipotent neural crest formation. **463**, 958–962.

Baker, D. A., Mille-Baker, B. and Wainwright, S. M. (2001). Mae mediates MAP kinase phosphorylation of Ets transcription factors in Drosophila. *Nature* **411**, 330–334.

Bassuk, A. G. and Leiden, J. M. (1995). A direct physical association between ETS and AP-1 transcription factors in normal human T cells. *Immunity* **3**, 223–237.

Baumgardt, M., Karlsson, D., Salmani, B. Y. and Bivik, C. (2014). Global programmed switch in neural daughter cell proliferation mode triggered by a temporal gene cascade. *Developmental Cell* **30**, 192–208.

Bei, L., Lu, Y. F., Bellis, S. L., Zhou, W. and Horvath, E. (2007). Identification of a HoxA10 activation domain necessary for transcription of the gene encoding □3 integrin during myeloid differentiation. *Journal of Biological …* **282**, 16846–16859.

Beitel, G. J., Tuck, S., Greenwald, I. and Horvitz, H. R. (1995). The Caenorhabditis elegans gene lin-1 encodes an ETS-domain protein and defines a branch of the vulval induction pathway. *genes & Development* **9**, 3149–3162.

Berset, T., Hoier, E. F., Battu, G., Canevascini, S. and Hajnal, A. (2001). Notch Inhibition of RAS Signaling Through MAP Kinase Phosphatase LIP-1 During C. elegans Vulval Development. *Science* **291**, 1055–1058.

Biggin, M. D. (2011). Animal transcription networks as highly connected, quantitative continua. *Developmental Cell* **21**, 611–626.

Bouazoune, K. and Kingston, R. E. (2012). Chromatin remodeling by the CHD7 protein is impaired by mutations that cause human developmental disorders. *PNAS* **109**, 19238–19243.

Boucherat, O., Chakir, J. and Jeannotte, L. (2012). The loss of Hoxa5 function promotes Notch-dependent goblet cell metaplasia in lung airways. *Biology open*.

Boxem, M. and van den Heuvel, S. (2001). lin-35 Rb and cki-1 Cip/Kip cooperate in developmental regulation of G1 progression in C. elegans. *Development* **128**, 4349–4359.

Brenner, S. (1974). The genetics of Caenorhabditis elegans. *Genetics* **77**, 71–94.

Breau, M. A., Wilkinson, D. G. and Xu, Q. (2013). A Hox gene controls lateral line cell migration by regulating chemokine receptor expression downstream of Wnt signaling.pp. 16892–16897.

Brodigan, T. M., Liu, J., (null), Kipreos, E. T. and Krause, M. (2003). Cyclin E expression during development in Caenorhabditis elegans. *developmental biology* **254**, 102–115.

Bromleigh, V. C. and Freedman, L. P. (2000). p21 is a transcriptional target of HOXA10 in differentiating myelomonocytic cells. *genes & Development* **14**, 2581–2586.

Burdine, R. D., Branda, C. S. and Stern, M. J. (1998). EGL-17(FGF) expression coordinates the attraction of the migrating sex myoblasts with vulval induction in C. elegans. *Development* **125**, 1083–1093.

Carlsson, P. and Mahlapuu, M. (2002). Forkhead transcription factors: key players in development and metabolism. *developmental biology* **250**, 1–23.

Cassada, R. C. and Russell, R. L. (1975). The dauerlarva, a post-embryonic developmental variant of the nematode Caenorhabditis elegans. *developmental biology* **46**, 326–342.

Celetti, A., Barba, P., Cillo, C. and Rotoli, B. (1993). Characteristic patterns of HOX gene expression in different types of human leukemia. *International Journal of Cancer* **53**, 237–244.

Chen, N. and Greenwald, I. (2004). The Lateral Signal for LIN-12/Notch in C. elegans Vulval Development Comprises Redundant Secreted and Transmembrane DSL Proteins. *Developmental Cell* **6**, 183–192.

Chen, Z. and Han, M. (2001). C. elegans Rb, NuRD, and Ras regulate lin-39-mediated cell fusion during vulval fate specification. *Current Biology* **11**, 1874–1879.

Cheng, W., Liu, J., Yoshida, H., Rosen, D. and Naora, H. (2005). Lineage infidelity of epithelial ovarian cancers is controlled by HOX genes that specify regional identity in the reproductive tract. *Nature medicine* **11**, 531–537.

Cheng, M., Olivier, P., Diehl, J. A. and Fero, M. (1999). The p21Cip1 and p27Kip1 CDK "inhibitors" are essential activators of cyclin D-dependent kinases in murine fibroblasts. *The EMBO Journal* **18**, 1571–1583.

Chng, Q. and Kenyon, C. (1999). egl-27 generates anteroposterior patterns of cell fusion in C. elegans by regulating Hox gene expression and Hox protein function. *Development* **126**, 3303–3312.

Chrisholm, A. (1991). Control of cell fate in the tail region of C. elegans by the gene egl-5. *Development* **111**, 921–932.

Christensen, S., Kodoyianni, V., Bosenberg, M., Friedman, L. and Kimble, J. (1996). lag-1, a gene required for lin-12 and glp-1 signaling in Caenorhabditis elegans, is homologous to human CBF1 and Drosophila Su (H). *Development* **122**, 1373–1383.

Clandinin, T. R., Katz, W. S. and Sternberg, P. W. (1997). Caenorhabditis elegansHOM-C Genes Regulate the Response of Vulval Precursor Cells to Inductive Signal. *developmental biology* **182**, 150–161.

Clark, S. G., Chisholm, A. D. and HORVITZ, H. R. (1993). Control of Cell Fates in the Central Body Region of C. elegans by the Homeobox Gene /in-39. *Cell* **74**, 43–55.

Clayton, J. E., van den Heuvel, S. J. L. and Saito, R. M. (2008). Transcriptional control of cell-cycle quiescence during C. elegans development. *developmental biology* **313**, 603–613.

Cohn, M. J., Patel, K., Krumlauf, R., Wilkinson, D. G., Clarke, J. D. and Tickle, C. (1997). Hox9 genes and vertebrate limb specification. *Nature* **387**, 97–101.

Collins, C. T. and Hess, J. L. (2015). Role of HOXA9 in leukemia: dysregulation, cofactors and essential targets. *Oncogene* 1–9.

Collins, C., Wang, J. and Miao, H. (2014). C/EBP is an essential collaborator in Hoxa9/Meis1-mediated leukemogenesis.pp. 9899–9904.

Corsi, A. K., Kostas, S. A., Fire, A. and Krause, M. (2000). Caenorhabditis elegans Twist plays an essential role in non-striated muscle development. *Development* **127**, 2041–2061.

Costa, M., Weir, M., Coulson, A., Sulston, J. and Kenyon, C. (1988). Posterior pattern formation in C. elegans involves position-specific expression of a gene containing a homeobox. *Cell* **55**, 747–756.

Couronne, O., Poliakov, A., Bray, N., Ishkhanov, T., Ryaboy, D., Rubin, E., Pachter, L. and Dubchak, I. (2003). Strategies and tools for whole-genome alignments. *Genome Research* **13**, 73–80.

Dale, T. C. (1998). Signal transduction by the Wnt family of ligands. *Biochemistry Journal* **329**, 209–223.

de Rosa, R., Grenier, J. K., Andreeva, T., Cook, C. E., Adoutte, A., Akam, M., Carroll, S. B. and Balavoine, G. (1999). Hox genes in brachiopods and priapulids and protostome evolution. *Nature* **399**, 772–776.

De Val, S., Chi, N. C., Meadows, S. M. and Minovitsky, S. (2008). Combinatorial regulation of endothelial gene expression by ets and forkhead transcription factors. *Cell* **135**, 1053–1064.

Du, W. and Pogoriler, J. (2006). Retinoblastoma family genes. *Oncogene* **25**, 5190–5200.

Duboule, D. (1994). Temporal colinearity and the phylotypic progression: a basis for the stability of a vertebrate Bauplan and the evolution of morphologies through heterochrony. *Dev. Suppl.* 135–142.

Eisenmann, D. M. (2005). Wnt signaling. *WormBook* 1–17.

Eisenmann, D. M., Maloof, J. N., Simske, J. S., Kenyon, C. and Kim, S. K. (1998). The β-catenin homolog BAR-1 and LET-60 Ras coordinately regulate the Hox gene lin-39 during Caenorhabditis elegans vulval development. *Development* **125**, 3667–3680.

Eissenberg, J. C. (2001). Molecular biology of the chromo domain: an ancient chromatin module comes of age. *Gene* **275**, 19–29.

Elledge, S. J. (1996). Cell cycle checkpoints: preventing an identity crisis. *Science* **274**, 1664–1672.

Euling, S. and Ambros, V. (1996). Heterochronic genes control cell cycle progress and developmental competence of C. elegans vulva precursor cells. *Cell* **84**, 667–676.

Esteban, N. C. and Spagnoli, F. M. (2014). Glimpse into Hox and tale regulation of cell differentiation and reprogramming. *Developmental dynamics* **243**, 76–87.

Farooqui, S., Pellegrino, M. W., Rimann, I., Morf, M. K., Müller, L., Fröhli, E. and Hajnal, A. (2012). Coordinated Lumen Contraction and Expansion during Vulval Tube Morphogenesisin Caenorhabditis elegans. *Developmental Cell* **23**, 494–506.

Fay, D. S. and Han, M. (2000). Mutations in cye-1, a Caenorhabditis elegans cyclin E homolog, reveal coordination between cell-cycle control and vulval development. *Development* 1–12.

Ferguson, E. L. and Horvitz, H. R. (1985). Identification and characterization of 22 genes that affect the vulval cell lineages of the nematode Caenorhabditis elegans. *Genetics* **110**, 17–72.

Frøkjaer-Jensen, C., Davis, M. W., Hopkins, C. E., Newman, B. J., Thummel, J. M., Olesen, S.-P., Grunnet, M. and Jorgensen, E. M. (2008). Single-copy insertion of transgenes in Caenorhabditis elegans. *Nature genetics* **40**, 1375–1383.

Garcia-Fernàndez, J. (2005). The genesis and evolution of homeobox gene clusters. *Nature Reviews Genetics* **6**, 881–892.

Garin, É., Lemieux, M. and Coulombe, Y. (2006). Stromal Hoxa5 function controls the growth and differentiation of mammary alveolar epithelium. *Developmental dynamics* **235**, 1858–1871.

Gavalas, A., Davenne, M., Lumsden, A., Chambon, P. and Rijli, F. M. (1997). Role of Hoxa-2 in axon pathfinding and rostral hindbrain patterning. *Development* **124**, 3693–3702.

Gellon, G. and McGinnis, W. (1998). Shaping animal body plans in development and evolution by modulation of Hox expression patterns. *Bioessays* **20**, 116–125.

Gilbert, P. M., Mouw, J. K., Unger, M. A. and Lakins, J. N. (2010). HOXA9 regulates BRCA1 expression to modulate human breast tumor phenotype. *The Journal of clinical investigation* **120**, 1535.

Gleason, J. E., Szyleyko, E. A. and Eisenmann, D. M. (2006). Multiple redundant Wnt signaling components function in two processes during C. elegans vulval development. *developmental biology* **298**, 442–457.

Glotzer, M., Murray, A. W. and Kirschner, M. W. (1991). Cyclin is degraded by the ubiquitin pathway. *Nature* **349**, 132–138.

Goetz, T. L., Gu, T. L. and Speck, N. A. (2000). Auto-inhibition of Ets-1 is counteracted by DNA binding cooperativity with core-binding factor □2. *Molecular and cellular biology* **20**, 81–90.

Go, M. J., Eastman, D. S. and Artavanis-Tsakonas, S. (1998). Cell proliferation control by Notch signaling in Drosophila development. *Development* **125**, 2031–2040.

Golden, J. W. and Riddle, D. L. (1984). The Caenorhabditis elegans dauer larva: developmental effects of pheromone, food, and temperature. *developmental biology* **102**, 368–378.

Graña, X. and Reddy, E. P. (1995). Cell cycle control in mammalian cells: role of cyclins, cyclin dependent kinases (CDKs), growth suppressor genes and cyclin-dependent kinase inhibitors (CKIs). *Oncogene* **11**, 211–219.

Green, J. L., Inoue, T. and Sternberg, P. W. (2010). Opposing Wnt Pathways Orient Cell Polarity during Organogenesis. *Cell* **134**, 646–657.

Guerry, F., Marti, C.-O., Zhang, Y., Moroni, P. S., Jaquiery, E. and Muller, F. (2007). The Mi-2 nucleosome-remodeling protein LET-418 is targeted via LIN-1/ETS to the promoter of lin-39/Hox during vulval development in C. elegans. *developmental biology* **306**, 469–479.

Haag, A., Gutierrez, P., Bühler, A., Walser, M., Yang, Q., Langouët, M., Kradolfer, D., Fröhli, E., Herrmann, C. J., Hajnal, A., et al. (2014). An in vivo EGF receptor localization screen in C. elegans Identifies the Ezrin homolog ERM-1 as a temporal regulator of signaling. *PLoS Genet.* **10**, e1004341.

Harterink, M., Kim, D. H., Middelkoop, T. C., Doan, T. D., Oudenaarden, A. V. and Korswagen, H. C. (2011). Neuroblast migration along the anteroposterior axis of C. elegans is controlled by opposing gradients of Wnts and a secreted Frizzled-related protein. *Development* **138**, 2915–2924.

Hershko, A. (1997). Roles of ubiquitin-mediated proteolysis in cell cycle control. *Current opinion in cell biology*.

Hochegger, H., Takeda, S. and Hunt, T. (2008). Cyclin-dependent kinases and cell-cycle transitions: does one fit all? *Nature Reviews Molecular Cell ….*

Hombría, J. C.-G. and Lovegrove, B. (2003). Beyond homeosis--HOX function in morphogenesis and organogenesis. *Differentiation* **71**, 461–476.

Hong, Y., Roy, R. and Ambros, V. (1998). Developmental regulation of a cyclin-dependent kinase inhibitor controls postembryonic cell cycle progression in Caenorhabditis elegans. *Development* **125**, 3585–3597.

Hunt-Newbury, R., Viveiros, R., Johnsen, R., Mah, A., Anastas, D., Fang, L., Halfnight, E., Lee, D., Lin, J., Lorch, A., et al. (2007). High-Throughput In Vivo Analysis of Gene Expression in Caenorhabditis elegans. *Plos Biology* **5**, 1981–1997.

Hwang, B. J. and Sternberg, P. W. (2004). A cell-specific enhancer that specifies lin-3 expression in the C. elegans anchor cell for vulval development. *Development* **131**, 143–151.

Iimura, T. and Pourquié, O. (2006). Collinear activation of Hoxb genes during gastrulation is linked to mesoderm cell ingression. *Nature* **442**, 568–571.

Izpisúa-Belmonte, J. C., Tickle, C., Dollé, P., Wolpert, L. and Duboule, D. (1991). Expression of the homeobox Hox-4 genes and the specification of position in chick wing development. *Nature* **350**, 585–589.

Jacobs, D., Beitel, G. J., Clark, S. G., Horvitz, H. R. and Kornfeld, K. (1998). Gain-of-function mutations in the Caenorhabditis elegans lin-1 ETS gene identify a C-terminal regulatory domain phosphorylated by ERK MAP kinase. *Genetics* **149**, 1809–1822.

Jacobs, Y., Schnabel, C. A. and Cleary, M. L. (1999). Trimeric association of Hox and TALE homeodomain proteins mediates Hoxb2 hindbrain enhancer activity. *Molecular and cellular biology* **19**, 5134–5142.

Janssen, N., Bergman, J. E. H., Swertz, M. A., Tranebjaerg, L., Lodahl, M., Schoots, J., Hofstra, R. M. W., van Ravenswaaij-Arts, C. M. A. and Hoefsloot, L. H. (2012). Mutation update on the CHD7 gene involved in CHARGE syndrome. *Hum. Mutat.* **33**, 1149-1160.

Jayaraman, G., Srinivas, R., Duggan, C. and Ferreira, E. (1999). p300/cAMP-responsive element-binding protein interactions with ets-1 and ets-2 in the transcriptional activation of the human stromelysin promoter. *Journal of Biological chemistry* **274**, 17342–17352.

Joshi, I., Minter, L. M., Telfer, J., Demarest, R. M., Capobianco, A. J., Aster, J. C., Sicinski, P., Fauq, A., Golde, T. E. and Osborne, B. A. (2009). Notch signaling mediates G1/S cell-cycle progression in T cells via cyclin D3 and its dependent kinases. *Blood* **113**, 1689–1698.

Kamath, R. S., Fraser, A. G., Dong, Y., Poulin, G., Durbin, R., Gotta, M., Kanapin, A., Le Bot, N., Moreno, S., Sohrmann, M., et al. (2003). Systematic functional analysis of the Caenorhabditis elegans genome using RNAi. *Nature* **421**, 231–237.

Kaufmann, E., Müller, D. and Knöchel, W. (1995). DNA recognition site analysis of Xenopus wingedhelix proteins. *Journal of molecular biology*.

Kenyon, C. (1986). A Gene Involved in the Development of the Posterior Body Region of C. elegans. *Cell* **46**, 477–487.

Kim, Y. and Nirenberg, M. (1989). Drosophila NK-homeobox genes. *Proceedings of the national Academy of Sciences of the United States of America* **86**, 7716–7720.

Kim, Y.-R., Oh, K.-J., Park, R.-Y., Xuan, N., Kang, T.-W., Kwon, D.-D., Choi, C., Kim, M., Nam, K., Ahn, K., et al. (2010). HOXB13 promotes androgen independent growth of LNCaP prostate cancer cells by the activation of E2F signaling. *Mol Cancer* **9**, 124.

Koh, K., Peyrot, S. M., Wood, C. G., Wagmaister, J. A., Maduro, M. F., Eisenmann, D. M. and Rothman, J. H. (2002). Cell fates and fusion in the C. elegans vulval primordium are regulated by the EGL-18 and ELT-6 GATA factors -- apparent direct targets of the LIN-39 Hox protein. *Development* **129**, 5171–5180.

Koreth, J. and van den Heuvel, S. (2005). Cell-cycle control in Caenorhabditis elegans: how the worm moves from G1 to S. *Oncogene* **24**, 2756–2764.

Korver, W., Roose, J. and Clevers, H. (1997). The winged-helix transcription factor Trident is expressed in cycling cells. *Nucleic Acids Research* **25**, 1715–1719.

Korswagen, H. C. (2002). Canonical and non-canonical Wnt signaling pathways in Caenorhabditis elegans: variations on a common signaling theme. *Bioessays* **24**, 801–810.

Kostic, I., Li, S. and Roy, R. (2003). cki-1 links cell division and cell fate acquisition in the C. elegans somatic gonad. *developmental biology* 1–11.

Kroeger, H., Jelinek, J., Estécio, M., He, R. and Kondo, K. (2008). Aberrant CpG island methylation in acute myeloid leukemia is accentuated at relapse. *Blood* **112**, 1366–1373.

Krumlauf, R. (1994). Hox genes in vertebrate development. *Cell* **72**, 191–201.

la Cova, de, C. and Greenwald, I. (2012). SEL-10/Fbw7-dependent negative feedback regulation of LIN-45/Braf signaling in C. elegans via a conserved phosphodegron. *genes & Development* **26**, 2524–2535.

Lemons, D. and McGinnis, W. (2006). Genomic evolution of Hox gene clusters. *Science* **313**, 1918–1922.

Lewis, E. B. (1978). A gene complex controlling segmentation in Drosophila. *Nature* **276**, 565–570.

Liang, H., Mao, X., Olejniczak, E. T., Nettesheim, D. G., Yu, L., Meadows, R. P., Thompson, C. B. and Fesik, S. W. (1994). Solution structure of the ets domain of Fli-1 when bound to DNA. *Nat. Struct. Biol.* **1**, 871–875.

Liu, J. and Fire, A. (2000). Overlapping roles of two Hox genes and the exd ortholog ceh-20 in diversification of the C. elegans postembryonic mesoderm. *Development* **127**, 5179–5190.

Lufkin, T. (2005). Hox Genes: Embryonic Development. *eLS*.

Macleod, K., Leprince, D. and Stehelin, D. (1992). The ets gene family. *Trends Biochem. Sci.* **17**, 251–256.

Mahfooz, N. S., Li, H. and Popadić, A. (2004). Differential expression patterns of the hox gene are associated with differential growth of insect hind legs. *PNAS* **101**, 4877–4882.

Maloof, J. N. and Kenyon, C. (1998). The Hox gene lin-39 is required during C. elegans vulval induction to select the outcome of Ras signaling. *Development* **125**, 180–191.

Maloof, J., Whangbo, J., Harris, J., Jongeward, G. and Kenyon, C. (1999). A Wnt signaling pathway controls hox gene expression and neuroblast migration in C. elegans. *Development* **126**, 37–49.

Maloof, J., Whangbo, J., Harris, J., Jongeward, G. and Kenyon, C. (1999). A Wnt signaling pathway controls hox gene expression and neuroblast migration in C. elegans. *Development* **126**, 37–49.

Mann, R. S. and Affolter, M. (1998). Hox proteins meet more partners. *Curr. Opin. Genet. Dev.* **8**, 423–429.

McGowan, C. H. and Russell, P. (1993). Human Wee1 kinase inhibits cell division by phosphorylating p34cdc2 exclusively on Tyr15. *The EMBO journal* **12**, 75–85.

McGowan, C. H. and Russell, P. (1995). Cell cycle regulation of human WEE1. *The EMBO journal* **14**, 2166–2175.

Medema, R. H., Kops, G. J., Bos, J. L. and Burgering, B. M. (2000). AFX-like Forkhead transcription factors mediate cell-cycle regulation by Ras and PKB through p27kip1. *Nature* **404**, 782–787.

Mello, C. C., Kramer, J. M., Stinchcomb, D. and Ambros, V. (1991). Efficient gene transfer in C. elegans: extrachromosomal maintenance and integration of transforming sequences. *The EMBO Journal* **10**, 3959–3970.

Miller, D. M. and Shakes, D. C. (1995). Immunofluorescence microscopy. *Methods Cell Biol.* **48**, 365–394.

Miller, L. M., Gallegos, M. E., Morisseau, B. A. and Kim, S. K. (1993). lin-31, a Caenorhabditis elegans HNF-3/fork head transcription factor homolog, specifies three alternative cell fates in vulval development. *genes & Development* **7**, 933–947.

Miller, M. E. and Cross, F. R. (2001). Cyclin specificity: how many wheels do you need on a unicycle? *J. Cell. Sci.* **114**, 1811–1820.

Moens, C. B. and Selleri, L. (2006). Hox cofactors in vertebrate development. *developmental biology* **291**, 193–206.

Moss, E. G., Lee, R. C. and Ambros, V. (1997). The Cold Shock Domain Protein LIN-28 Controls Developmental Timing in C. elegans and Is Regulated by the lin-4 RNA. *Cell* **88**, 637–646.

Mukhopadhyay, A., Deplancke, B., Walhout, A. J. M. and Tissenbaum, H. A. (2008). Chromatin immunoprecipitation (ChIP) coupled to detection by quantitative real-time PCR to study transcription factor binding to DNA in Caenorhabditis elegans. *Nat Protoc* **3**, 698–709.

Nalbantoglu, B., Tekir, S., Ülgen, K. (2011) Wnt Signaling Network in Homo Sapiens. *Edited by Paula Bubulya.*

Nilsson, I. and Hoffmann, I. (2000). Cell cycle regulation by the Cdc25 phosphatase family. *Prog Cell Cycle Res* **4**, 107–114.

Niu, W., Lu, Z. J., Zhong, M., Sarov, M., Murray, J. I., Brdlik, C. M., Janette, J., Chen, C., Alves, P., Preston, E., et al. (2011). Diverse transcription factor binding features revealed by genome-wide ChIP-seq in C. elegans. *Genome Research* **21**, 245–254.

Nusser-Stein, S., Beyer, A., Rimann, I., Adamczyk, M., Piterman, N., Hajnal, A. and Fisher, J. (2012). Cell-cycle regulation of NOTCH signaling during C. elegans vulval development. *Molecular Systems Biology* **8**, 1–14.

Overdier, D. G., Porcella, A. and Costa, R. H. (1994). The DNA-binding specificity of the hepatocyte nuclear factor 3/forkhead domain is influenced by amino-acid residues adjacent to the recognition helix. *Molecular and cellular biology* **14**, 2755–2766.

Pan, C.-L., Howell, J. E., Clark, S. G., Hilliard, M., Cordes, S., Bargmann, C. I. and Garriga, G. (2006). Multiple Wnts and frizzled receptors regulate anteriorly directed cell and growth cone migrations in Caenorhabditis elegans. *Developmental Cell* **10**, 367–377.

Park, M. and Krause, M. W. (1999). Regulation of postembryonic G(1) cell cycle progression in Caenorhabditis elegans by a cyclin D/CDK-like complex. *Development* **126**, 4849–4860

Pearson, J. C., Lemons, D. and McGinnis, W. (2005). Modulating Hox gene functions during animal body patterning. *Nature Reviews Genetics* **6**, 893–904.

Peeper, D. S., Upton, T. M., Ladha, M. H., Neuman, E., Zalvide, J., Bernards, R., DeCaprio, J. A. and Ewen, M. E. (1997). Ras signaling linked to the cell-cycle machinery by the retinoblastoma protein. *Nature* **386**, 177–181.

Pellegrino, M. W. and Hajnal, A. (2014). The transcription factor VAB-23 links vulval cell fate specification and morphogenesis. *Worm* **1**, 170–175.

Pellegrino, M. W., Farooqui, S., Fröhli, E., Rehrauer, H., Kaeser-Pebernard, S., Muller, F., Gasser, R. B. and Hajnal, A. (2011). LIN-39 and the EGFR/RAS/MAPK pathway regulate C. elegans vulval morphogenesis via the VAB-23 zinc finger protein. *Development* **138**, 4649–4660.

Penigault, J.-B. and Felix, M.-A. (2011). High sensitivity of C. elegans vulval precursor cells to the dose of posterior Wnts. *developmental biology* **357**, 428–438.

Petersen, J. M., Skalicky, J. J. and Donaldson, L. W. (1995). Modulation of Transcription Factor Ets-1 DNA Binding: DNA-Induced Unfolding of an xo Helix. *Science* **269**, 1866–1869.

Phelan, M. L. and Rambaldi, I. (1995). Cooperative interactions between HOX and PBX proteins mediated by a conserved peptide motif. *Molecular and cellular biology* **15**, 3989–3997.

Powers, T. P. and Amemiya, C. T. (2004). Evidence for a Hox14 paralog group in vertebrates. *Curr. Biol.* **14**, R183–4.

Prasad, B. C. and Clark, S. G. (2006). Wnt signaling establishes anteroposterior neuronal polarity and requires retromer in C. elegans. *Development* **133**, 1757–1766.

Qi, R., An, H., Yu, Y., Zhang, M., Liu, S., Xu, H., Guo, Z., Cheng, T. and Cao, X. (2003). Notch1 signaling inhibits growth of human hepatocellular carcinoma through induction of cell cycle arrest and apoptosis. *Cancer Research* **63**, 8323–8329.

Rechsteiner, M. and Rogers, S. W. (1996). PEST sequences and regulation by proteolysis. *Trends Biochem. Sci.* **21**, 267–271.

Regős, Á., Lengyel, K., Takács-Vellai, K. and Vellai, T. (2013). Identification of novel cis-regulatory regions from the Notch receptor genes lin-12 and glp-1 of Caenorhabditis elegans. *Gene Expression Patterns* **13**, 66–77.

Rezsohazy, R. (2014). Non□transcriptional interactions of Hox proteins: Inventory, facts, and future directions. *Developmental dynamics* **243**, 117–131.

Rezsohazy, R., Saurin, A. J., Maurel-Zaffran, C. and Graba, Y. (2015). Cellular and molecular insights into Hox protein action. *Development* **142**, 1212–1227.

Rodriguez-Paredes, M., Ceballos-Chavez, M., Esteller, M., Garcia-Dominguez, M. and Reyes, J. C. (2009). The chromatin remodeling factor CHD8 interacts with elongating RNA polymerase II and controls expression of the cyclin E2 gene. *Nucleic Acids Research* **37**, 2449–2460.

Rogers, C., Jayasena, C., Nie, S. and Bronner, M. E. (2012). Neural crest specification: tissues, signals, and transcription factors. *WIREs Developmental Biology* **1**, 52–68.

Roy, S. H., Clayton, J. E., Holmen, J., Beltz, E. and Saito, R. M. (2011). Control of Cdc14 activity coordinates cell cycle and development in Caenorhabditis elegans. *Mechanisms of Development* **128**, 317–326.

Ruvkun, G., Ambros, V., Coulson, A., Waterston, R., Sulston, J. and Horvitz, H. R. (1989). Molecular genetics of the Caenorhabditis elegans heterochronic gene lin-14. *Genetics* **121**, 501–516.

Saito, R. M., Perreault, A., Peach, B., Satterlee, J. S. and van den Heuvel, S. (2004). The CDC-14 phosphatase controls developmental cell-cycle arrest in C. elegans. *Nat Cell Biol* **6**, 777–783.

Salser, S. J., Loer, C. M. and Kenyon, C. (1993). Multiple HOM-C gene interactions specify cell fates in the nematode central nervous system. *genes & Development* **7**, 1714–1724.

Sapir, A., Choi, J., Leikina, E., Avinoam, O. and Valansi, C. (2007). AFF-1, a FOS-1-regulated fusogen, mediates fusion of the anchor cell in C. elegans. *Developmental Cell* **12**, 683–698.

Schiedlmeier, B., Santos, A. C. and Ribeiro, A. (2007). HOXB4's road map to stem cell expansion.pp. 16952–16957.

Schindelin, J., Arganda-Carreras, I., Frise, E., Kaynig, V., Longair, M., Pietzsch, T., Preibisch, S., Rueden, C., Saalfeld, S., Schmid, B., et al. (2012). Fiji: an open-source platform for biological-image analysis. *Nat. Methods* **9**, 676–682.

Schindler, A. J. and Sherwood, D. R. (2012). Morphogenesis of the Caenorhabditis elegans vulva. *WIREs Dev Biol* **2**, 75–95.

Schmid, T. and Hajnal, A. (2015). Signal transduction during C. elegans vulval development: a NeverEnding story. *Curr. Opin. Genet. Dev.* **32**, 1–9.

Schnetz, M. P., Handoko, L., Akhtar-Zaidi, B., Bartels, C. F., Pereira, C. F., Fisher, A. G., Adams, D. J., Flicek, P., Crawford, G. E. and LaFramboise, T. (2010). CHD7 targets active gene enhancer elements to modulate ES cell-specific gene expression. *PLoS Genet.* **6**, e1001023.

Sharrocks, A. D. (2001). The ETS-domain transcription factor family. *Nat. Rev. Mol. Cell Biol.* **2**, 827–837.

Shaye, D. D. and Greenwald, I. (2002). Endocytosis-mediated downregulation of LIN-12/Notch upon Ras activation in Caenorhabditis elegans. *Nature* **420**, 686–690.

Shemer, G. and Podbilewicz, B. (2002). LIN-39/Hox triggers cell division and represses EFF-1/fusogen-dependent vulval cell fusion. *genes & Development* **16**, 3136–3141.

Sherr, C. J. and Roberts, J. M. (1999). CDK inhibitors: positive and negative regulators of G1-phase progression. *genes & Development* **13**, 1501–1512.

Sherwood, D. R., Butler, J. A., Kramer, J. M. and Sternberg, P. W. (2005). FOS-1 promotes basement-membrane removal during anchor-cell invasion in C. elegans. *Cell* **121**, 951–962.

Siegfried, K. R. and Kimble, J. (2002). POP-1 controls axis formation during early gonadogenesis in C. elegans. *Development* **129**, 443–453.

Sorge, S., Ha, N., Polychronidou, M. and Friedrich, J. (2012). The cis□regulatory code of Hox function in Drosophila. *The EMBO journal* **31**, 3323–3333.

Srinivasan, S., Dorighi, K. M. and Tamkun, J. W. (2008). Drosophila Kismet regulates histone H3 lysine 27 methylation and early elongation by RNA polymerase II. *PLoS Genet.* **4**, e1000217.

Sriuranpong, V., Borges, M. W., Ravi, R. K., Arnold, D. R., Nelkin, B. D., Baylin, S. B. and Ball, D. W. (2001). Notch signaling induces cell cycle arrest in small cell lung cancer cells. *Cancer Research* **61**, 3200–3205.

Sternberg, P. W. (1988). Lateral inhibition during vulval induction in Caenorhabditis elegans. **335**, 551–554.

Sternberg, P. W. (2005). Vulval development. *WormBook* 1–28.

Sternberg, R. H. P. (1992). The gene lin-3 encodes an inductive signal for vulval development in C. elegans. **358**, 470–476.

Stevaux, O. and Dyson, N. J. (2002). A revised picture of the E2F transcriptional network and RB function. *Curr. Opin. Cell Biol.* **14**, 684–691.

Sulston, J. E. and Horvitz, H. R. (1977). Post-embryonic Cell Lineages of the Nematode, Caenorhabditis elegans. *developmental biology* **56**, 110–156.

Sun, M., Song, C. X. and Huang, H. (2013). HMGA2/TET1/HOXA9 signaling pathway regulates breast cancer growth and metastasis.pp. 9920–9925.

Sundaram, M. V. (2004). Vulval development: the battle between Ras and Notch. *Current Biology* **14**, R311–R313.

Sundaram, M. V. (2005). The love-hate relationship between Ras and Notch. *genes & Development* **19**, 1825–1839.

Sundaram, M. V. (2006). RTK/Ras/MAPK signaling. *WormBook* 1–19.

Szabó, E., Hargitai, B., Regős, Á., Tihanyi, B. and Barna, J. (2009). TRA-1/GLI controls the expression of the Hox gene lin-39 during C. elegans vulval development. *developmental biology* **330**, 339–348.

Takacs-Vellaia, K., b, Vellaia, T., b, Chenc, E. B., Zhangb, Y., Guerryb, F., c, M. J. S. and Muller, F. (2007). Transcriptional control of Notch signaling by a HOX and a PBX/EXD protein during vulval development in C. elegans. *developmental biology* **302**, 661–669.

Takada, I., Mihara, M., Suzawa, M., Ohtake, F., Kobayashi, S., Igarashi, M., Youn, M.-Y., Takeyama, K.-I., Nakamura, T., Mezaki, Y., et al. (2007). A histone lysine methyltransferase activated by non-canonical Wnt signaling suppresses PPAR-γ transactivation. *Nat Cell Biol* **9**, 1273–1285.

Tan, P. B., Lackner, M. R. and Kim, S. K. (1998). MAP Kinase Signaling Specificity Mediated by the LIN-1 Ets/LIN-31 WH Transcription Factor Complex during C. elegans Vulval Induction. *Cell* **93**, 569–580.

Taniguchi, Y. (2014). Hox transcription factors: modulators of cell-cell and cell-extracellular matrix adhesion. *BioMed research international*.

Tetsu, O. and McCormick, F. (1999). Beta-catenin regulates expression of cyclin D1 in colon carcinoma cells. *Nature* **398**, 422–426.

Thompson, B., Tremblay, V., Lin, G. and Bochar, D. (2008). CHD8 Is an ATP-Dependent Chromatin Remodeling Factor That Regulates {beta}-Catenin Target Genes. *Molecular and Cellular Biology* **28**, 3894–3904.

Thummel, R., Ju, M., Sarras, M. P. and Godwin, A. R. (2007). Both Hoxc13 orthologs are functionally important for zebrafish tail fin regeneration. *Dev Genes Evol* **217**, 413–420.

Trinkaus, J. P. (1969). Cells into organs: the forces that shape the embryo.

Van Auken, K., Weaver, D., Robertson, B., Sundaram, M., Saldi, T., Edgar, L., Elling, U., Lee, M., Boese, Q. and Wood, W. B. (2002). Roles of the Homothorax/Meis/Prep homolog UNC-62 and the Exd/Pbx homologs CEH-20 and CEH-40 in C. elegans embryogenesis. *Development* **129**, 5255–5268.

van den Heuvel, S. (2005). Cell-cycle regulation. *WormBook* 1–16.

Vermeulen, K., Van Bockstaele, D. R. and Berneman, Z. N. (2003). The cell cycle: a review of regulation, deregulation and therapeutic targets in cancer. *Cell Prolif.* **36**, 131–149.

Vissers, L. E. L. M., Ravenswaaij, C. M. A. V., Admiraal, R., Hurst, J. A., Vries, B. B. A. de, Janssen, I. M., Vliet, W. A. V. D., Huys, E. H. L. P. G., Jong, P. J. de, Hamel, B. C. J., et al. (2004). Mutations in a new member of the chromodomain gene family cause CHARGE syndrome. *Nature genetics* **36**, 955–957.

Wagmaister, J. A., Gleason, J. E. and Eisenmann, D. M. (2006a). Transcriptional upregulation of the C. elegans Hox gene lin-39 during vulval cell fate specification. *Mechanisms of Development* **123**, 135–150.

Wagmaister, J. A., Miley, G. R., Morris, C. A., Gleason, J. E., Miller, L. M., Kornfeld, K. and Eisenmann, D. M. (2006b). Identification of cis-regulatory elements from the C. elegans Hox gene lin-39 required for embryonic expression and for regulation by the transcription factors LIN-1, LIN-31 and LIN-39. *developmental biology* **297**, 550–565.

Wang, B. B., Müller-Immergluck, M. M., Austin, J., Robinson, N. T., Chisholm, A. and Kenyon, C. (1993). A homeotic gene cluster patterns the anteroposterior body axis of C. elegans. *Cell* **74**, 29–42.

Wang, M. and Sternberg, P. W. (2000). Patterning of the C. elegans 1 degrees vulval lineage by RAS and Wnt pathways. *Development* **127**, 5047–5058.

Weigel, D., Jürgens, G., Küttner, F., Seifert, E. and Jäckle, H. (1989). The homeotic gene fork head encodes a nuclear protein and is expressed in the terminal regions of the Drosophila embryo. *Cell* **57**, 645–658.

Whangbo, J. and Kenyon, C. (2010). A Wnt Signaling System that Specifies Two Patterns of Cell Migration in C. elegans. *Molecular Cell* 851–858.

Wood, W. B. (1988). Introduction to C. elegans Biology. *Cold Spring Harbor Monograph Archive* **17**, 1–16.

Wolpert, L. (1992). Gastrulation and the evolution of development. *Development* **116**, 7–13.

Yang, L. (2005). The roles of two C. elegans HOX co-factor orthologs in cell migration and vulva development. *Development* **132**, 1413–1428.

Yoo, A. S., Bais, C. and Greenwald, I. (2004). Crosstalk between the EGFR and LIN-12/Notch pathways in C. elegans vulval development. *Science* **303**, 663–666.

Yoshida, N., Yoshida, S., Araie, M., Handa, H. and Nabeshima, Y. (2000). Ets family transcription factor ESE-1 is expressed in corneal epithelial cells and is involved in their differentiation. *Mechanisms of Development* **97**, 27–34.

Zhang, X. and Greenwald, I. (2011). Spatial Regulation of lag-2 Transcription During Vulval Precursor Cell Fate Patterning in Caenorhabditis eleganslag-2. *Genetics* **188**, 847–858.

Žigman, M., Laumann-Lipp, N., Titus, T. and Postlethwait, J. (2014). Hoxb1b controls oriented cell division, cell shape and microtubule dynamics in neural tube morphogenesis. *Development* **141**, 639–649.

7

Appendix

7.1 Abbreviations

ΔCT	Delection of the C Terminus
1°	Primary cell fate
2°	Secondary cell fate
3°	Tertiary cell fate
A-P	Anterior - Posterior
A-Rvl	Anterior Reverse vulva
aas	Amino-acids
AC	Anchor Cell
CDK	Cyclin Dependent Kinase
CKI	Cyclin Kinase Inhibitor
DNA	Desoxyribonucleic acid
E. coli	Escherichia coli
Expl	Exploted
gf	Gain of function
GFP	Green fluorescent protein
HRP	Horseradish peroxidase
L1-4	Larval stage 1-4
lf	Loss of function
LIN	Lineage defective
M	Molar
MosSCI	Mos1-mediated single copy insertion (MosSCI)
Muv	Multivulva
NA	No applicable
NC	No confirmed
NF	No found
NGM	Nematode Growth Media
ODR	Oligos Daniel Roiz
OMP	Oligos Mark Pellegrino
OSN	Oligos Stefanie Nusser-Stein
P-Rvl	Posterior Reverse vulva
P1-12	Posterior ventral Ectoblast 1-12
P1-12.a	Anterior decendant of the P Ectoblast 1-12
P1-12.p	Posterior decendant of the P Ectoblast 1-12
PAGE	Polyacrylamide gel electrophoresis
PBS-T	Phosphate Buffered Saline Tween-20
PCR	Polymerase chain reaction
PHA	Phasmid neuron A
PHB	Phasmid neuron B
PVDF	Polyvinylidene difluoride

Pvl	Produring vulva
Rb	Retinoblastoma (Human gene)
rf	Reduction of function
RNAi	RNA interference
SDS	Sodium dodecyl sulfate
SNP	Single nucleotide Polymorphism
STET	Sucrose, Triton X-100, EDTA and Tris Buffer
Str	Sterile
TF	Transcription Factor
U	Units
VPCs	Vulval Precursor Cells
Vul	Vulvaless
WT	Wild-type
zhEx	Zurich Extrachromosomal array
zhIs	Zurich Integrated array

7.2 Curriculum Vitae

Personal Data

Name:	Daniel Maria ROIZ LAFUENTE
Day of birth:	July 27, 1987
Nationality:	Spanish
Hometown:	Seville (Spain)
Matriculation No.:	10-764-033

Education

2010 – 2015	**PhD Dr. Sc. nat.** Doctoral thesis: "The HOX LIN-39, NOTCH LIN-12 and Forkhead LIN-31 coordinately control the cell cycle of the *C. elegans* vulva". Carried out under the supervision of Prof. Dr Alex Hajnal, Institute of Molecular Life Sciences, University of Zurich, Switzerland.
Summer 2010	**Biology Undergraduate Summer School (BUSS)** Project title: "Expression analysis of the *ttr* protein family in *C. elegans"*. Carried out in the laboratory of Prof. Dr. Alex Hajnal, Institute of Molecular Life Sciences, University of Zurich, Switzerland.
2005 – 2010	***Licenciado* in Biology** University of Seville, Spain
2003 – 2005	***Bachelaurate* (Type B – Natural Sciences)** Colegio Portaceli, Sevilla, Spain
1999 – 2003	**Secondary School (Type B – Natural Sciences)** Colegio Santo Angel De la Guarda, Sevilla, Spain
1993 – 1998	**Primary School** Colegio Santo Angel De la Guarda, Sevilla, Spain

Oral Presentations

"The *hox* gene lin-39 controls cell cycle progression during *C. elegans* vulval development"
Daniel Roiz, Philipp Leu and Alex Hajnal
Basel Worm Meeting 2013; Friedrich Miescher Institute; Basel; Switzerland, 2013

Poster Presentations

"The *hox* gene *lin-39* coordinates vulval cell cycle progression"
Daniel Roiz, Juan Miguel Escobar-Restrepo and Alex Hajnal
Berlin *C. elegans* Meeting 2014, Berlin, Germany, 2014

"LIN-39/HOX controls cell cycle progression in *C. elegans* vulva development"
Daniel Roiz and Alex Hajnal
17th International Congress of Developmental Biology, Cancun; Mexico, 2013

***"C. elegans* as a model to investigate the molecular functions of CHD-7, the homolog of the CHARGE syndrome gene"**
Daniel Roiz and Alex Hajnal
SDB 71st Annual Meeting, Montreal, Canada, 2012

"The chromo-helicase domain protein CHD-7 is a putative regulator of WNT-ligands"
Daniel Roiz and Alex Hajnal
18th International C. elegans Meeting, University of California, Los Angeles, USA, 2011

"*chdl*: a putative wnt-ligand regulator"
Daniel Roiz and Alex Hajnal
IMLS Retreat, Wildhaus, Switzerland, 2011

Teaching experiences

2010 – date Assistant in various courses from M.Sc. in biology and Medical faculty.
Bio 326: *"Modern genetics and genomics"*

Bio 260: "*Molecular Biology*"
Medical course: "*Zellwachstum und Zelltod in C. elegans"*

2012 - 2013 Supervision of a M.Sc. project
"LIN-39 is essential for the proliferation of Vulval Precursor Cells in *Caenorhabditis elegans"*. Philipp Leu, Institute of Molecular Life Sciences, University of Zurich, Switzerland.

7.3 Acknowledgements

First at all, I would like to thank Prof. Alex Hajnal and Stefanie Nusser-Stein whom without support I would not be writing these lines. Both of them bet for me after few weeks working as a summer student and made everything possible to accommodate me as PhD student. Moreover, Alex has always exceeded my expectations understanding my mind-set and my ambitions, supporting me when I most needed and taking me to the right path when I was completely lost.

I also warmly thank Erika Fröhli and Juan Miguel Escobar Restrepo. Both have been my friends, psychologists and, sometimes, my hands during these 5 years in the Hajnal lab. Without them the outcome I present in this thesis would have been much poorer if being at all. Obviously I cannot forget many other lab member that have played very important roles in and out the lab during this time, especial thanks go to Sarfarazhussain Farooqui, "my best enemy" Itay Nakdimon and Philipp Leu, my first and last master student whose energy and love for science helped me when I most needed.

In addition, I need to thank the Young Scientist Network and all the members I had the pleasure to work with. Up to date, it has been the most enriching experience I can recall. It has helped me to build my personality and my skills far beyond the lab and has definitely marked my future path.

I want to thank my family, especially my parents who have supported me unconditionally and my brother Norberto. He has been guiding me in the distant: supporting me, even when not authorizing, understanding my fears and being, in summary, my best friend. The friend that only few people has the good luck to find in life.

I have no words to thank my girlfriend Anna. She has complemented and balanced me since the first day we met in a bar of Seville, compromising at times her own development for me and my career. This PhD is also hers!

Finally my friends, *the Machotes,* in special: Ruben Gómez, who opened his house in Zurich for me and never closed, Lander Casado and Carlos Puig. Moreover, I would like to mention Boris Battistini, who always brings me a new perspective. I will always keep all of you, named here or not, in my memory.